BRGM
L'ENTREPRISE AU SERVICE DE LA TERRE

Ademe

INSTITUT MIXTE
DE RECHERCHES GÉOTHERMIQUES

seismic studies on the HDR site of Soultz-sous-Forêts during Phase IIa

décembre 1992
R 36 411

BRGM

L'ENTREPRISE AU SERVICE DE LA TERRE

Ademe

INSTITUT MIXTE
DE RECHERCHES GÉOTHERMIQUES

seismic studies on the HDR site of Soultz-sous-Forêts during Phase IIa

A. Beauce
R.H. Jones
H. Fabriol
C. Hulot

décembre 1992
R 36 411

BRGM - IMRG
B.P. 6009 - 45060 ORLÉANS CEDEX 2 - France - Tél. : (33) 38.64.31.72

ABSTRACT

During Phase IIa (1990-1991) of the european HDR Soultz project, two 50 h-hydraulic injection tests at flowrates of 7 and 15 l/s were carried out at the bottom of the 2000 m deep GPK1 borehole. These tests complemented a first hydraulic experiment achieved during Phase I at a lower flowrate of 3 l/s.

In order to monitor the microseismicity induced by these tests, two boreholes used during phase I (N° 4609 and 4598) were abandonned, and two old oil wells (N° 4601 and 4550) were recovered and deepened in order to penetrate in the granitic basement.

New seismic probes componed of 3-axis accelerometers were designed and deployed at the bottom of three boreholes in cooperation with Camborne School of Mines. Grounting of these probes with zirconium marbles failed. This network was supplemented with hydrophone(s) installed in a new borehole EPS1 sited at about 600 m SSE of GPK1. This borehole, drilled during this phase, reached a depth of 2200 m but only the first 2000 meters were accessible during these experiments.

More than 400 induced seismic events were recorded which of them about 60% were located. Seismicity spread out to form a cloud with a NNW-SSE elongation in general agreement with the stress field deduced from BHTV and *in-situ* measurements, and grew downward to stop NNW of GPK1 bottom at a depth of 2200 m. Combined analysis of P-wave polariy data and stress field showed that the sesimicity could have occured on subvertical joints striking in the direction of the maximum horizontal stress direction.

A permanent and a mobile seismic network were installed at surface by Institut de Physique du Globe de Strasbourg in order to monitor the natural local seismicity of the Soultz region and eventually events associated with the hydraulic tests. No local, nor induced events were recorded by this network; however a natural local event was recorded by the downhole network suggesting that the region is subject to a low magnitude level seismic activity.

Various active seismic surveys were also carried out during this phase in association with Camborne School of Mines : cross-hole surveys between GPK1 and EPS1 before and after hydraulic stimulations, and tube wave VSP survey in GPK1. Comparison of the located induced microseismicity with a previous walkaway survey achieved in 1988 showed that a subvertical structural trend could have act as a barrier to the seismic growth to the NNE of GPK1.

CONTENTS

	INTRODUCTION	**7**
1.	**SEISMIC NETWORKS AND ACTIVE SEISMIC STUDIES**	**9**
1.1.	**Borehole seismic network**	**9**
1.2.	**Downhole seismic probes and surface links**	**12**
1.3.	**Data acquisition**	**13**
1.4.	**Comments on installation of the downhole seismic probes**	**13**
1.5.	**Surface seismic network**	**14**
1.6.	**Other seismic experiments**	**15**
1.7.	**Velocity model**	**17**
2.	**MONITORING OF THE MICROSEISMICITY INDUCED BY THE HYDRAULIC EXPERIMENTS**	**21**
2.1.	**Microseismicity induced during the 7 l/s hydraulic experiment**	**21**
2.1.1.	Hydraulic parameters and seismic locations	21
2.1.2.	Evolution of the induced microseismicity during the 7 l/s experiment	23
2.1.3.	Amplitudes distributions	26
2.2.	**Microseismicity induced during the 15 l/s hydraulic experiment**	**29**
2.2.1.	Hydraulic parameters and seismic locations	29
2.2.2.	Evolution of the induced microseismicity during the 15 l/s experiment	31
2.2.3.	Amplitudes distributions	31
2.3.	**Locations of the overall microseismicity and error estimations.**	**35**
2.4.	**Fault plane solutions**	**35**
2.5.	**Comparison of the 1991 induced seismicity and the 1988 active seismic surveys**	**39**
	CONCLUSIONS	**43**
	REFERENCES	**45**
	LIST OF FIGURES	**47**
	LIST OF TABLES	**49**
	LIST OF ANNEXES	**51**

INTRODUCTION

The HDR site of Soultz/Forêts in Alsace (NE of France) was chosen in 1986 for scientific HDR investigation. The site is on the western side of a very large thermal anomaly which extends over about 3000 km^2 in the Rhine graben valley. This site overlaps the old Pechelbronn oil field where various deep wells drilled in the early 50's are available.

During Phase I of the project (1987-1988), a first borehole (GPK1) was drilled which reached a final depth of 2000 m and various scientific investigations were undertaken during this period. Bottom hole temperature of GPK1 reached 140°C and the top of the granite is sited at 1377 m measured depth. The granite is covered by a sedimentary series. A first hydraulic injection was made at the bottom zone of this borehole with a relatively low flow rate of 3.3 l/s for a period of 50 hours. Induced seismicity recorded was detected by 3-axis geophone probes deployed in three old recovered oil wells at depth ranging from 850 to 1350 m. A small amount of the detected seismicity could be located and this showed a trend to grow towards greater depths than the injection zone.

During the feasability phase of the scientific prototype (Phase IIa) which began in 1990, a new borehole (EPS1) has been drilled to a depth of 2200 m at about 500 m distance from GPK1 and reached a bottom hole temperature of about 150°C. In order to complete the Phase I work and test the behaviour of the granite in response to fluid injections, two new 50h-hydraulic stimulations were undertaken in GPK1 in July 1991 with respective flowrates of 7 l/s and 15 l/s.

To monitor the seismic response of the granite during these experiments, three boreholes have been reopened and redrilled to penetrate into the granite. Three 3-axis accelerometer probes were built and were deployed at the bottom of these deepened holes. The seismic network was completed by a string of hydrophones installed into EPS1. More than 400 induced seismic events were recorded during the Phase IIa injection tests and about 60% of these were located.

The results presented in this report were obtained within the framework of a cooperation between BRGM/IMRG and the Camborne School of Mines Hot Dry Rock Project.

The first part of this report presents the seismic networks used during the hydraulic tests and also refers to active seismic work undertaken during this phase of the project.

Chapter 2 focuses on the two hydraulic experiments and discusses the results of the induced seismicity.

1. SEISMIC NETWORKS AND ACTIVE SEISMIC STUDIES

1.1. SEISMIC BOREHOLE NETWORK

This section presents the borehole network where the seismic probes used for the microseismic monitoring of the hydraulic experiments undertaken during Phase IIa were deployed. However the seismic boreholes used in phase I are first reviewed.

Background:

During the period 1987-1988 (Phase I), three recovered oil wells sited around GPK1 were used, which were as follows:

Borehole N°	Depth (m)	Temp. (°C)	Total dist. from GPK1 bottom (m)
4598	843	104	1201
4609	963	114	1042
4616	1360	124	764

Table 1 - Characteristics of the seismic boreholes used during phase I

A seismic probe was deployed at the bottom of each of these boreholes. These probes which were built in cooperation with CNRS Garchy, were composed of three orthogonally mounted geophones (natural frequency: 20 Hz) and were grouted either by cement (N° 4598) when it was possible, or by zirconium marbles poured from the well head (boreholes 4609 and 4616).

A first 50h long hydraulic test, undertaken in GPK1 between 1968 m and bottom hole, took place in December 1988 at a flow rate of 3.3 l/s. Results of this test are discussed in Beauce *et al*, 1991.

One major difficulty encountered during this pre-feasibility period was that seismic data recorded during the hydraulic experiment were not of sufficient quality to allow reliable locations. This was mainly due to the fact that two of the three seismic sensors were sited in the sedimentary cover which dramaticaly attenuates the seismic signals.

In order to solve this problem, it was decided to deepen the wells to reach at least a depth of about 100 m inside the granite. Unfortunately, this was not possible. Borehole 4609 contained oil and there was no authorization to use it for this new phase. Borehole 4598 had a tool left at the bottom after its original drilling as an oil well in the 1950's.

Under such circumstances, and as nobody from the project have expressed any interest to use them for other eventual purposes, these boreholes, 4609 and 4598 have been cemented and abandoned in June 1991 (Degouy, 1991).

Phase IIa:

For this phase, well 4616 and two new boreholes (4601 and 4550) were reopened and redrilled (Degouy *et al.*, 1992). Figure 1 shows their locations and table 2 presents their characteristics.

Well N°	4616	4550	4601	EPS1	GPK1
Longitude (m)	1004635.95	1004983.9	1003533.55	1004890.75	1004689.05
Latitude (m)	152447.55	152308.84	151165.3	151618.3	152057.34
Depth (m)	1414	1500	1604	2227.2	2000
Elevation (m)	156.51	151.17	169.63	174.93	152.82
Depth of tubing (m)	1385	1416.95	1521.55	1989.96	1420
Temp. (°C)	123	133	127	150	140

Table 2 - Coordinates of the various boreholes used during Phase IIa

Elevations are refered to top of well head and geographic coordinates are in Lambert. Depths are referred to ground level.

Borehole 4616 could not be deepened because metallic junks were found at the bottom. A suspended 4 1/2" tubing was installed in all the boreholes 4616, 4550 and 4601.

Each of these boreholes were equiped for this phase with a three-axis accelerometer tool developed in cooperation with Camborne School of Mines (noted CSM in the foregoing text).

In addition to these seismic observation boreholes, another well (EPS1) was used in order to deploy CSM's hydrophone tools (either one single hydrophone or a string of 2 hydrophones) during hydraulic experiments. EPS1, was initially drilled with a target depth of 3500 m; but, due to various technical problems, its final depth was 2227 m (but only the first 2004 m were accessible during the hydraulic tests performed in July 1991).

As a conclusion, the seismic network for this phase of the project was made of 3 three-axis accelerometers probes plus either one or two hydrophones.

In April 1991, trajectory surveys for all these boreholes were made inside the tubing by the company NEYRFOR, using a gyroscopic tool. The measured trajectories are given in Annex 1.

Final coordinates referred to top of GPK1 well head and after corrections of altitude and deviations of the boreholes are given in table 3:

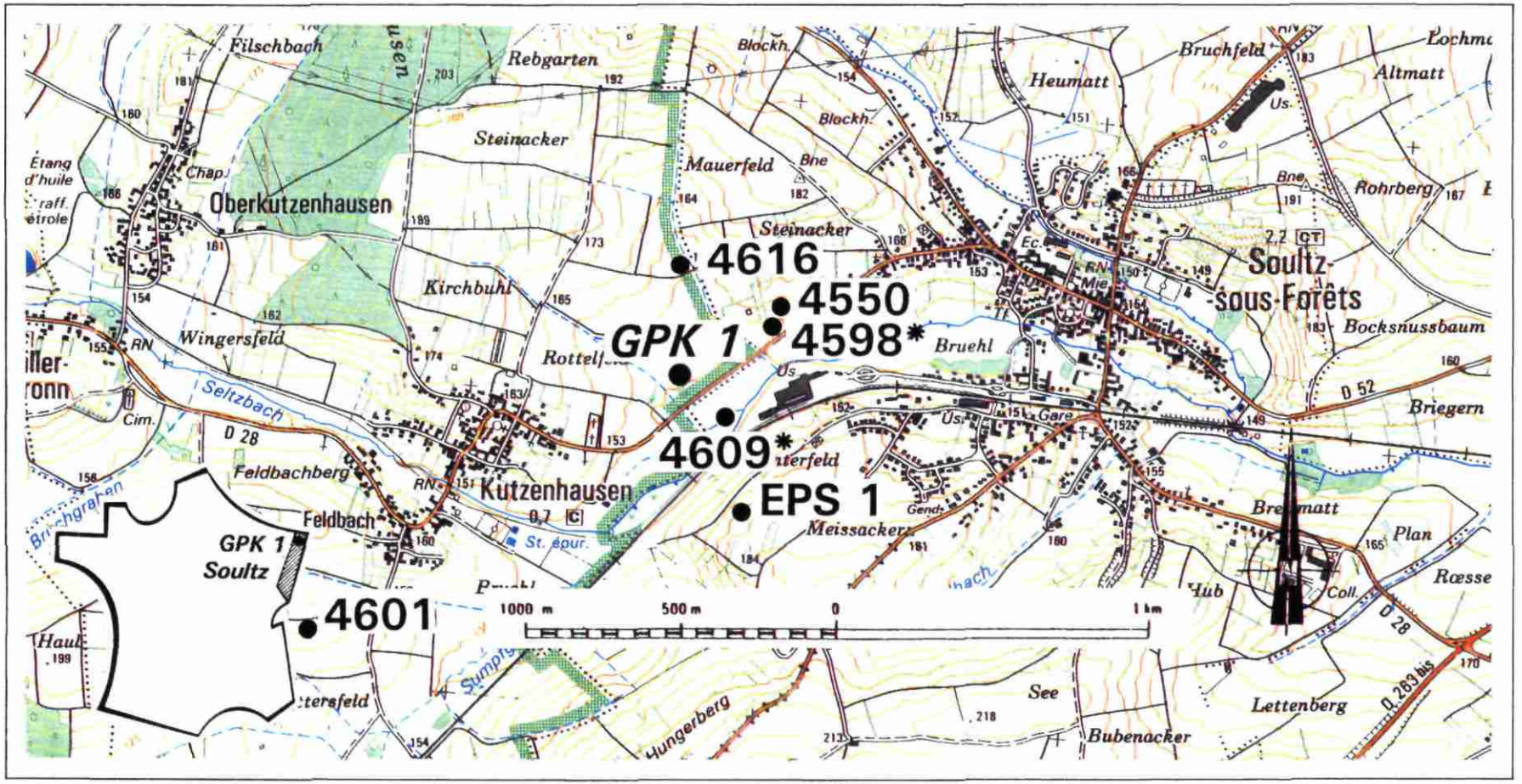

Figure 1 - Situation map of the project and seismic borehole network (✱ : boreholes only used during Phase IIa).

SENSOR N°	X (m)	Y (m)	Z (m)	Depth in granite (m)
4616	-45.03	353.61	-1382.81	7
4550	285.23	205.12	-1492.63	87
4601	-1118.05	-864.35	-1580.76	26
Hydro 1	197.45	-363.95	-1917.24	≈500
Hydro 2	210.45	-353.95	-1974.82	≈500

Table 3 - Coordinates of the seismic probes referred to GPK1 well head

1.2. DOWNHOLE SEISMIC PROBES AND SURFACE LINKS

Five seismic tools were designed to withstand the hard conditions of the Soultz site (temperature above 125°C, salinity of around 100 g/l) in cooperation with CSM. External diameter of these probes are 86 mm and they are 1 m long.

Each probe is composed of three accelerometers disposed at right angles from one another. Sensors used were modified 8318 Bruel & Kjaer accelerometers with basic sensitivity of 0.78 V/g. These accelerometers have a resonance frequency at 6.5 kHz and a flat response up to 1 kHz. A downhole gain of 1000 was used for probes deployed in boreholes 4616 and 4550. A 4000 gain was used only for the probe deployed in borehole 4601, the farthest one from the injection point. Electronic components were tested for high temperatures (up to 200°C) and tool housing were also tested for pressure.

Data from the probes were analog transmitted to the surface by a 7/16" 7 conductors cable (Camesa 7H42RTZ) with tefzel/teflon insulated conductors able to withstand the temperatures encountered in the various boreholes.

The surface data acquisition system was split into two separate parts, the laboratory and the outstations. The laboratory rack housed the system power supply, the power distribution card and the filters for each outstation. The outstation boxes regulated the bulk power supply, sending a regulated +/-15 V supply to the sondes, and converted the signals to differential mode, and then transmiting the differential signals back to the laboratory.

The connexion between outstations and main laboratory was insured by 5 armoured and screened cables pairs, buried in the ground at about 2 m deep. Various types of buried cables were used:

. Connexion to borehole N° 4616, 4550 and 4601 : SYLEC SYT2
. Connexion to borehole EPS1 : ANIXTER A7P520005 LF Type 2

(NB: for the connexion EPS1-Laboratory, an old logging cable used during phase I was also buried as a spare in addition to the Anixter one).

The data allocation was the following: pairs 1, 2 and 3 for respectively vertical, horizontal 1, and horizontal 2 signals. The remaining pairs were used respectively for grounding the system and the power supply.

1.3. DATA ACQUISITION

Analog data was transmitted from well the heads to an online computer (micro-Vax) situated on site. The data were antialias filtered at 1500 Hz using a Butterworth lowpass filter and selected sampling rate was 5000 sps/channel. Events were triggered by a Datalab unit and the time window for data acquisition was 1.6 s. The software (METAL2) provided by CSM allows visualisation of the seismograms, picking of seismic waves onsets during the monitoring and least square based locations of the events.

1.4. COMMENTS ON INSTALLATION OF THE DOWNHOLE SEISMIC PROBES

Probe n° 1 was first deployed in borehole 4616 during the period November 1990 to March 1991 and no failure occurred during this testing period under operational conditions. The probe was then recovered.

The seismic probes were deployed in May 1991 using CSM's winch: probe n° 2 in borehole 4616, n° 3 in borehole 4550, n° 4 in borehole 4601.

Various calibration shots were fired from the surface (1 kg of dynamite near each well head) in order to test the functioning of the probes.

One week after the deployment of the probes, it was decided to attempt the grouting of the probes by means of 125 kg of zirconium marbles (∅ = 425 to 1180 microns) poured onto the probe from each wellhead. After this operation, various difficulties were encountered, the major ones being as follows:

Borehole 4550:

The day after the grouting operation, the probe sited in borehole 4550 failed. During the pull-out operation, the probe got stuck at 1407 m. This depth is very near the casing shoe. After various further unsuccessful attempts to pull out the probe from the surface, it was decided to use a workover rig to clean the borehole (Degouy, 1991). The logging cable broke at the cable head weak point of the tool (so no cable was left in the borehole) and tool n° 3 was left at the bottom. During this operation the cable was also damaged at a distance of 110 m from the surface wellhead and a torpedo was made to replace this damaged section. A new tool (n° 5) was then deployed on June 25th.

The technique of grouting the seismic sondes using zirconium marbles was used successfully during Phase I in boreholes 4616 and 4609 and no difficulties were encountered. The reason why the probes got stuck in Phase II was probably due to a combination of factors. The main differences between the two phases were the diameters of the tubings used during phase II which were less than in Phase I, and the possible presence of grease or oil inside the tubing. The smaller diameter tubing means that as the tool re-enters the tubing from the openhole section the clearence between the tool and the tubing is greatly reduced. These factors mean it is much more likely that the zirconium marbles could form a bridge within the tubing which would block the passage of the tool.

Borehole 4616:

In this well, the zirconium marbles made a bridge, near the surface, at the interface between the water-oil and the air inside the well. This bridge was destroyed by the use of a compressed air

machine, and the marbles were ejected out of the borehole (at least one half of the total quantity poured inside the borehole was recovered and controlled at the surface).

On 26th of June, the probe deployed into this borehole showed problems on the power line which led to the obligation to pull it out and change it for the revised probe n° 1. After the deployment of this new tool, the measured depth made with the same depth counter as was used previously, was less than that observed previously (1387 m instead of the 1409 m encountered before): so, apparently the seismic probe was deployed only 7 m inside the granite.

In these conditions, and as no spare system was quickly available on site and no time was left to undertake a further cementation procedure before the hydraulic experiment began, it was decided not to cement the probes.

The general point must be stressed that the problems of grouting the seismic sondes in the seismic observation boreholes is intimately related to the well completions for the seismic observation boreholes. The seismic network consists of only a bare minimum of sensors and as this is the case every effort should be made to maximise the information which can be recovered from each well/sensor. This requires the secure grouting of the seismic sondes.

1.5. SURFACE SEISMIC NETWORK

In order to complement the information produced by the downhole seismic network, various seismic sensors have been deployed on the surface. Two types of surface network have been installed by the Institut de Physique du Globe de Strasbourg (IPGS) (Hoang Trong Pho *et al.*, 1991).

- **Permanent network:** The purpose of this network was to monitor the natural local seismicity around the Soultz site and to complete the existing regional network of IPGS. Three sites were instrumented around GPK1 at distances ranging from 4 to 7 km (see figure 2). This network was operational in May 1991.

Each site is composed of one 3-axis accelerometer unit plus a vertical seismograph and the data are transmitted to the Soultz site and to Strasbourg. Data are then sampled at 150 sps/channel and collected on a PC which allows the triggering of the events. Coordinates of this network are given in the following table:

Station name	Latitude	Longitude	Elevation (m)
HOFFEN	N 48°56'30"	E 7°56'50"	150
SURBOURG	N 48°54'53"	E 7°51'08"	200
LANGENBERG	N 48°58'50"	E 7°48'19"	500

Table 4 - Coordinates of the surface permanent IPGS network

- **Mobile network:** This temporary seismic network was installed in July 1991 in order to monitor the hydraulic injection experiments. It was composed of 8 mobile seismographic stations deployed in circle at a radius of 1 km around the GPK1 borehole. At each station, a 1 Hz vertical sensor was

installed and the data was transmitted to the site to be recorded on magnetic tape and continuously plotted on paper.

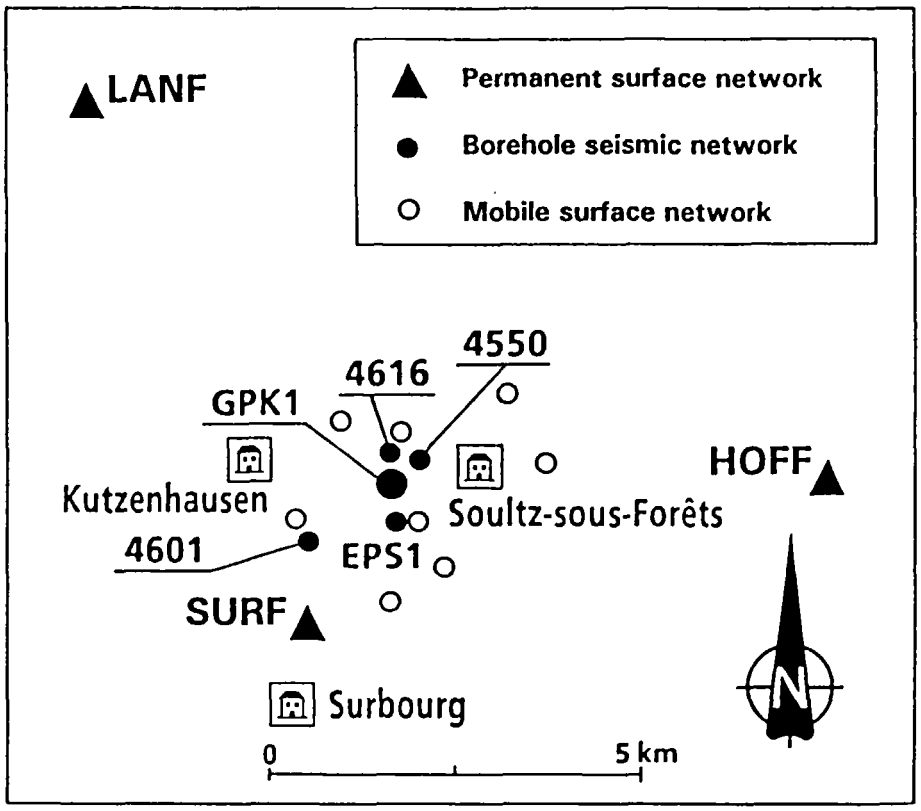

Figure 2 - Situation map of the permanent and mobile surface seismic network

During the whole hydraulic experiment no seismic events were recorded, either induced events or natural local events. However, it must be noted that one local seismic event was recorded by the downhole seismic network (on 15/07/1991 at 3:30 local time), which did not trigger the surface network. The plot of this event is presented in figure 3, which shows clear P and S arrivals on the probe sited in borehole 4550. Rough analysis of this event shows that it occurred at a location of about 10 km NNE from the site.

1.6. OTHER SEISMIC EXPERIMENTS

In addition to the microseismic monitoring survey undertaken at Soultz site during this phase of the project, active seismic surveys were undertaken by Camborne School of Mines Hot Dry Rock Project in collaboration with BRGM/IMRG. They will be briefly listed and summarized with reference to the corresponding extended reports. The surveys were as follows:

- **Cross-hole surveys:** Two surveys between the boreholes EPS1 and GPK1 were carried out; the first one before the hydraulic experiments and the latter one after them. The objective of these surveys was to image the circulation of the injected water inside the granite and to compare the results with the induced seismicity related to the hydraulic injections.

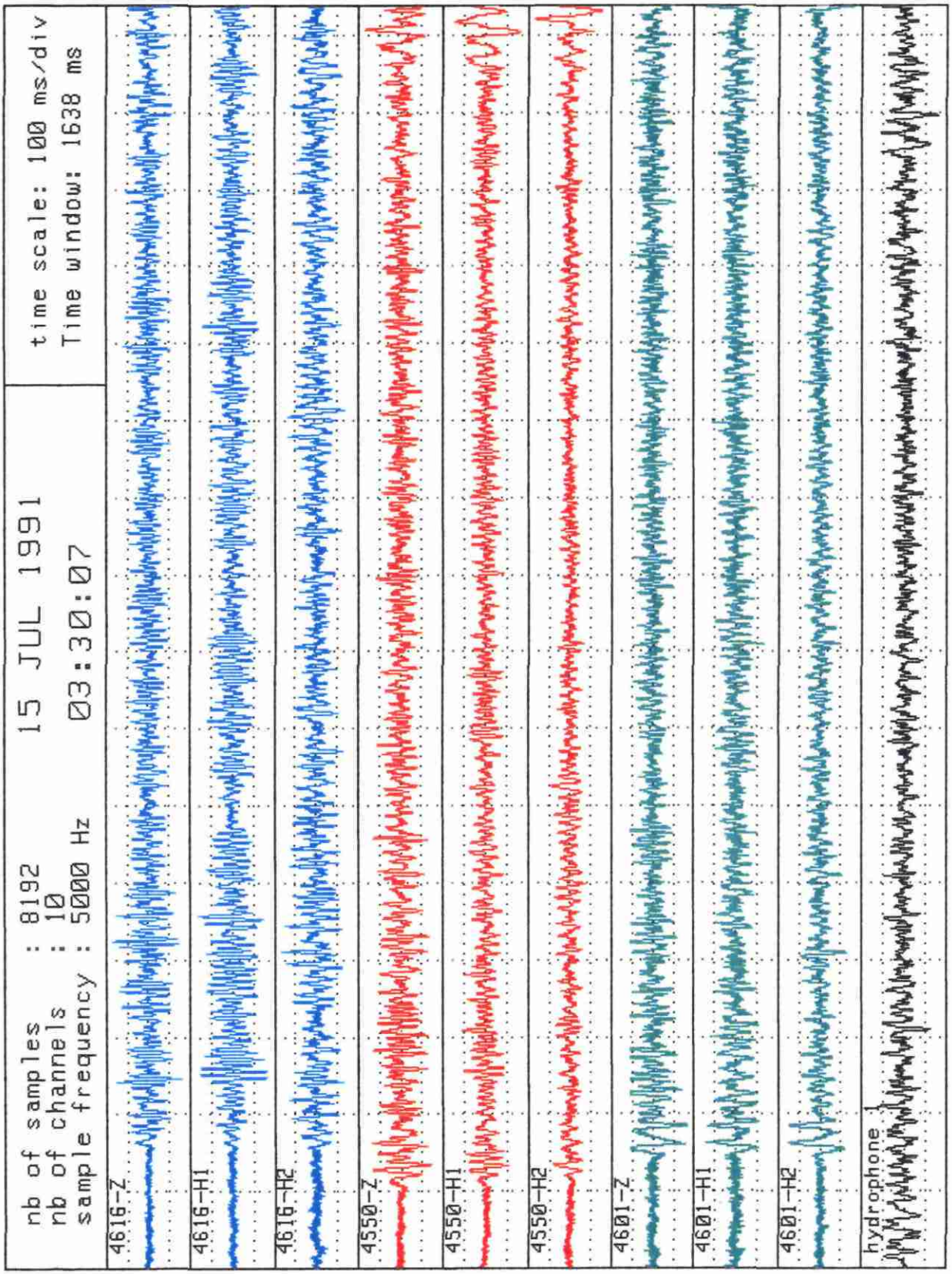

Figure 3 - Sismograms of a natural local event recorded on the downhole seismic network during the hydraulic stimulations. (Normalized amplitudes).

Field operation reports are presented in Stewart et al, 1991. For the pre-stimulation survey, the CSM sparker tool (input energy of 1000 Joules) was deployed in GPK1 from 1782 to 1992 m and the hydrophone string was deployed in EPS1 from 1825 m to 1945 m. The post-stimulation survey covered a more extensive depth range, i.e. from 1722 to 1812 m for the source in GPK1 and from 1675 to 1945 m for the receiver. Spacing for both surveys was 30 m.

Results of these surveys are discussed in Stewart *et al.*, 1992. From a technical point of view, sparker and hydrophones operated well during both surveys. Clear signals were recorded for propagation distances through the granite of about 400 m without stacking. For higher distances up to 550 m, a 24 fold stack was necessary to allow reliable interpretation of the P-wave onsets.

Velocity tomograms were produced for each survey as well as a difference tomogram, which reveals the differences between the two surveys. Although a low-velocity feature located at about 1800 m in GPK1, which corresponds to the main productive zone in this borehole, has been pointed out, no particular trends in relation with the injected water propagation inside the granitic rock mass were revealed: we must also note, see section 2.2.1 of this report, that most of the seismicity occurred far below the zone illuminated by the seismic rays.

- **Tube wave VSP surveys in GPK1:** The aim of these surveys undertaken by CSM HDR Project staff, was to characterize the main joints (location, orientation and intrinsic permeability) intersecting borehole GPK1. Field operations are presented in Stewart *et al.*, 1991, and interpretation of the data in Jones, 1991. Three source positions were used near the wellheads of boreholes 4616, 4550 and 4601. 125 g explosive shots were fired in ponds sited at the surface; the receiver used was the CSM's hydrophone deployed in GPK1 at depths ranging from 1400 m to 1995 m MD with a 5 m spacing.

Major structural features were found at depths of 1680 m, 1820 m and 1960 m, all of them with fairly shallow dipping angles of about 14° to 20° from horizontal. Azimuths of these features are more widely dispersed from N212° to N337°.

1.7. VELOCITY MODEL

In order to obtain a velocity field around GPK1, and thus to allow reliable locations of the microseismic events induced by the hydraulic injections, a calibration shot of 300 g of HMX explosives was fired by Schlumberger at a depth of 1992 m in GPK1. For this purpose, the three 3-axis probes and the hydrophone string were respectively deployed in the boreholes 4616, 4550, 4601 and in the borehole EPS1.

Clear P-wave onsets were produced on all the sensors of the network (figure 4); only one S-wave arrival was observed on probe 4616. The P-wave calculated velocities are given in table 5.

PROBE	P-wave velocity (km/s)
4616	5.715
4550	5.745
4601	5.465
Hydrophone (top)	5.940
Hydrophone (bot)	5.930

Table 5 - P-wave velocities deduced from the calibration shot fired in GPK1

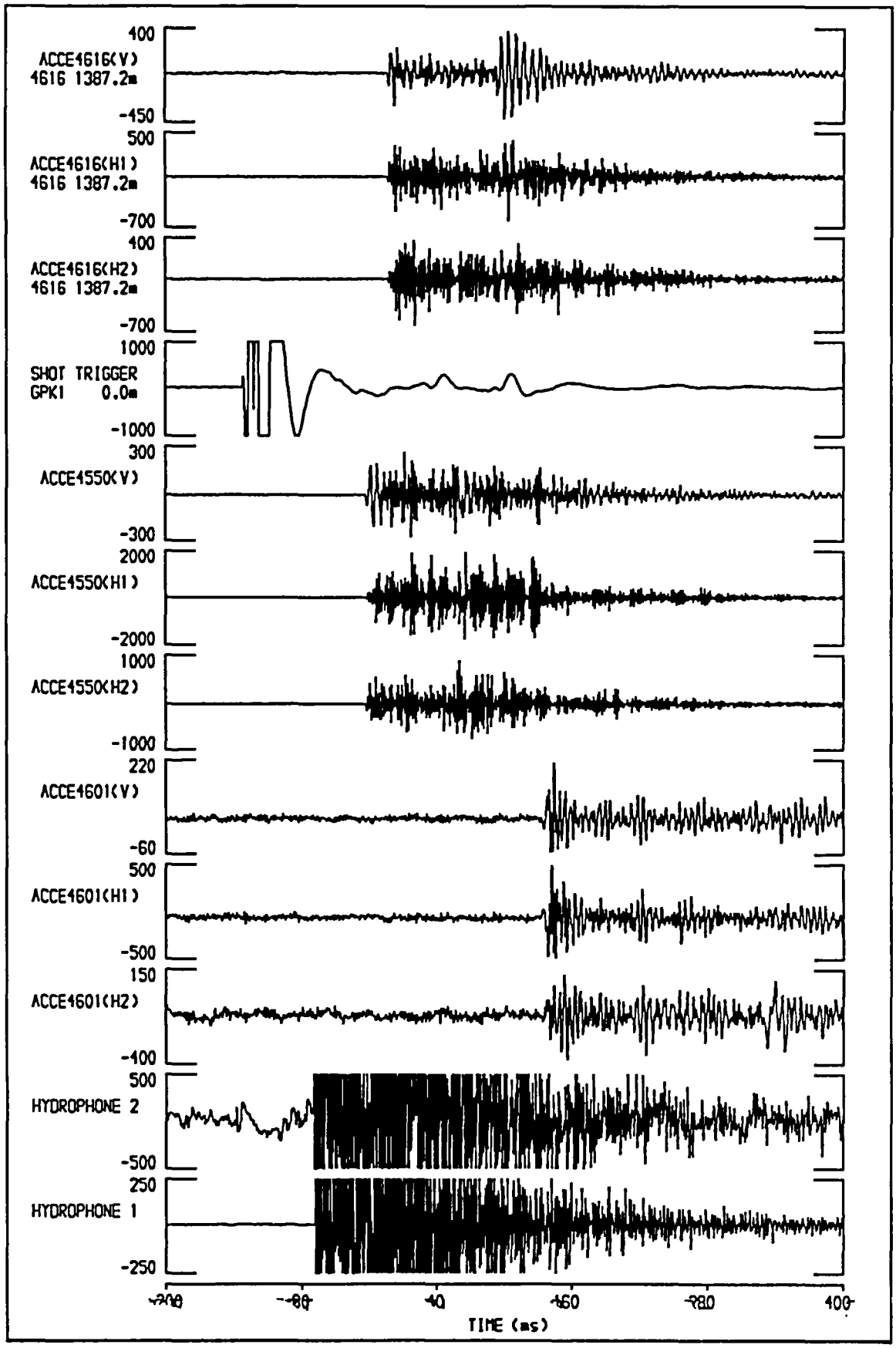

Figure 4 - Sismograms of the calibration shot fired in GPK1 at 1992 m depth.

The velocities between pairs GPK1-4616 and GPK1-4550 are very similar. During Phase I, two 200g explosive shots were also fired at the bottom of GPK1 and the deduced medium velocity was 5.680 km/s between GPK1 and 4616 (and we have to bear in mind that probe 4616 during this first phase was sited just above the granite-buntsandstein interface).

Compared to these values, the measured velocities between EPS1 and GPK1 appear to be too high. However, borehole EPS1 is highly deviated and errors in its survey could produce significant variations in the calculated velocities. As an example, an error of about 30 m in the horizontal coordinates of the bottom of EPS1 would change the calculated P-wave velocity between GPK1 and EPS1 by 0.3 km/s.

The velocity distribution measured during the cross-hole survey between GPK1 and EPS1 gave results with similar values (Stewart *et al.*, 1991): for propagation distances ranging from 350 m to 400 m (i.e. same order of distances as for the calibration shot), the calculated velocities were 5.95 km/s. For higher distances, the velocity distribution seems to be aligned on a linear fit (V = 5.85 km/s), but P-wave onsets were also more emergent and therefore difficult to pick.

More problematic is the low velocity measured between GPK1 and 4601. In this case the raypath is long (about 1470 m) and it is unlikely that this could be due to well survey errors (it will require a 100 m error to account for the observed velocity differences). The seismic reflexion profiles undertaken in 1984 in this region have pointed out a very complex tectonic structure with faults affecting the sedimentary cover of the Soultz site and also the granite mass. The schema presented on figure 5 shows on a NE-SW vertical section the relative positions of the boreholes 4601 and GPK1 in its structural context. The bottom of the borehole 4601 is clearly sited very near to the Kutzenhausen fault and moreover the Soultz fault is also located between the two boreholes. These facts may help to explain the anomalous velocity measured between GPK1 and EPS1. As we do not have any quantitative information which could lead to a reliable explanation, we are not really able to draw any more definite conclusions at this time about the nature of the velocity anomaly.

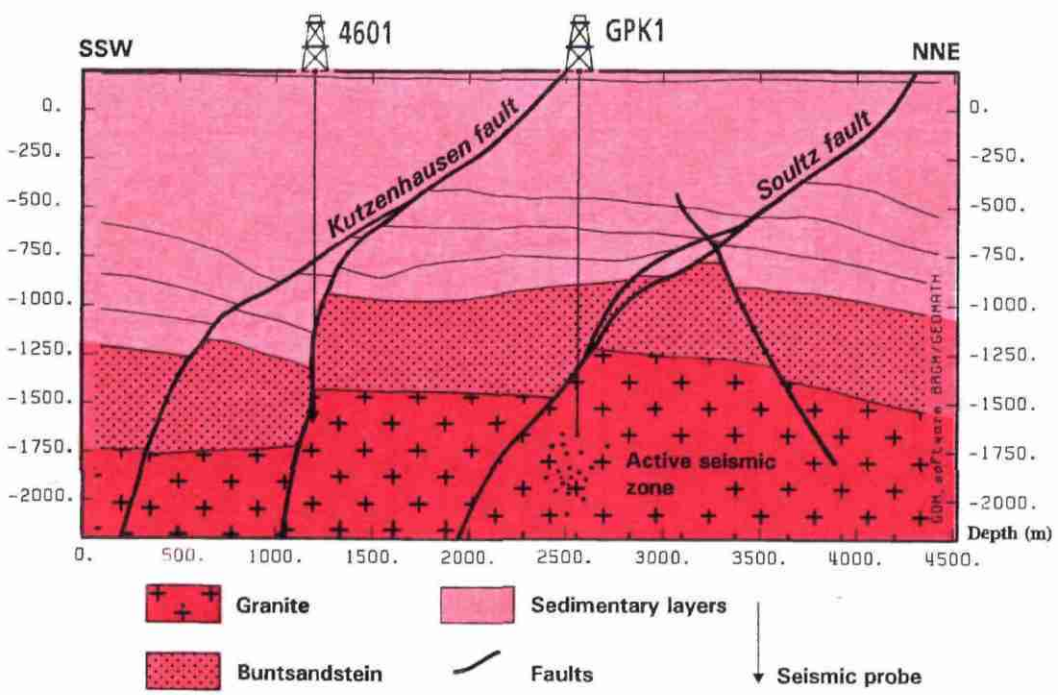

Figure 5 - Geological SSW-NNE cross-section between GPK1 and borehole 4601

In such conditions, and in order to not perturbate the locations of the induced seismicity and to preserve a relative homogeneity in the results, it has been decided not to use the timings picked on this probe for the locations.

The final velocity model adopted for locations is an isotropic model with an average P-wave velocity of 5.85 km/s and an S-wave velocity of 3.35 km/s. Station delays have been introduced in the location processing which are as follows:

Sensor n°	P delays (in ms)
4616	3.
4550	3.
(4601)	(18.)
hyd (top)	0.
hyd (bot)	0.

Vp = 5.85 km/s
Vs = 3.35 km/s

Table 6 - P-wave station delays corrections

No S-wave delays have been considered as S-wave were difficult to measure from the calibration shot and so the velocity is only known approximately.

2. MONITORING OF THE MICROSEISMICITY INDUCED BY THE HYDRAULIC EXPERIMENTS

The purpose of Phase I (1988) was to investigate the hydromechanical properties of the crystalline basement near the bottom of the borehole GPK1. The main test was a 3.3 l/s injection of 520 m^3 of water for 50 h in a vertical fracture created between 1968 and 1991 m depth (Jung, 1991). Two important results were obtained for the 1988 programme:

- stress conditions in the Rhine Graben are very favourable for hydraulic fracturing at depths of about 2 km, due to a very low minor horizontal stress, and consequently the direction of the stimulation grows in the direction perpendicular to it;

- the hydraulic behaviour of GPK1 was consistent with a borehole being connected to a major fault or fractured zone in the vicinity of the borehole; the interpretation of the tests show it was of apparently infinite transmissibility and extent i.e. a constant head boundary condition.

During Phase IIa (1991), it was decided to investigate in more details and to a greater extent the rock around the bottom of GPK1. Two hydraulic fracturing/injection experiments were performed, already termed the 7 l/s and 15 l/s experiments respectively.

Table 7 gives a list of the seismic data files used during these two experiments:

Experiment	Data File	Comments
7 l/s test	STZSTI01	1 hydrophone in EPS1
7 l/s test (packer reseated)	STZSTI02	1 hydrophone in EPS1
15 l/s test	STZSTI03	2 hydrophones in EPS1
no injection/low flow test	STZSTI04 STZSTI05	1 hydrophone in EPS1

Table 7 - Seismic data file names

A list of all the events recorded during these injections tests is given in Annex 2, complemented wihen their locations were appropriate.

2.1. MICROSEISMICITY INDUCED DURING THE 7 L/S HYDRAULIC EXPERIMENT

2.1.1. Hydraulic parameters and seismic locations

The 7 l/s hydraulic stimulation started on July 11th at 15h, over a 26 m-long vertical section of GPK1, between a packer sited at 1965 m and the bottom hole. After six and a half hours, and an

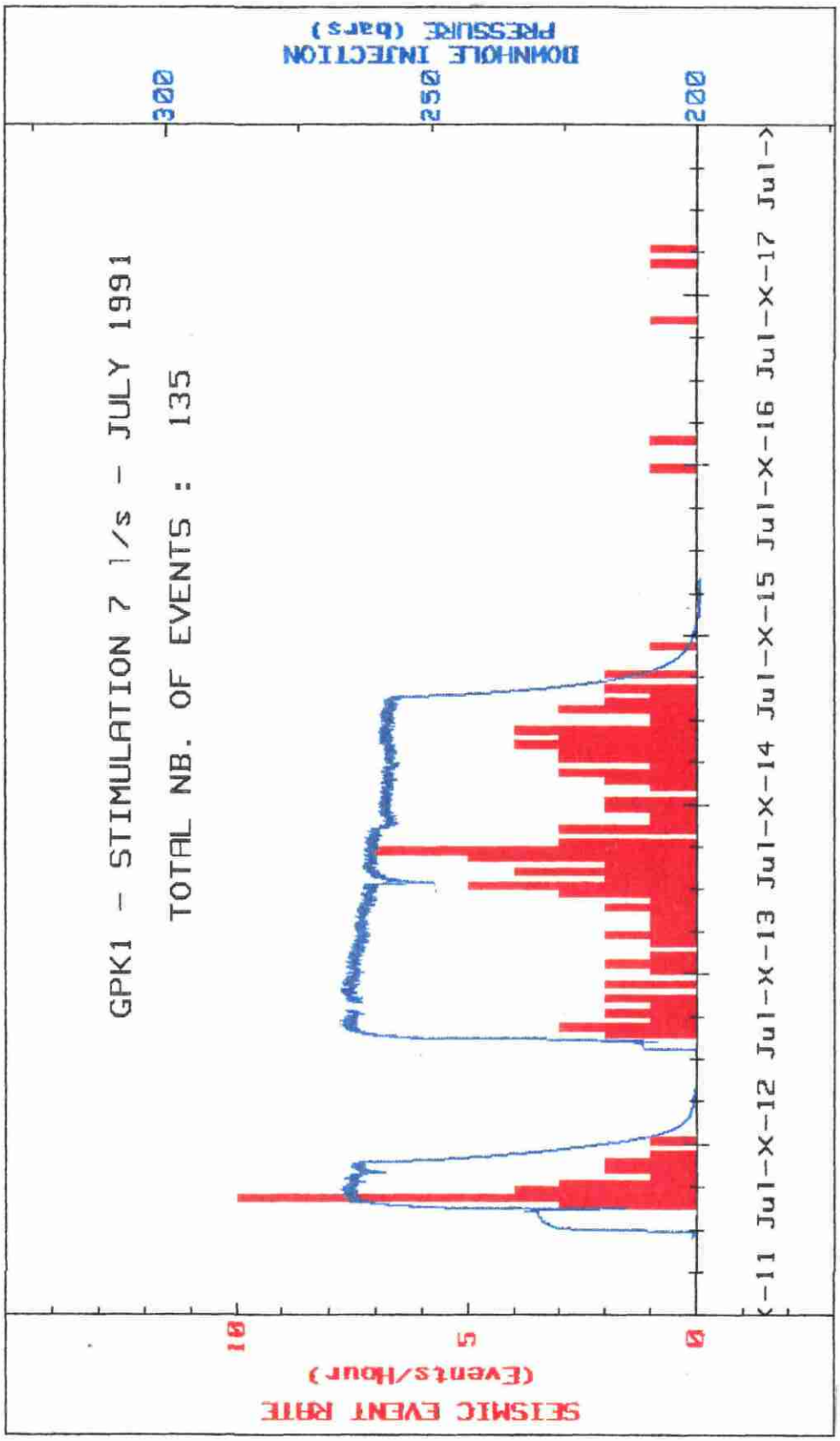

Figure 6 - Seismic event rate and downhole pressure recorded during the 7 l/s hydraulic test.

injected volume of about 160 m^3, the experiment was stopped as the pressure in the annulus began to increase. The injection re-started at 13:15 on 12th and carried on for the next 50 hours.

Figure 6 shows a plot of the seismic event rate and down-hole pressure recorded during this period. A total of 135 microseismic events were induced during this test and seismic rate decreased immediatly that the injection stopped.

As for Phase I, the largest seismic event rate corresponds to the beginning of the injection. Afterwards, as the downhole pressure decreased, the event rate also decreased.

Following Jung (1992), this indicates the presence of shearing on joints throughout the test. The general movement of the seismic front away from the well is consistent with the outward movement of a pressure front throughout the test.

Among all the seismicity recorded during this test, 60% of the events have been interpreted and located, the isotropic velocity model presented in § 1.7 being used for the locations. During this test, only one hydrophone was deployed in the borehole EPS1. As the timings from probe 4601 were not used for the locations, we have a network consisting of only three sensors, such a network must be coplanar. So location results gave dual solutions which form a mirror image relected in the plane defined by the three sensors. For typical surface installed networks this is not a problem as one solution is in the air, however for an underground network both solutions are within the rock. The decision to choose the deeper of the pair of solutions was based on the results obtained when there were more sensors and a non-coplanar network, i.e. when two hydrophones were deployed as in the 15 l/s injection (STZSTI03).

The recorded events show clear P and S wave onsets on the different probes of the network (see figure 7). It must be noted that the probe deployed in the borehole 4601 recorded only about 20% of the whole recorded seismic activity. Various examples of events and corresponding spectra are presented in Annex 3.

The significance of the location of seismicity versus time will be discussed in detail in section 2.1.2. Figures 8 to 10 present the hypocenter locations in plan view and in two vertical sections: N60°E and N150°E respectively.

These directions are chosen as they are approximately parallel to the maximum and minimum horizontal stress direction (respectively N140-160° and N50-70°) as determined by Rummel *et al.*, 1989.

2.1.2. Evolution of the induced microseismicity during the 7 l/s experiment

The evolution of the seismicity as a function of time during this test is presented in Annex 4, in successive 4h-duration time windows.

The microseismicity starts southward of GPK1 between 1950 m and 2100 m depth, along a SE dipping zone intersecting the GPK1 axis 60 m beneath its bottom. This trend extends until the injection stops, due to an abnormal pressure increase in the annulus. As the injection restarts the seismicity migrates slowly away from GPK1 but always in a southeasterly direction and in the same depth range. Some events are located a considerable distance from GPK1, but it should be borne in mind that during the first experiment the use of only one hydrophone increases the uncertainty in hypocenter determination. From 13th of July at 2h, events begin to migrate northwest of GPK1,

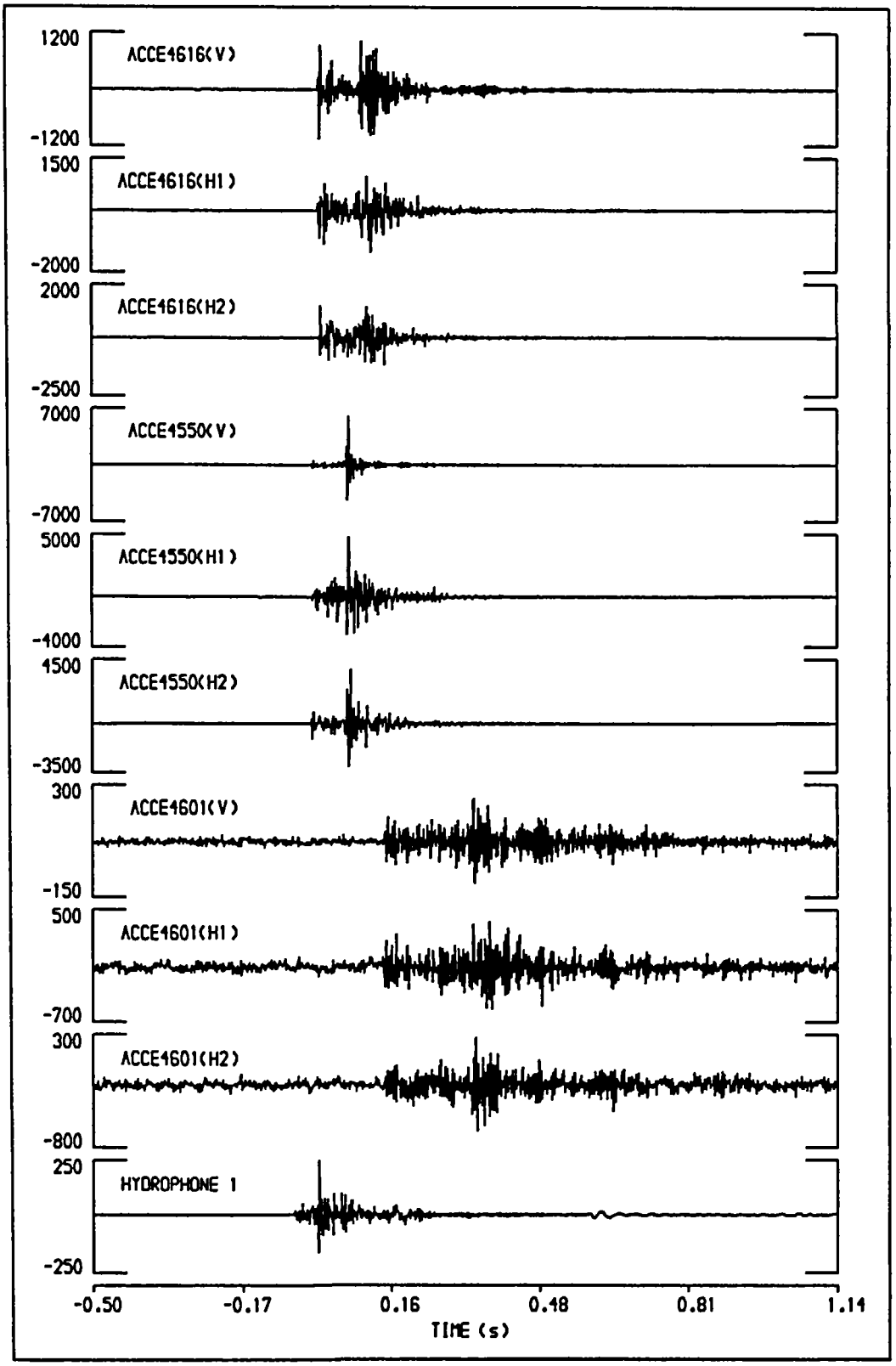

Figure 7 - Example of an induced event recorded during the 7 l/s hydraulic test. (STZSTI01 - Event 26 - 11/07/1991 - 17:27:54).

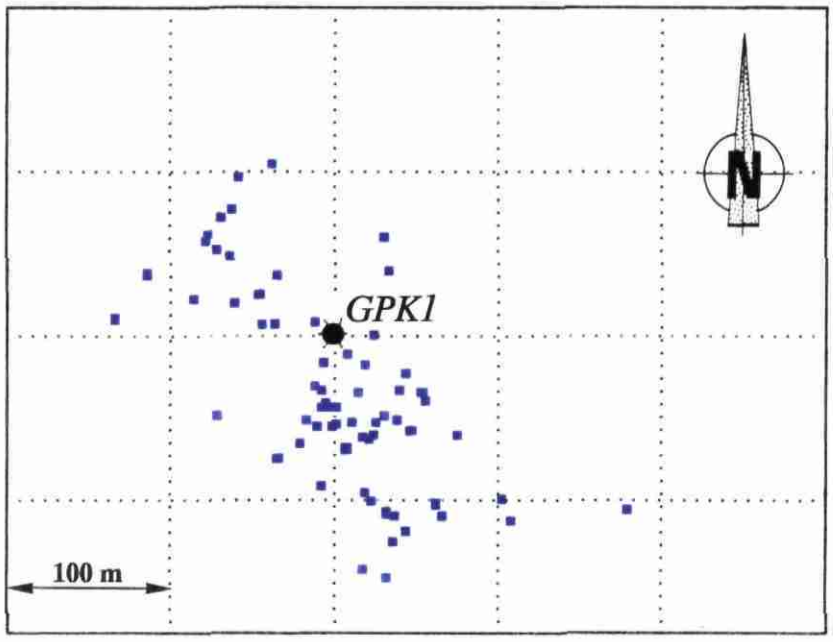

Figure 8 - Locations of the microseismic events induced during the 7 l/s hydraulic test. Map view.

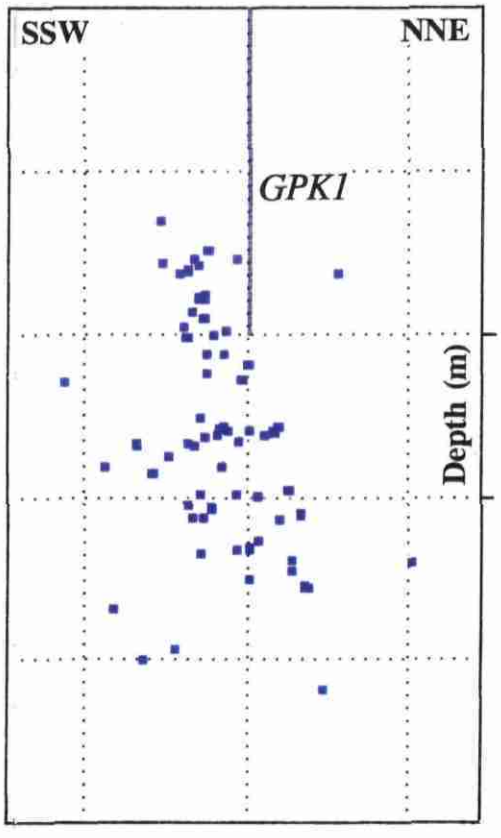

Figure 9 - Vertical N60° cross-section.

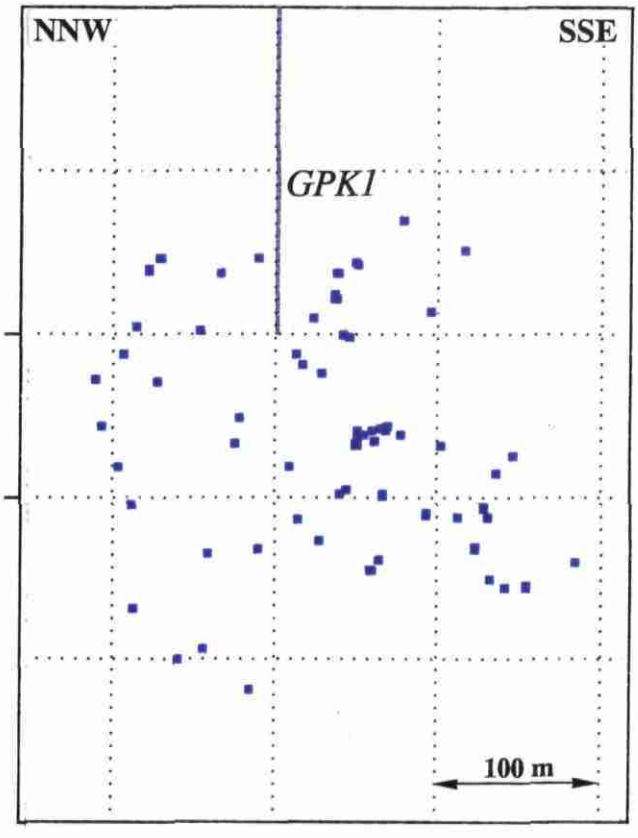

Figure 10 - Vertical N150° cross-section.

initially above the bottom, afterwards deepening progressively. For the final 4h period the end of the experiment, only one event is located above the bottom of GPK1, the depths of the others range from 2000 to 2200 m.

During the hydraulic fracturation experiment undertaken in 1988 at a flow rate of 3.3 l/s in the same conditions as during this phase, 58 events were recorded of which only 12 were located. Though the precision of the locations is higher in phase IIa, we observe that seismicity of phase I is located roughly in the same zone (figure 11) as the seismicity recorded at the beginning of the 7 l/s, and, as is shown below, at the beginning of the 15 l/s experiment. That is to say: close to GPK1 bottom, along a NW-SE trend and between 1950 and 2100 m. So the fracture network stimulated at the beginning of each experiment is the same.

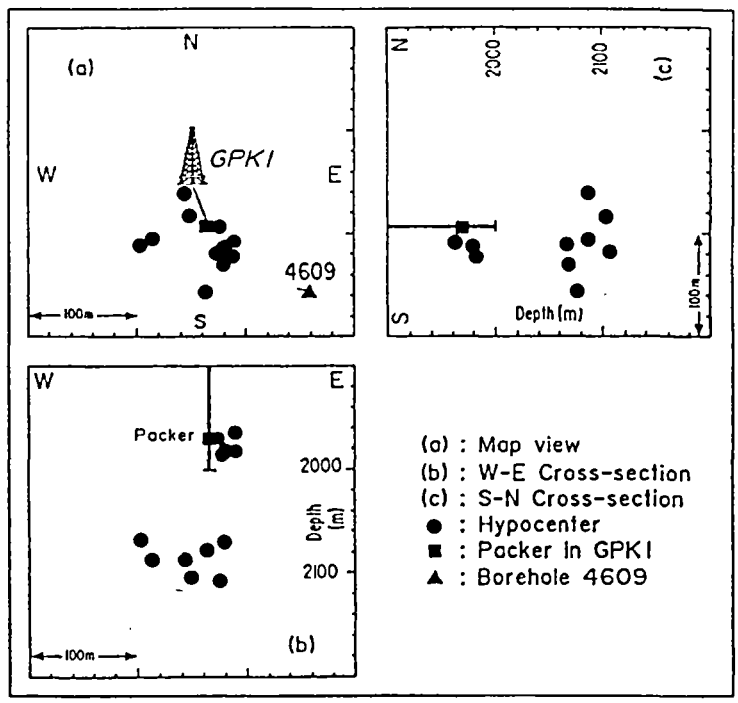

Figure 11 : Locations of seismic events induced during the 3 l/s hydraulic test undertaken in 1988.

2.1.3. Amplitudes distributions

As the seismic probe could not be cemented they were prone to resonances. This means that the amplitudes recorded do not accurately reflected the amplitudes of the seismic waves in the rock. Thus we only have considered the relative amplitudes measured on the hydrophone deployed at the bottom of EPS1. In figures 12 to 14 or each located event, the diameter of the circle centered on the hypocenter is proportional to the amplitude peak to peak of the S-wave measured on the hydrophone 1.

On figure 12, epicenters are roughly distributed along a NW-SE direction and the striking feature is the concentration of events on a dipping axis towards the E on the N60 vertical section (Figure 13). On the contrary, the projection of hypocenters on a N150 vertical section, perpendicular to the former (Figure 14), shows a scattered distribution which is consistent with the concentration of events on a NW-SE trend.

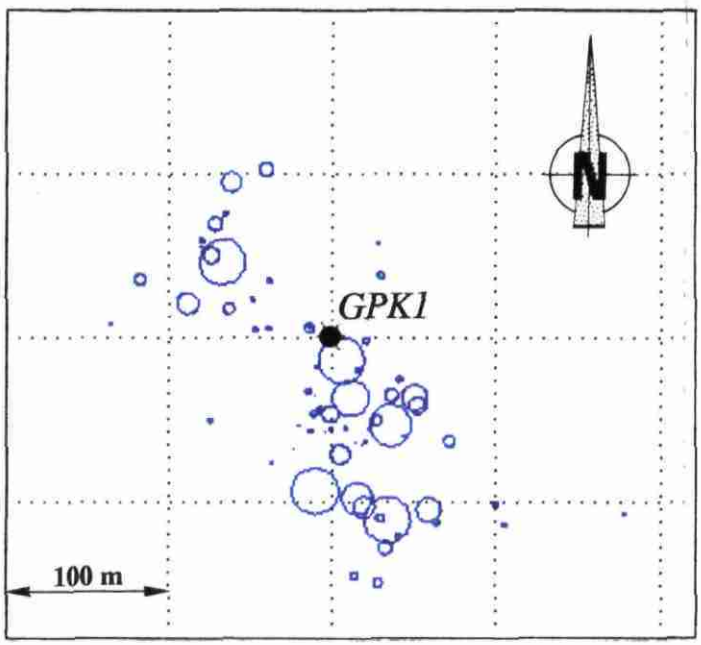

Figure 12 - Maximum amplitudes distributions of the microseismic events induced during the 7 l/s hydraulic test and recorded on the hydrophone deployed at the bottom of EPS1. Map view.

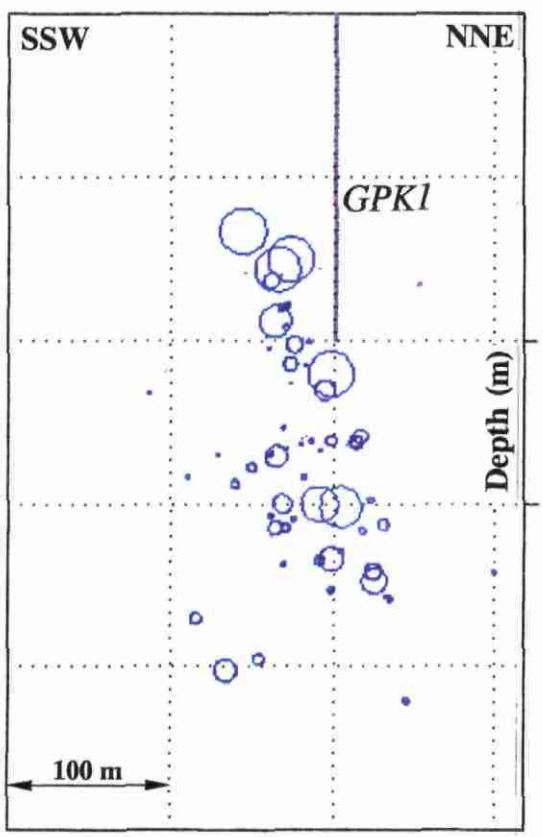

Figure 13 - Vertical N60° cross-section.

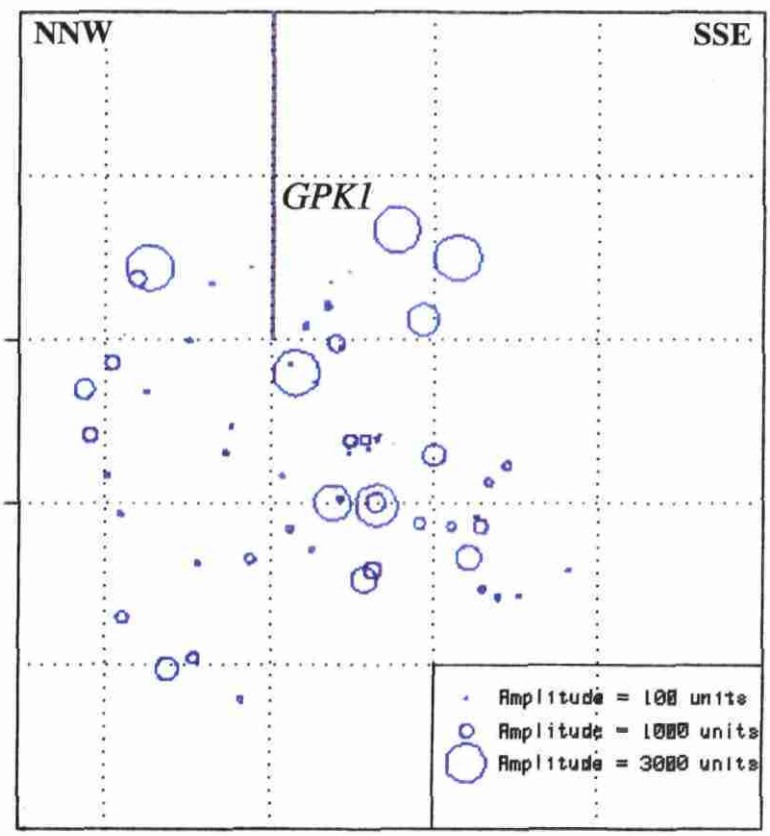

Figure 14 - Vertical N150° cross-section.

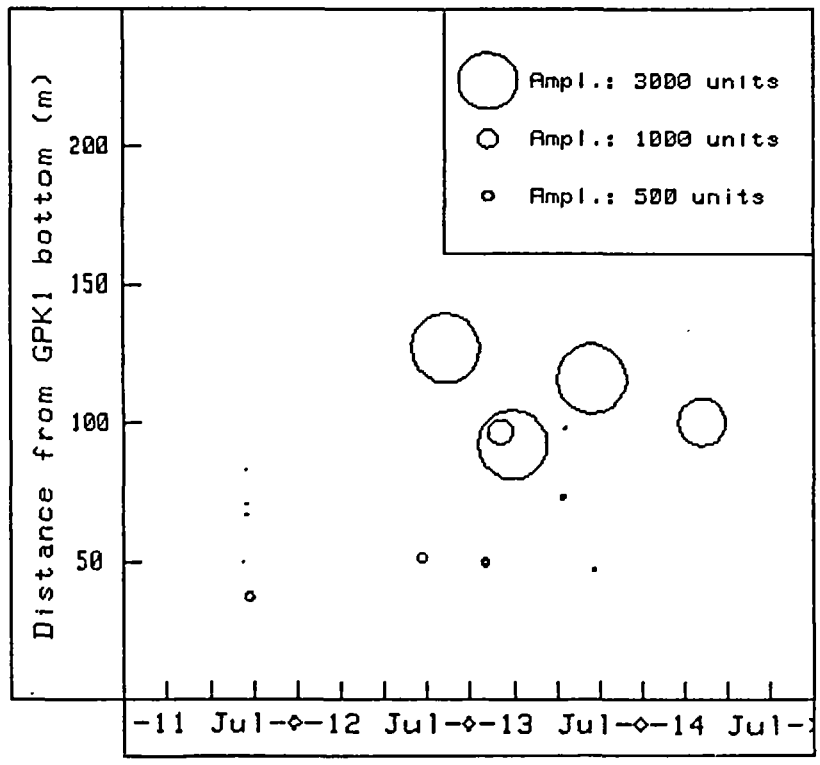

Figure 15 - Distances from GPK1 bottom and maximum amplitudes distributions versus time for events located above 2000 m. (Hydraulic test: 7 l/s).

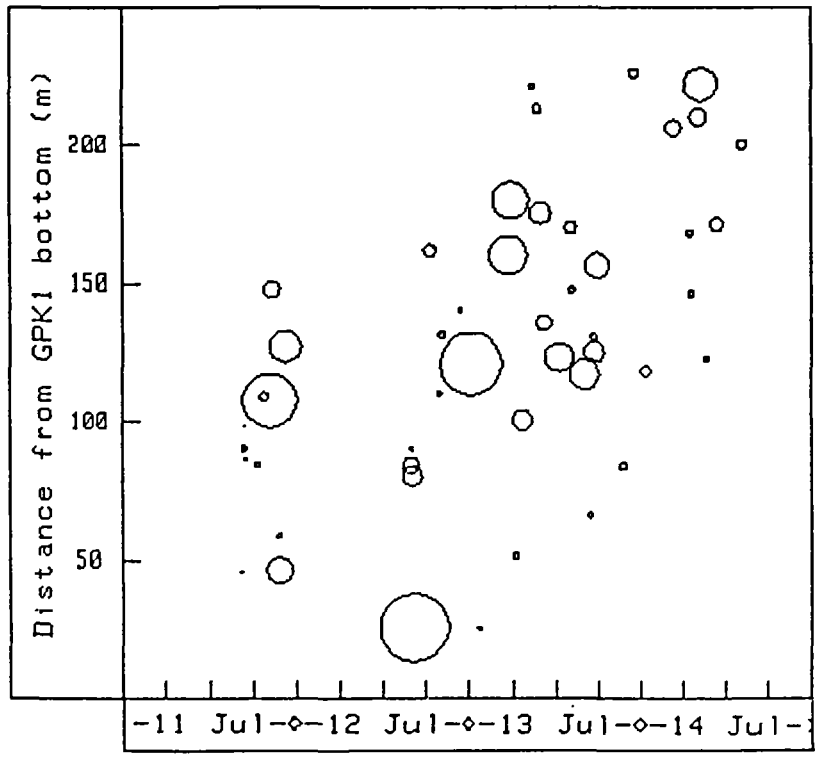

Figure 16 - Distances from GPK1 bottom and maximum amplitudes distributions versus time for events located below 2000 m. (Hydraulic test: 7 l/s).

Proportionally, there are more events of higher amplitude above 2000 m depth than below (see in particular figure 14). In the same way, for the events located beneath 2000 m depth, the high amplitude events are surrounded by many low amplitude events.

This can be synthesized on a diagram of the event amplitude versus time and distance to GPK1 borehole bottom. The events are split up in two parts: events with depths above 2000 m (Figure 15) and with depths below 2000 m (Figure 16).

Comparing both figures, we observe how most of the induced seismicity migrates with time downward and away from GPK1 bottom and how events of higher amplitude can occur behind the progression of the low amplitude seismicity front. This particular fact has already been observed in laboratory study of fluid pressure diffusion on rock samples (Kranz *et al.*, 1990). As was stated before, the number of events located above 2000 m is much less than below but with proportionally higher amplitudes.

2.2. MICROSEISMICITY INDUCED DURING THE 15 L/S HYDRAULIC EXPERIMENT

2.2.1. Hydraulic parameters and seismic locations

The 15 l/s injection in GPK1 started on 18th of July at 9 a.m. and lasted about 50 hours in similar conditions to the previous experiment. A total volume of 2700 m^3 of fresh water was injected. Figure 17 shows the downhole injection pressure recorded during this test and the associated seismic event rate. The first event occurred after an injected volume of 35 m^3 and a total of 239 induced events were recorded. In comparison with the previous test, the average seismic rate (4 events/hour) was double.

It must be also pointed out that two peaks of seismicity (more than 10 events/hour) were observed, as important as the first peak appearing just after the beginning of the injection. The second peak corresponds to the start of seismicity concentration northwest of GPK1 at about 2200 m depth as we shall see later. A third peak of just under ten events per hour is related to the same zone as the second peak.

A gap in seismic activity can be observed from July 18th at 18h to July 19th at 2h, in coincidence with an increase of downhole pressure. This overpressure is however an artefact due to an increase of the flowrate created by an adjustment of the rotation of the injection pump. The other anomaly which occurred later on (July 19th at 8h) is also meaningless in term of an eventual physical response of the granite: it was only due to the switching of the injection pumps (Jung, personal communication). Nevertheless, it should be noted that a gap of the seismic event rate occur just before the start of the deepening of the induced seismicity.

Moreover the seismicity still persisted at a rate of 2 events/hour during the 12h following the end of the stimulation, suggesting the existence of a remanent pressurized zone sited away from the borehole injection interval.

During this stimulation, the 2-hydrophones string was deployed in EPS1 and timings from 4601 were not used. The hydrophones were removed from EPS1 and replaced by the single unit on 20 of July at 4 p.m., after the end of the 15 l/s injection test.

Figures 18 to 20 presents the overall located seismicity during this test.

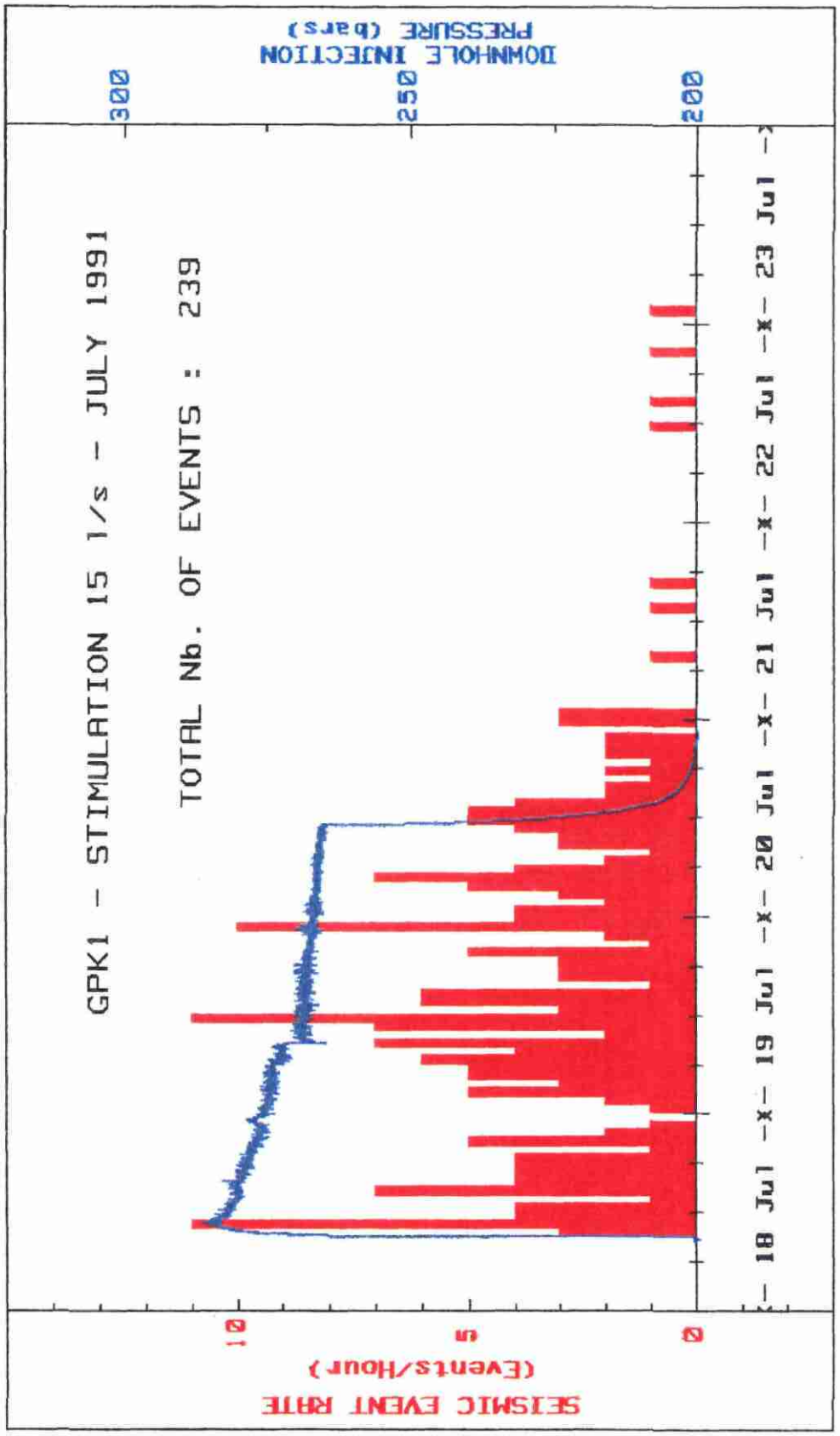

Figure 17 - Seismic event rate and downhole pressure recorded during the 15 l/s hydraulic test.

2.2.2. Evolution of the induced microseismicity during the 15 l/s experiment

As for the 7 l/s experiment, the evolution of the seismicity with time is presented in Annex 5 using 4h time windows.

There is a relative similarity between the growth of microseismicity in the first eight hours of both experiments. At the beginning of the 15 l/s experiment, events are located south and southeast of GPK1 and extend upwards and downwards with respect to the borehole bottom. Then, the seismic gap aforementioned begins from 18th of July at 18h, to 19th of July at 2h. At the end of this gap, seismicity moves northeastward from GPK1. As in the 7 l/s case, events occur above and beneath 2000 m depth, then from 19th of July at 16h, a large peak of seismicity appears, concentrated northwest of GPK1, between 2100 and 2300 m depth. This deeper zone remains the major active zone during the next 24h, with the exception of some sparse events located above 2100 m. Starting from 20th of July at 4h, a change occurs and seismicity appears again southeast of GPK1 and above the borehole bottom. The figure between 4h and 8h on 20th of July shows the striking feature of an elongated NW-SE axis in the horizontal plan. Nevertheless this trend disappears after 12h, and, at the end of the injection, seismicity is concentrated 100 m westwards from GPK1 at about 2200 m depth. During the post-stimulation experiments (step injection tests) several events occur, at a considerable distance from GPK1. As for 7 l/s stimulation, hypocenters locations are less precise, due to the reduction in the number of hydrophones in EPS1 from two to one.

2.2.3. Amplitudes distributions

The amplitudes of the located events are shown in figures 21 to 23, in the same way as for the 7 l/s experiment. The main trend of the distribution of seismicity in the horizontal plane is still NW-SE, but the amplitudes are larger. The eastward dipping axis of the 7 l/s experiment is still active, but less clear on the N60E projection since it is relayed by a westward dipping concentration of events beneath 2150 m depth (Figure 21). In this case, the low amplitudes do not surround the highest ones; on the contrary, several high amplitude events are located on the envelope of the seismic cloud.

The diagrams (Figures 24, 25) amplitude-time-distance, are treated separately for events with depths above (Figure 24) and beneath 2000 m (Figure 25) respectively. Once again most of the seismicity migrates downward with time and, surprisingly, the activity above 2000 m starts again on 20th of July again at 16h, and continues beyond the 15 l/s experiment with three small events. It should be noted that the activity beneath 2000 m and after the injection end includes several large amplitude events.

There does not appear to be a simple link between injection pressure and event magnitude, or in the case considered here, signal amplitude. In all these diagrams it can be seen that large and small amplitude events are scattered throughout the data. This is consistent with the view that the seismicity is caused by the activation of existing joints within the rock mass rather than the formation of new joints within the rock mass in the simulated region. Thus the signal amplitude of the events is related to the pattern of pre-existing joints, but the event rate is related to the injection rate or pressure.

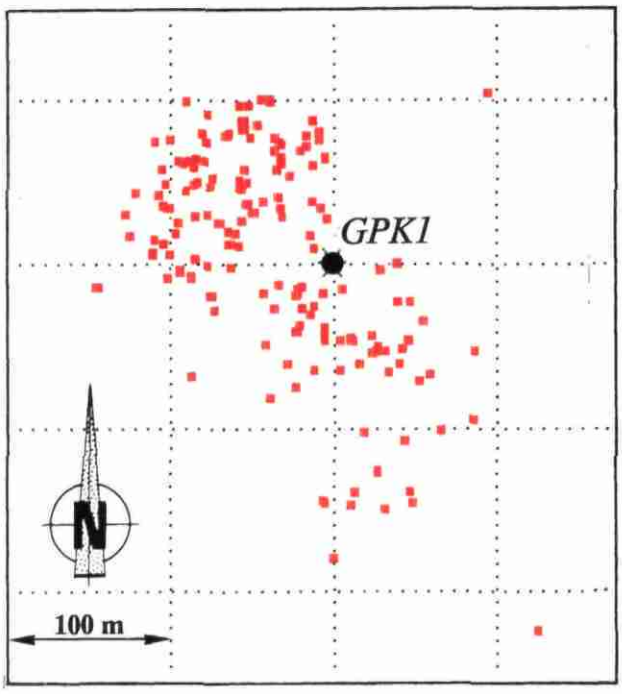

Figure 18 - Locations of the microseismic events induced during the 15 l/s hydraulic test. Map view.

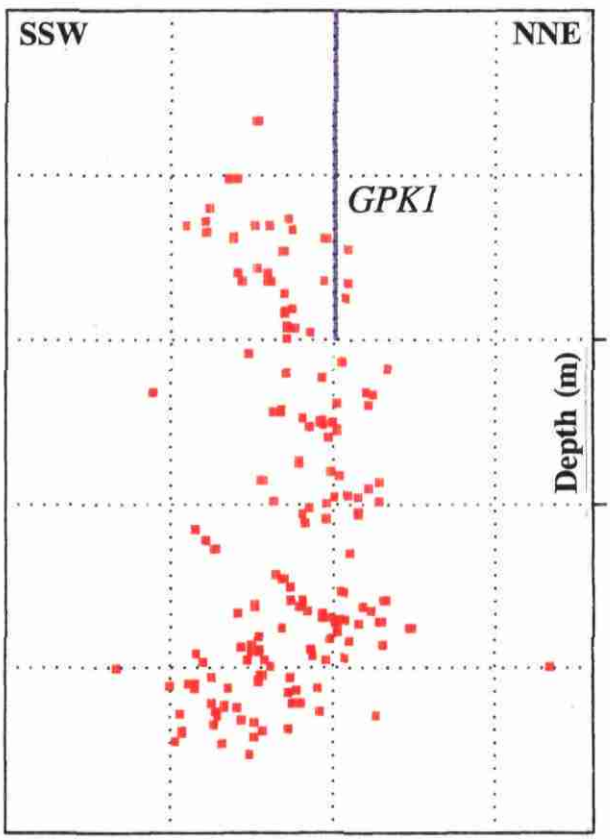

Figure 19 - Vertical N60° cross-section.

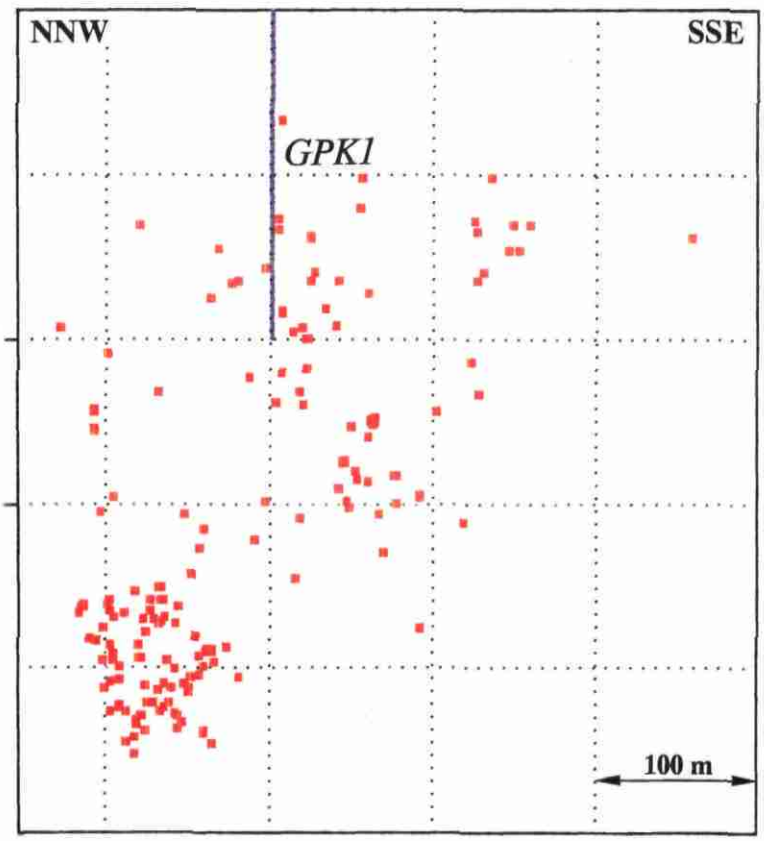

Figure 20 - Vertical N150° cross-section.

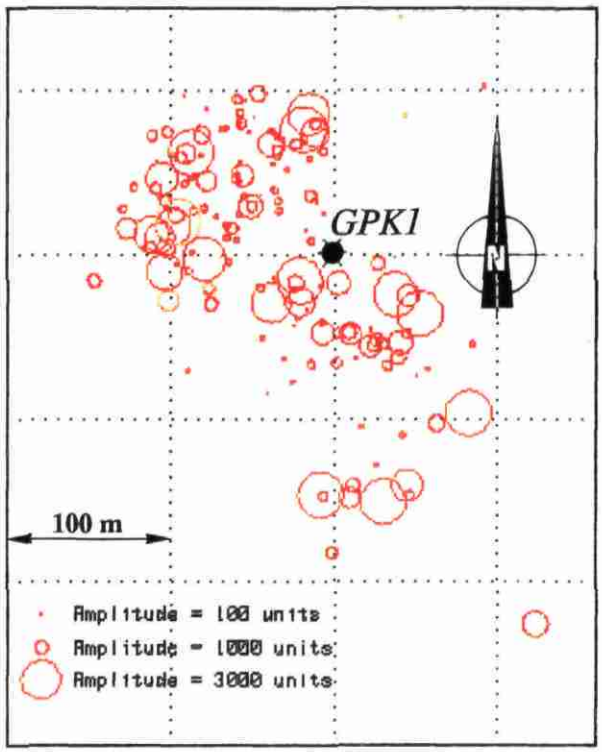

Figure 21 - Maximum amplitudes distributions of the microseismic events induced during the 15 l/s hydraulic test and recorded on the hydrophone deployed at the bottom of EPS1. Map view.

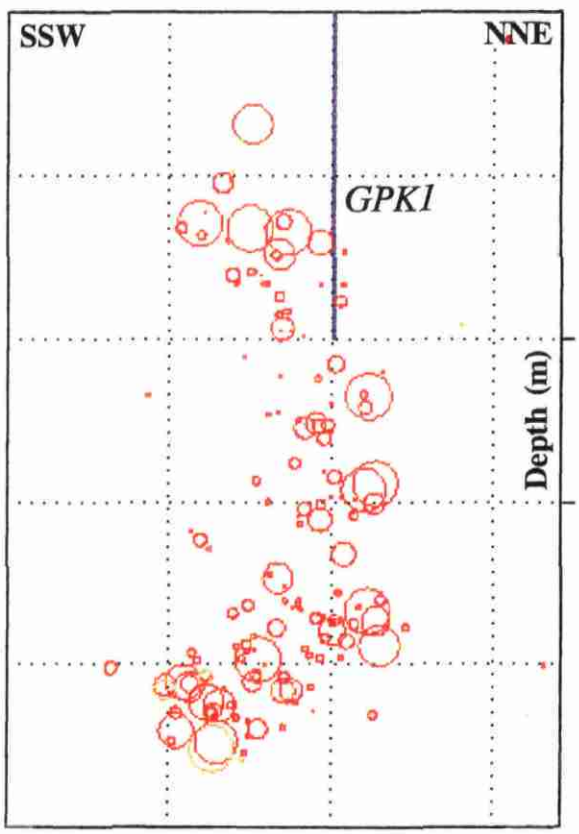

Figure 22 - Vertical N60° cross-section.

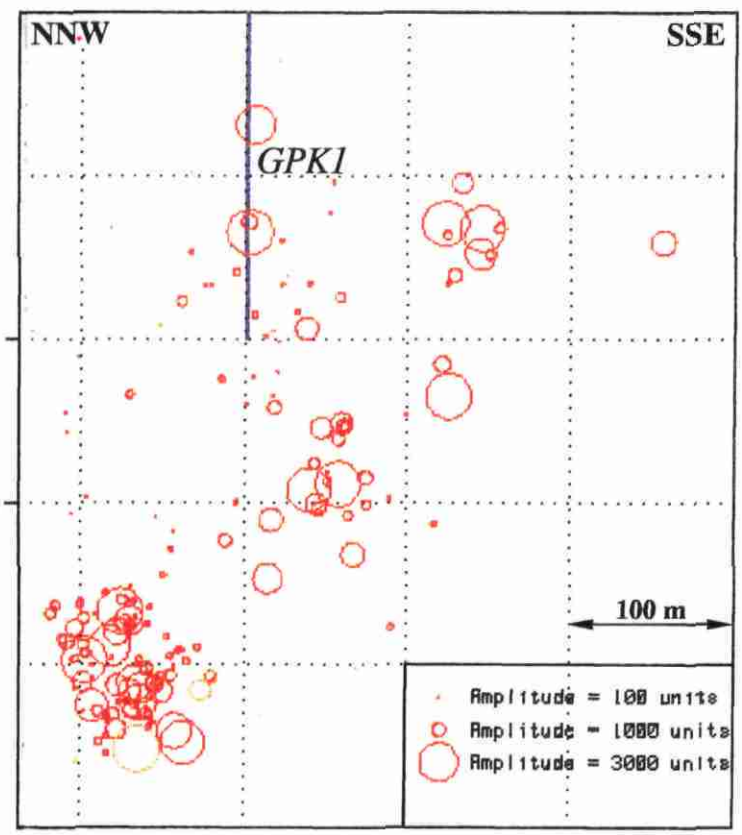

Figure 23 - Vertical N150° cross-section.

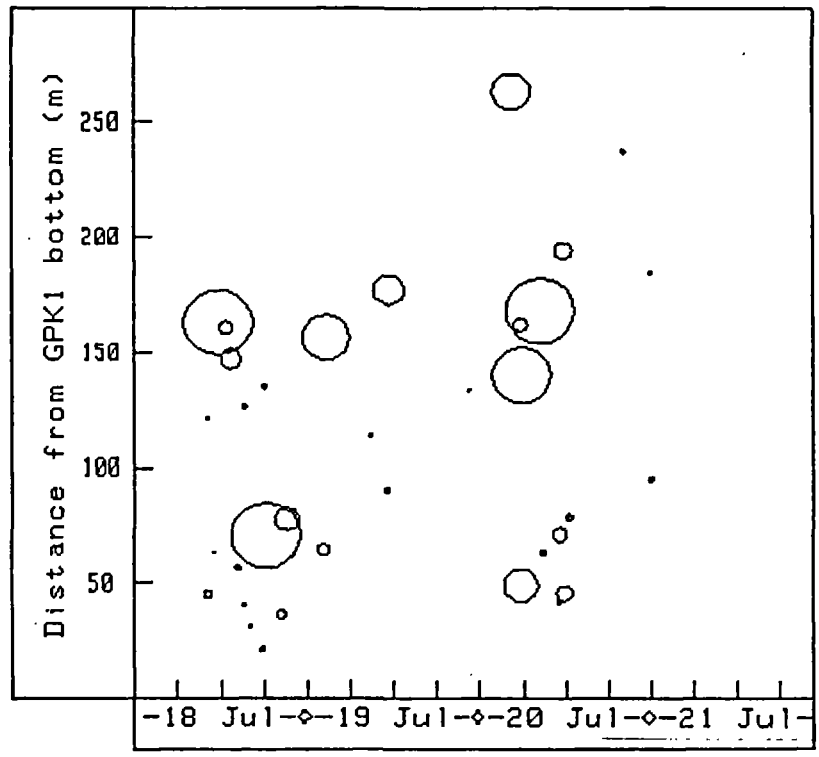

Figure 24 - Distances from GPK1 bottom and maximum amplitudes distributions versus time for events located above 2000 m. (Hydraulic test: 15 l/s).

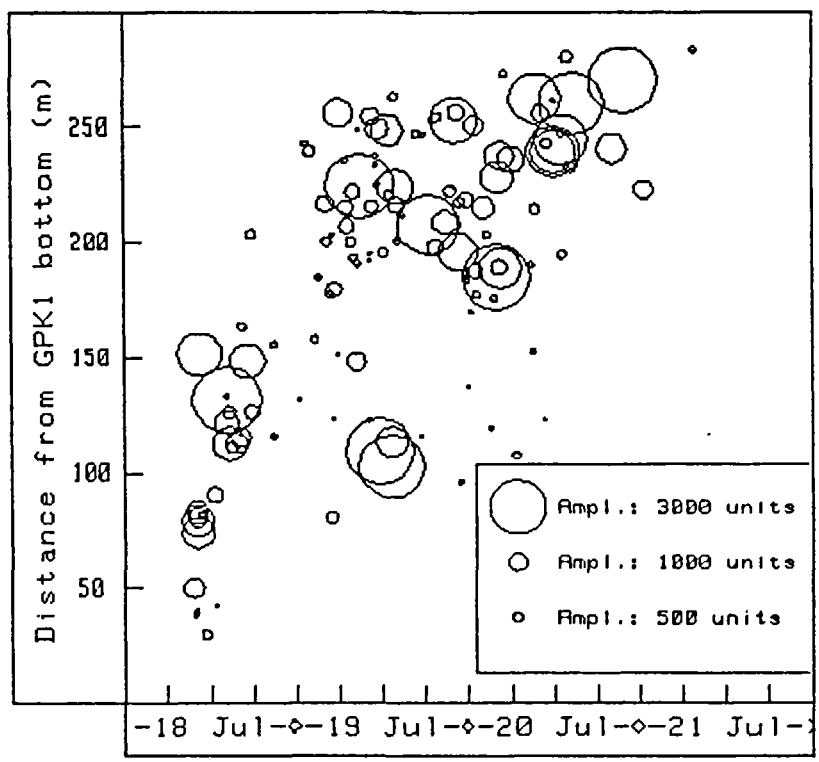

Figure 25 - Distances from GPK1 bottom and maximum amplitudes distributions versus time for events located below 2000 m. (Hydraulic test: 15 l/s).

2.3. LOCATIONS OF THE OVERALL MICROSEISMICITY AND ERROR ESTIMATIONS

The overall located microseismicity induced during the various aforementionned hydraulic tests are summarized on figures 26 to 28. Moreover, an important parameter that must be taken into account in addition to the locations of the events, is the error estimation attached to this determination. It must be remembered that during the course of the experiments the number of seismic stations changed: during the 7 l/s experiment and after the 15 l/s experiment only one hydrophone was deployed in EPS1, meanwhile during the 15 l/s two hydrophones were deployed in EPS1. So, the configuration of the recording network has changed and hence number of timings used to locate the events typical changed, as did the degree of confidence of the location results.

The error estimation procedure is explained in Jones, 1992. Briefly, this algorithm takes into account the experimental configuration (i.e. network geometry and velocity model) and a normal distibution of error pickings to obtain an error ellipsoid in space; this ellipsoid is then scaled by the observed station residuals values of the event. Statistically, the distribution of errors presents 2 peaks if we considered the locations results associated to the network configuration with 1 hydrophone or 2 hydrophones; these maxima indicate that the locations have respectivelly precisions of about +/- 40 m and +/- 20 m for one standard deviation on the time pickings of P and S waves (i.e. for a 70% confidence limit). Moreover, not only the absolute values varies, but also the shape and orientation of the error ellipses.

In order to illustrate these remarks, Annex 6 presents errors ellipses projected on two orthogonal views calculated on selected events which have shown good signal to noise ratio.

Various orientations of the error ellipsoid could be observed, linked to the stations configuration which have recorded the event. These views also clearly illustrate, for the particular case of the deeper seismic cloud sited on NW of GPK1, that the precision of the locations are quite accurate to suppose that all these events represent the failure of different joints.

Figure 29 shows the 99.7% confidence ellipsoids for the seismicity from both the 7 and 15 l/s injections viewed from the south-west. The error ellipsoids are rendered as solid objects. The larger the error ellipsoid the greater is the uncertainty in the location of the microearthquake. For the purposes of this figure some of the most inaccurate locations have been excluded so as not to obscure the more accurate locations. Of particular interest is the group of locations at the bottom left of the figure. The fact that the error ellipsoids do not overlap suggests the microearthquakes are spatially distinct and do not represent repeated failure at the same point on the same joint.

2.4. FAULT PLANE SOLUTIONS

With the few sensors available added to the fact that the sensors were not properly grouted and so do not provide reliable amplitude information, it has been impossible to determine quantitative fault plane solutions. However, results based on P-wave polarity onsets recorded during the hydraulic experiments are presented in Annex 7 in order to characterize some events. Plots of the 54 located events where P-wave polarity picks recorded on the seismic sensors and hydrophone(s) could be determined with confidence are also given, in addition with the various populations which could have been deduced from this analysis.

A normal course of analysis in earthquake seismology is to produce fault plane solutions and then from these to attempt to determine the stress field in that region. However at the Soultz site our knowledge of the stress field is greater than that of the fault planes. Because of this situation the

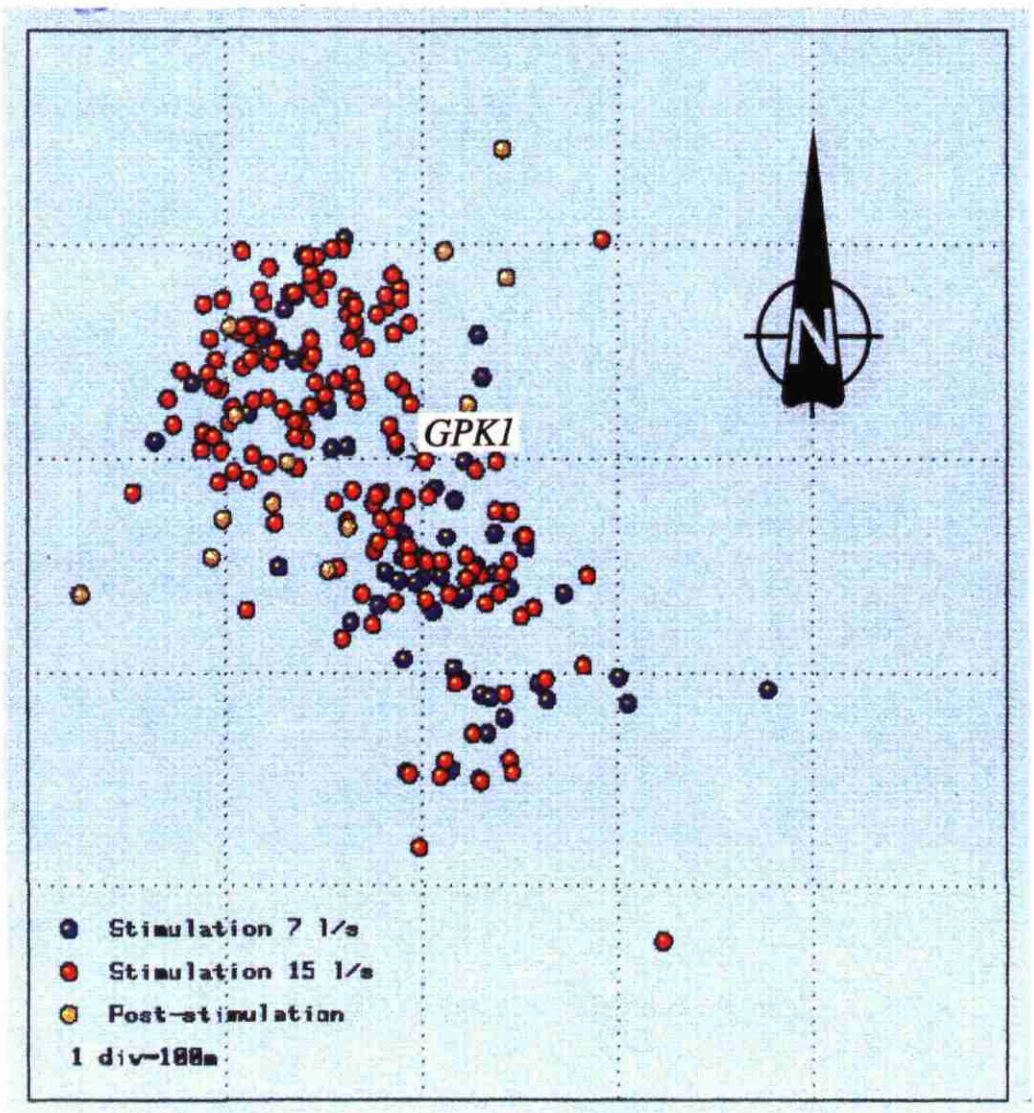

Figure 26 - Map view of the overall microseismicity located during the hydraulic tests.

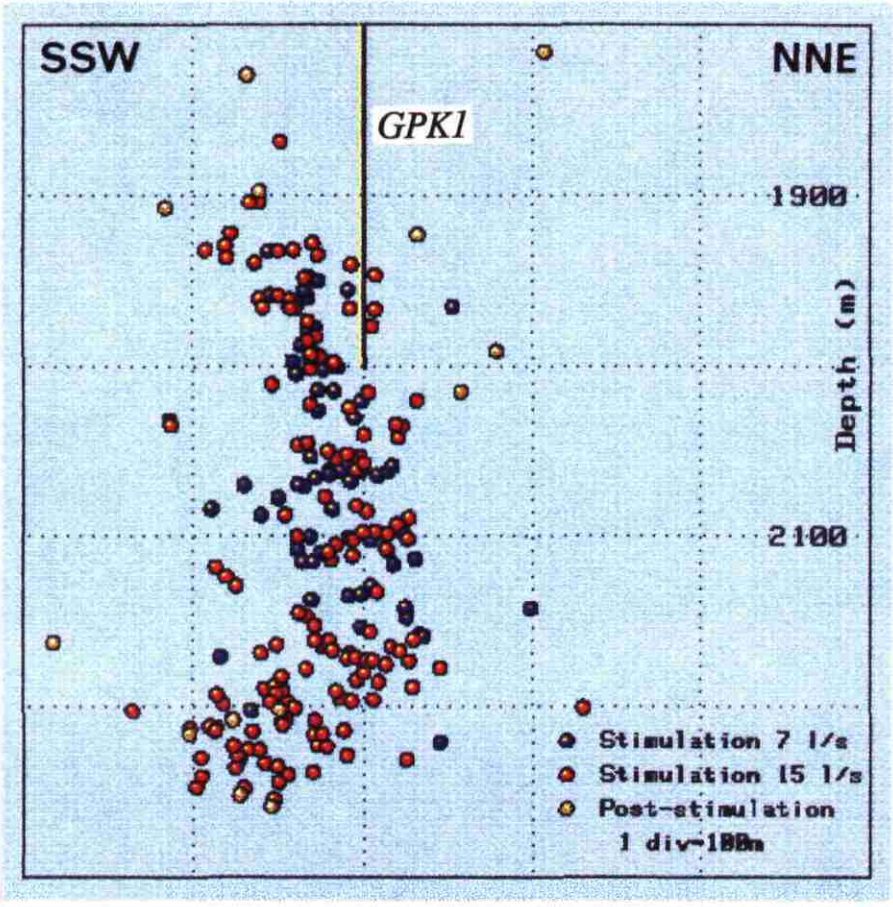

Figure 27 - Vertical N60° cross-section.

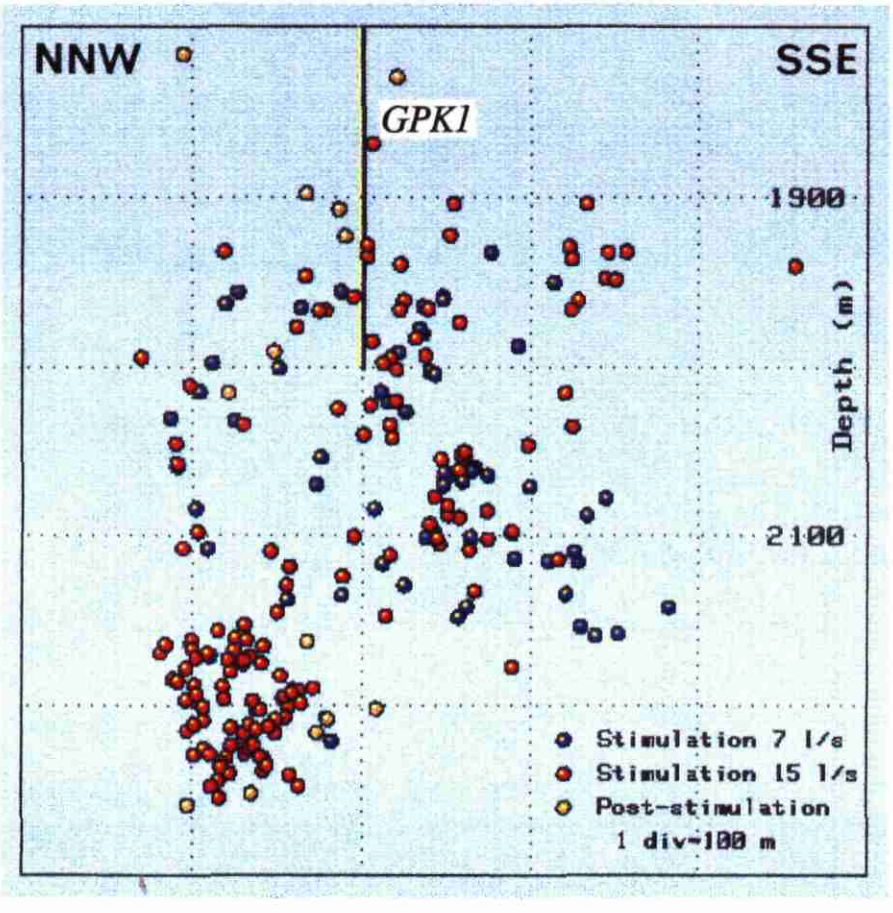

Figure 28 - Vertical N150° cross-section.

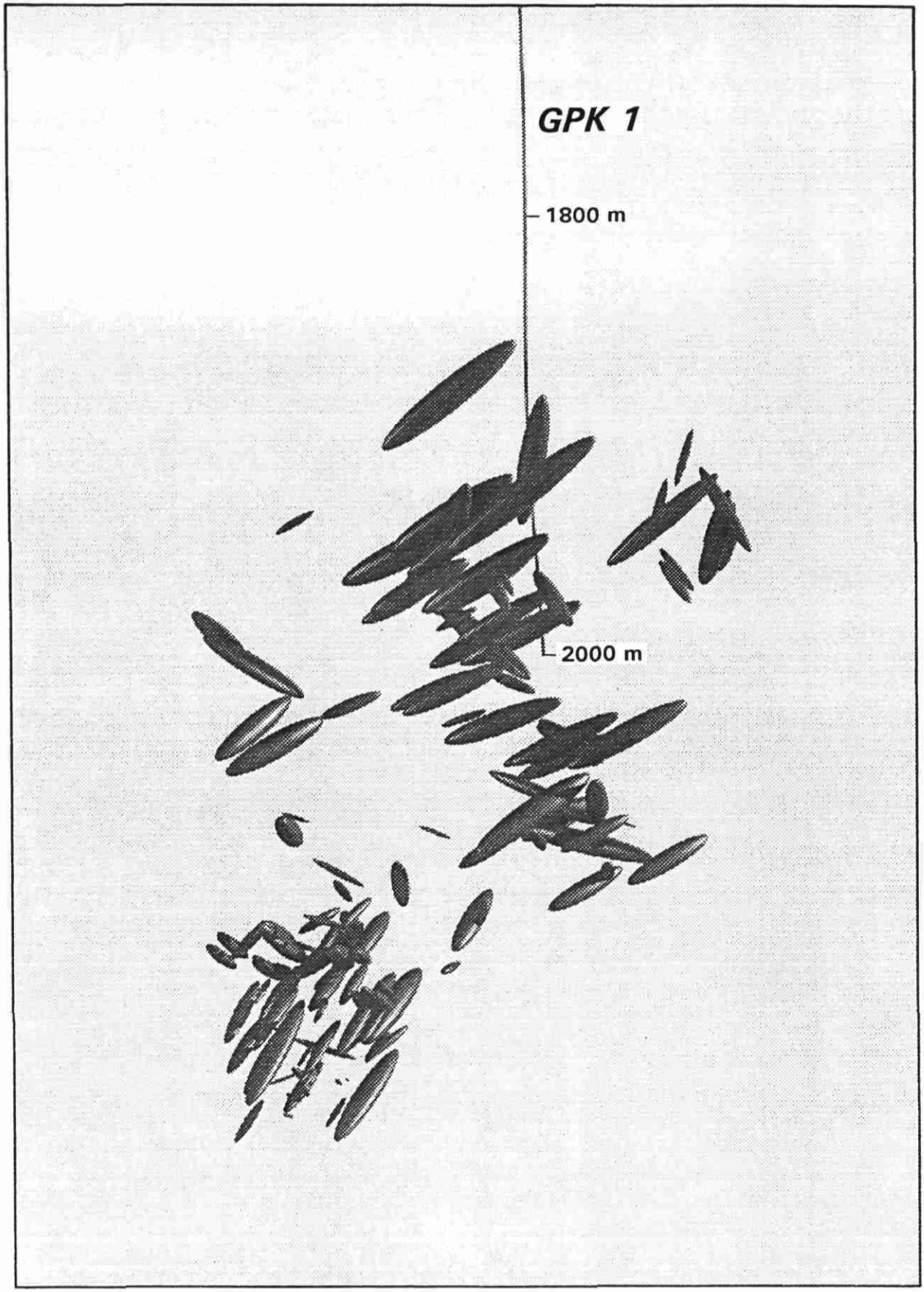

Figure 29 - Ellipsoid errors for the microseisms induced during both the 7 and the 15 l/s injection tests. Side view for the SW.

method of analysis adopted here has been to find the fault plane solution which is consistent with the P-wave polarities and which would require the minimum excess pore pressure, for each event. By doing this at least the simplest possible set of fault planes solutions which can account for the data can be produced.

This method was applied to the Soultz data for all events with three or more P-wave polarity picks. The resulting failure planes are plotted in figure 30. This figure shows that all the polarity data can be accounted for by failure on planes which are near vertical and which have a strike direction similar to that of the principle horizontal stress, which is the intermediate stress direction. Although the diagram shows two failure planes it should be pointed out that these are the minimum stress failure planes and for all the events considered a second failure planes belonging to the other family also existed and typically this only required a slightly higher pore pressure to cause failure. This means that it is not possible to determine whether joints dipping to the east or west or both are those that dominate the seismic development of the reservoir.

2.5. COMPARISON OF 1991 INDUCED SEISMICITY WITH 1988 ACTIVE SEISMIC SURVEYS

Various active seismic surveys were undertaken in 1988 with Schlumberger. Three offset seismic profiles (OSP) and a Vertical seismic profile (VSP) together with a Walkaway along a N54° line jointing GPK1 and well 4550.

Several features appeared on the Walkaway and VSP surveys, which have been described in Beauce *et al.*, 1991 which are related either to fractured/altered zones observed in the borehole, or to induced events locations. On figures 31 and 32, hypocenters of the events recorded respectively during the 7 l/s and the 15 l/s hydraulic experiments have been projected and superimposed on the Walkaway section. The trend dipping towards the east, along which the first events of both experiments are aligned, correlates well with a dipping reflector sited at 2000 m, west of the borehole.

The seismicity located in Phase I at 2100 m depth was linked to the 2100 m reflector. Some seismicity also appeared in the same zone during the 7 l/s experiment and even during the 15 l/s one. Most of it belongs to a cluster sited 50 m southwest of GPK1.

Moreover, as the hydraulic injection experiments proceeded, the front of seismicity was growing downward but seems to be stopped on the northeastern part of GPK1: on the walkaway section, a sub-vertical feature or discontinuity dipping towards the west (marked F2) which terminates the reflectors sited at depths between 2000 and 2200 m is also observed in this region. This feature could mark a fault which acts as a barrier to the growth of the seismicity in this direction if the fault is hydraulically active.

The active deep seismic zone located beneath 2150 m corresponds to the interval between two important reflectors observed on the active seismic surveys. The second one, at 2250 m depth corresponds to the bottom of this cluster of seismicity. Nevertheless we know those events are sited more than 100 m out of the plane of the Walkaway section. A simpler explanation may be that the progression of the front of induced seismicity might have been stopped simply by the termination of the injection and not by a tectonic or lithologic barrier.

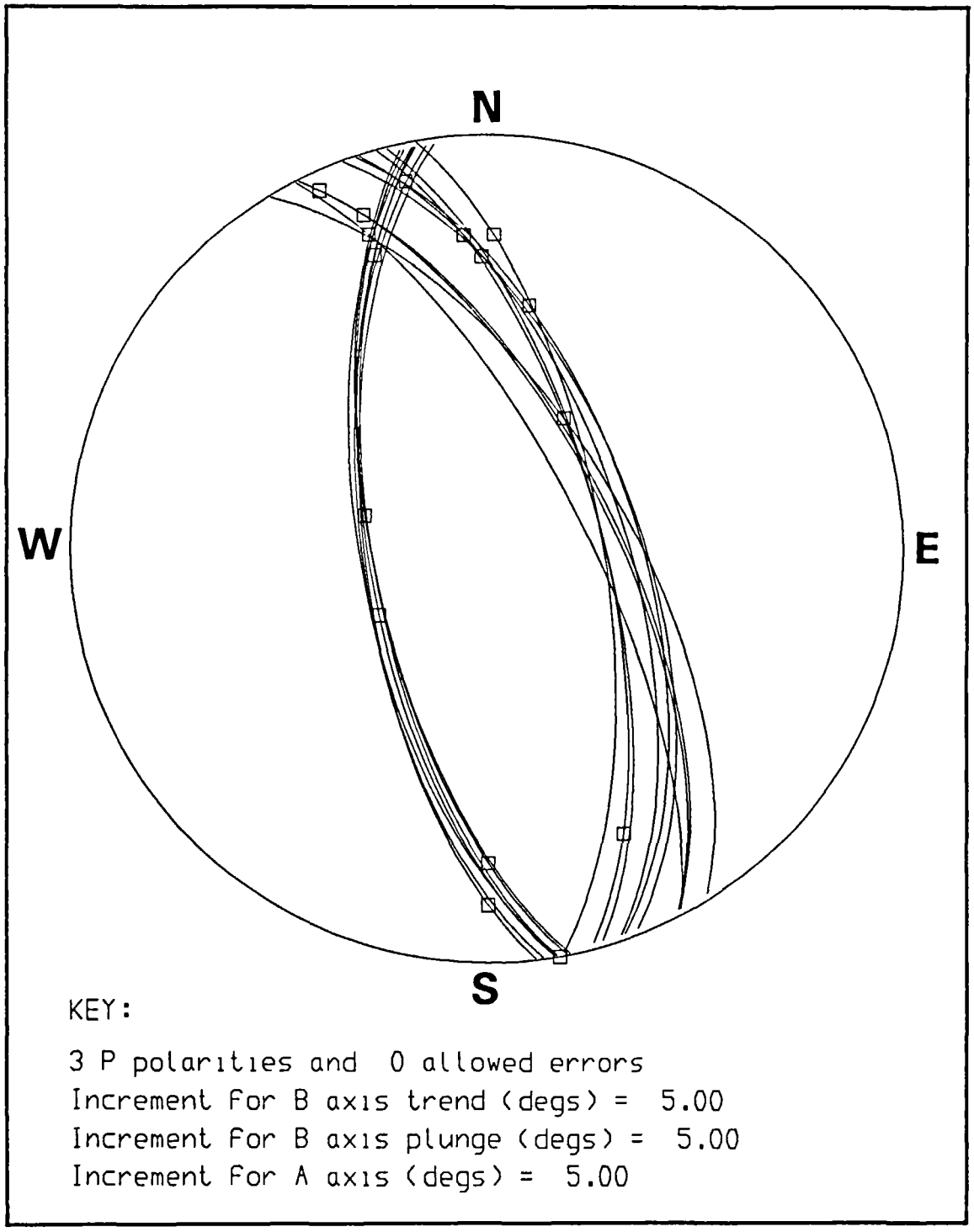

Figure 30 - Fault plane solutions consistent with P-wave polarities and requiring minimum excess pore pressure.

Voir calque dans document papier

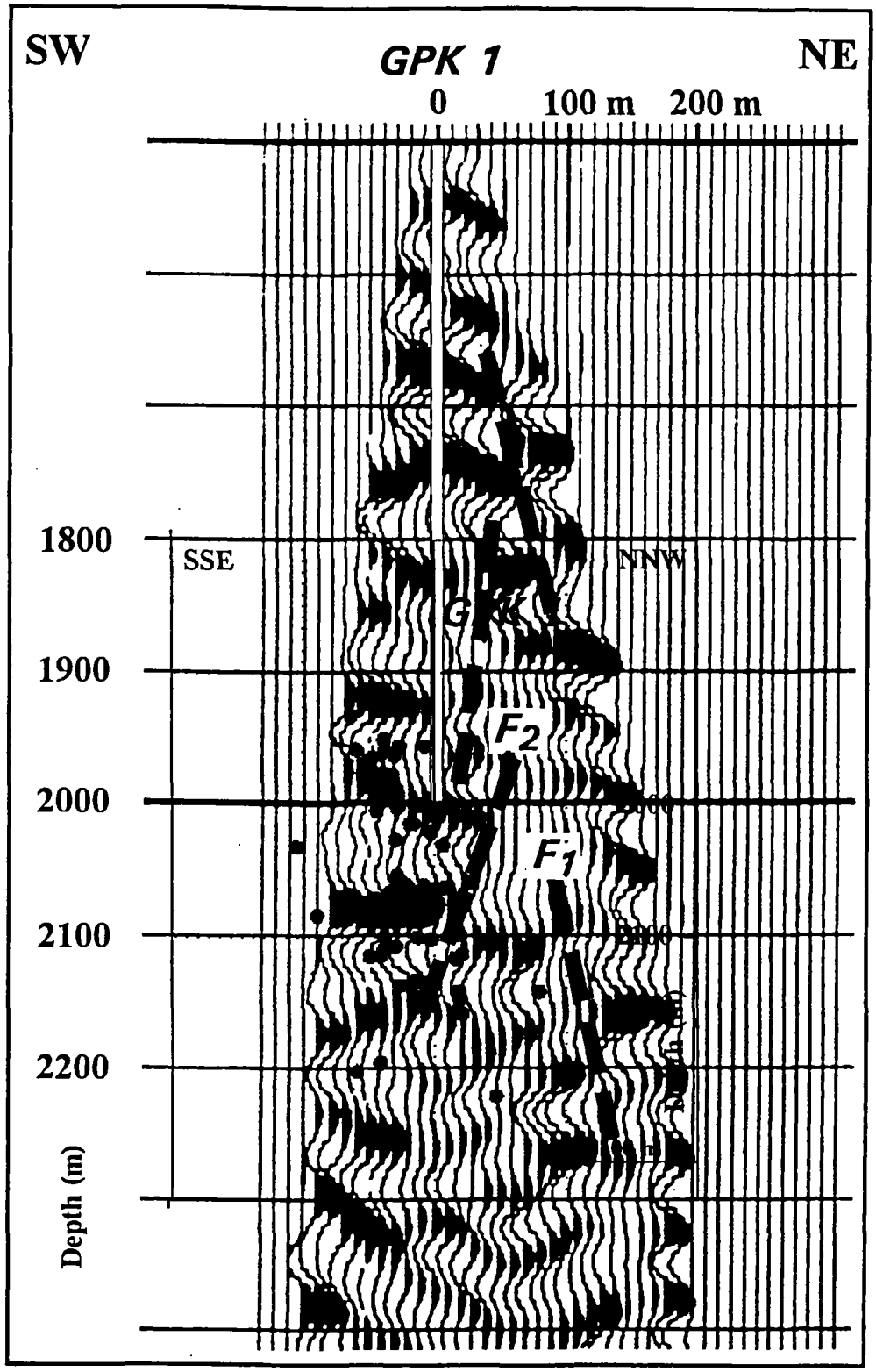

Figure 31 - Walkaway section along a N54° line associated with the induced seismicity recorded during the 7 l/s hydraulic test.

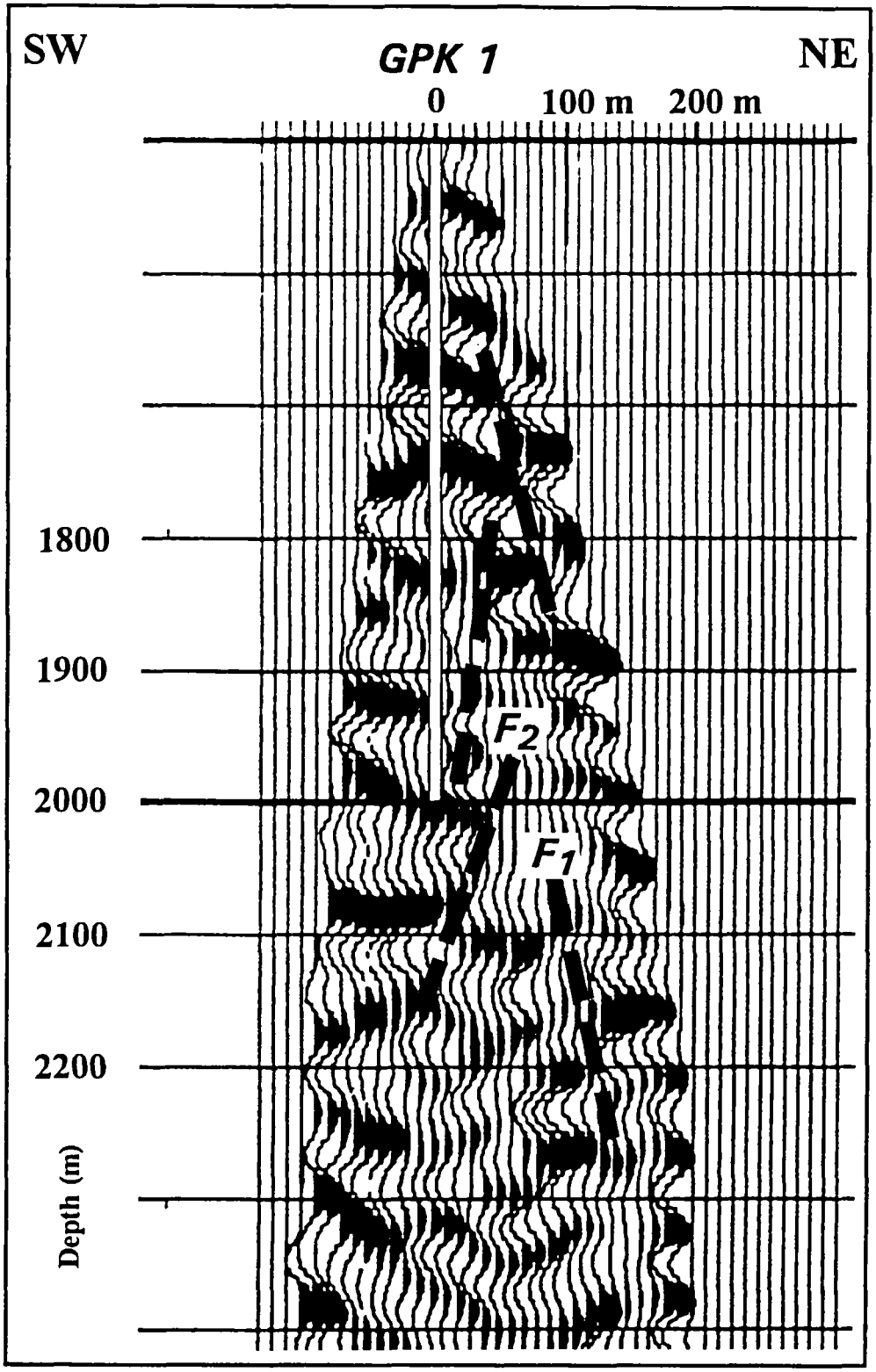

Figure 31 - Walkaway section along a N54° line associated with the induced seismicity recorded during the 7 l/s hydraulic test.

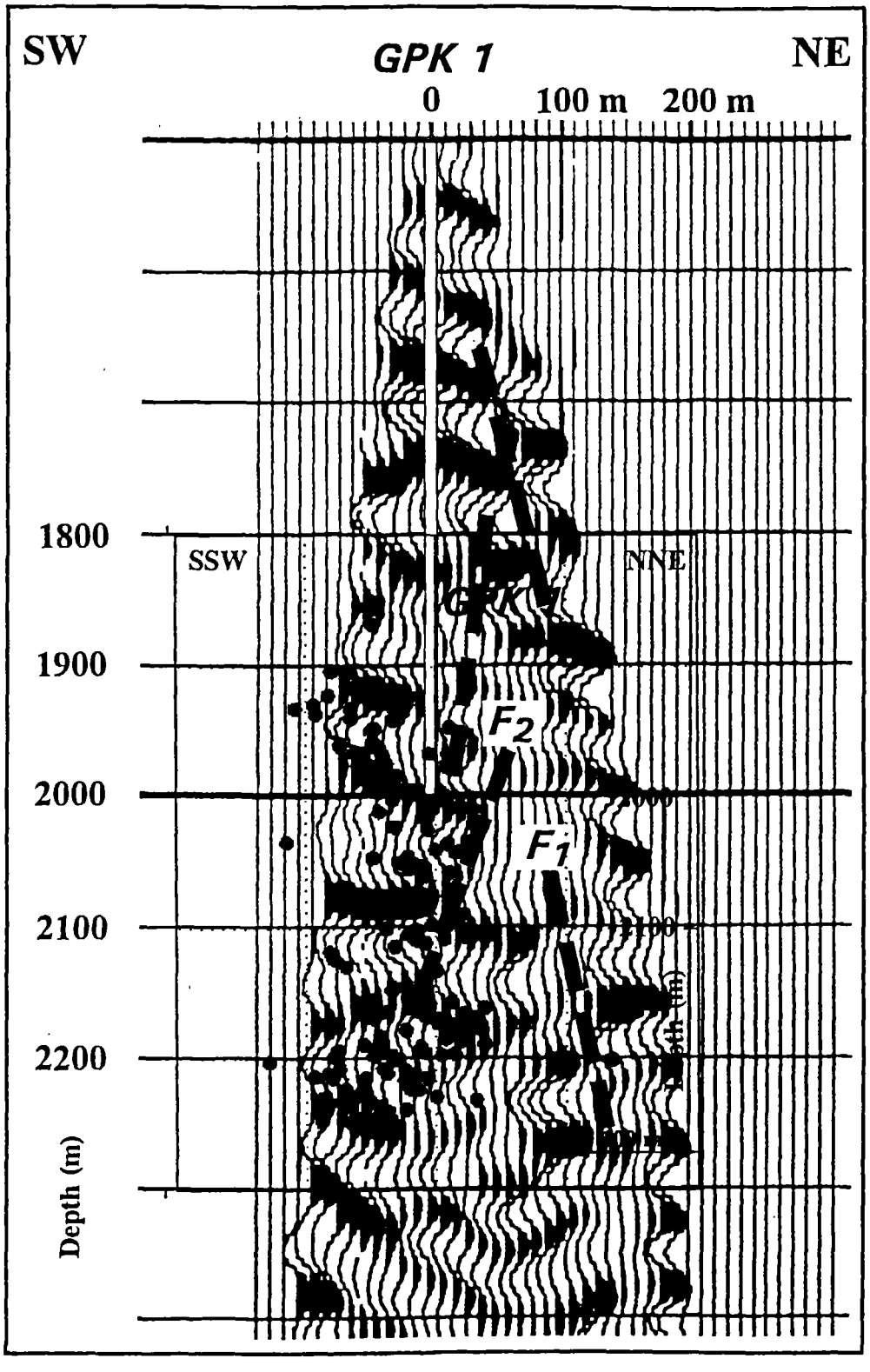

Figure 32 - Walkaway section along a N54° line associated with the induced seismicity recorded during the 15 l/s hydraulic test.

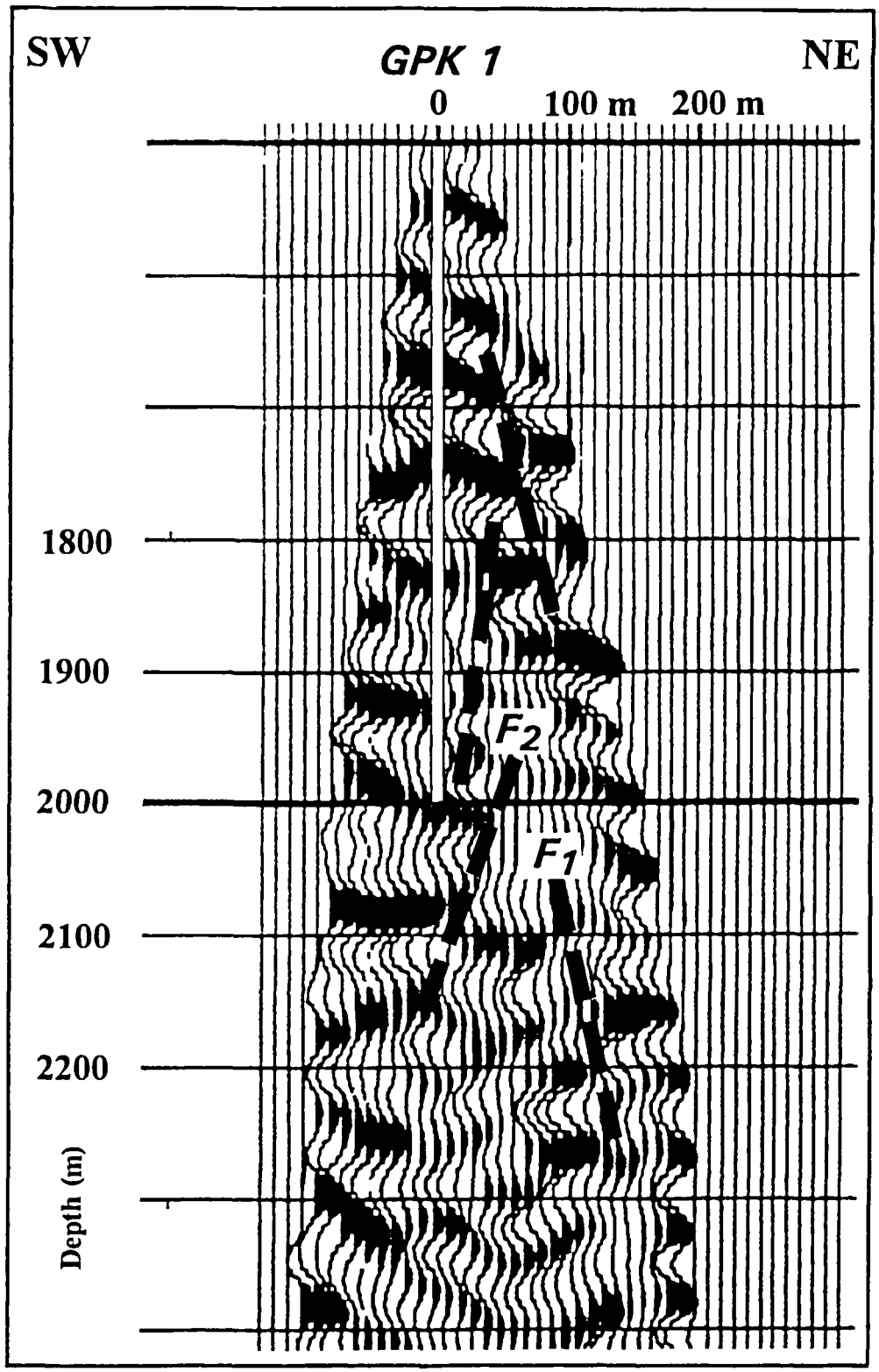

Figure 32 - Walkaway section along a N54° line associated with the induced seismicity recorded during the 15 l/s hydraulic test.

CONCLUSIONS

During Phase IIa of the HDR Soultz project, the two hydraulic stimulations undertaken at the bottom of GPK1 borehole induced more than 400 microseismic events recorded on the downhole network.

Overall the seismic cloud propagates along a NNW-SSE trend which is in agreement with the orientation of the present maximum horizontal stress component measured by other methods (BHTV and in situ measurements).

The seismicity grows downward during both experiments i.e. the 7 l/s and the 15 l/s injections. The events progression follows a subvertical feature from NNW to SSE of GPK1 and from depths ranging from 1950 m down to 2150 m. During the 15 l/s test and after an injection of about 1000 m^3, a connection with a deeper seismic zone occurs: this new seismic zone sited at about 2150-2250 m depth and NNW of the injection zone remains the only active region and does not present any tendency to grow during the test period: the seismic events are confined in a region of about 50 m radius until the end of the injection and this zone remains the only active zone during the 24 hours after the injections cease. Later, its activity continues in addition to a reactivation of the zone sited near the injection interval.

Seismicity still remains after the injections cease at a relatively high rate and persists for several days, indicating that a remanent pressure is maintained in the granite for some time after the end of the injections. These events are located mainly in the deeper aforementionned zone and near the injection interval of GPK1.

In correlation with the walkaway section line, the growth of seismicity seems to be stopped towards the NNE of GPK1 by a natural subvertical feature. The seismic region defined between 1950 and 2150 m depths could be connected to the deeper zone via this feature.

Analysis of the P-wave polarity data in conjunction with the stress field shows that the seismicity could have occurred on sub-vertical joints striking in the direction of the maximum principal horizontal stress direction. However it is not possible, by just examining the P-wave polarity data, to determine whether it is the east or west dipping joints, or indeed both sets of joints, which are the most important.

Comparison between active seismic results (crosshole and tube wave VSP surveys) and the induced seismicity does not give complementary information on the propagation of the injected fluid inside the granite: this was due to the fact that the zones illuminated by the active seismics were sited above the bottom of GPK1 whereas most of the seismicity occurs below the bottom of GPK1.

During the injection experiments, permanent and mobile surface networks did not record any induced seismicity, nor natural local seismicity. However, it must be noted that the downhole network did record a natural event, which could not be located, suggesting that a very low magnitude level natural seismicity does exist in this region.

In order to allow further quantitative studies in particuliar on fault plane solutions and to obtain reliable results, the work undertaken and results produced clearly point to the necessity for a proper grouting procedure of the sensors at depths in this situation. It also shows that a more dense network is required. These problems will need to be addressed for the next phase of the project.

REFERENCES

BEAUCE A., JONES R., FABRIOL H., TWOSE C., HULOT C. (1992) - Microseismic monitoring of hydraulic experiments undertaken during Phase IIa of the Soultz HDR Project (Alsace-France), 17th Workshop on *Geothermal Reservoir Engineering*, Stanford (USA), Jan 2931, 1992, 6 p.

BEAUCE A., FABRIOL H.,LE MASNE D.,CAVOIT C., MECHLER P., CHEN X.K. (1991) - Seismic studies on the HDR site of Soultz-sous-Forêts (Alsace-France), *Geothermal Science and Technologie*, Vol 3(1-4), p. 239-266.

BEAUCE A., FABRIOL H., HULOT C. (1991) - Seismic monitoring of the hydraulic stimulations undertaken at Soultz-sous-Forêts, Field report, note technique, BRGM SGN/IRG N91-145.

DEGOUY M. (1991) - Rapport d'execution des travaux de nettoyage du puits 4550, 4 juillet 1991, CFG 44/91/SFE, 2 p.

DEGOUY M., VILLENEUVE B. and WEBER R. (1992) - Logistical support and development of the Soultz hot dry rock site: seismic observation wells and well EPS1, 1990-1991 Soultz-sous-Forêts (France), Final report, report N° 92CFG09, 41 p.

HOANG T.P., HELM J.R., CARA M. (1991) - Programme de surveillance sismique à Soultz/Forêts, Rapport final ARC Géothermie des roches fracturées, avril 1992, p. 151-163.

JONES R. (1992) - Further analysis of Soultz Phase IIa stimulation seismic data, Technical note, March 1992, CSM TN03/99, 19 p.

JONES R. (1991) - Analysis of Soultz Phase IIa tubewave VSP's, Technical report, Dec. 1991, CSM TN03/96, 20 p.

JONES R., BEAUCE A., TWOSE C, FABRIOL H., HULOT C., NICHOLLS J. (1991) - Soultz Phase 2 stimulation seismic monitoring field report, Technical note CSM TN03/92, 12 p.

JUNG R. (1992) - Connecting a borehole to a nearby fault by means of hydraulic fracturing, *Geothermal Resources Council Transactions*, Vol. 16, Oct. 1992, p. 433-437.

JUNG R. (1991) - Hydraulic fracturing and hydraulic testing in the granitic section of borhole GPK1, Soultz/Forêts. *Geotherm. Sci. & Tech.*,Vol 3, N° 1-4, p. 149-197.

KRANTZ R.L., SATOH T., NISHIZAWA O., KUSUNOSE K., TAKAHASHI M., MASUDA K., HIRATA A. (1990) - Laboratory study of fluid pressure diffusion in rock using acoustic emissions. *Journ. Geophys. Res.*, Vol 95, N° B13, p. 21593-21607.

RUMMEL F., BAUMGARTNER J. (1991) - Hydraulic fracturing stree measurements in the granitic section of borehole GPK1, Soultz/Forêts. *Geotherm. Sci. & Tech.*, Vol. 3, N° 1-4, p. 199-215.

STEWART R., JONES R. (1992) - Analysis of Soultz cross-hole data, Technical note, March 92, CSM TN03/100, 40 p.

STEWART R., FABRIOL H., BEAUCE A., NICHOLLS J. (1991) - Soultz crosshole survey operations report, Technical note, Dec 1991, CSM TN03/97, 32 p.

STEWART R., FABRIOL H., NICHOLLS J., BEAUCE A. (1991) - Soultz VSP operations report, Aug. 1991, Technical note, CSM TN03/91, 10 p.

LIST OF FIGURES

Figure 1 - Situation map of the project and seismic borehole network

Figure 2 - Situation map of the permanent and mobile surface seismic network

Figure 3 - Sismograms of a natural local event recorded during the hydraulic experiment period

Figure 4 - Sismograms of the calibration shot fired in GPK1 at 1992 m depth.

Figure 5 - Geological SSW-NNE cross-section between GPK1 and 4601

Figure 6 - Seismic event rate and downhole pressure recorded during the 7 l/s hydraulic test

Figure 7 - Example of an induced event recorded during the 7 l/s hydraulic test

Figures 8 to 10 - Locations of the microseismic events induced during the 7 l/s hydraulic test

Figure 11 - Location of the induced seismicity recorded in 1988

Figures 12 to 14 - Amplitudes distributions of the events induced during the 7 l/s hydraulic test

Figure 15 - Distances and amplitudes distributions of the events located above 2000m depth

Figure 16 - Distances and amplitudes distributions of the events located below 2000m depth

Figure 17 - Seismic event rate and downhole pressure recorded during the 15 l/s hydraulic test

Figures 18 to 20 - Locations of the microseismic events induced during the 15 l/s hydraulic test

Figures 21 to 23 - Amplitudes distributions of the events induced during the 15 l/s hydraulic test

Figure 24 - Distances and amplitudes distributions of the events located above 2000m depth

Figure 25 - Distances and amplitudes distribution of the events located below 2000m depth

Figures 26 to 28 - Locations of the overall seismicity induced during the hydraulic experiments

Figure 29 - Error ellipsoids of the events located during the hydraulic experiments.

Figure 30 - Fault plane solution consistent with P-wave polarities and requiring minimum excess pore pressure

Figure 31 - Walkaway section associated with the induced seismicity recorded during the 7 l/s hydraulic test

Figure 32 - Walkaway section associated with the induced seismicity recorded during the 15 l/s hydraulic test

LIST OF TABLES

Table 1 - Characteristics of the seismic boreholes used during Phase I

Table 2 - Coordinates of the various boreholes used during Phase IIa

Table 3 - Coordinates of the seismic probes referred to GPK1 well head

Table 4 - Coordinates of the permanent surface IPGS network

Table 5 - P-wave velocities deduced from the calibration shot fired in GPK1

Table 6 - P-wave station delays corrections

Table 7 - Seismic data files names and comments

LIST OF ANNEXES

ANNEX 1 - Trajectory surveys of boreholes 4616, 4550, 4601 and EPS1

ANNEX 2 - List of events and locations

ANNEX 3 - Seismic event examples

ANNEX 4 - Evolution of the induced seismicity during the 7 l/s experiment

ANNEX 5 - Evolution of the induced seismicity during the 15 l/s experiment

ANNEX 6 - Location errors on selected events

ANNEX 7 - List of events characterized by their P-wave polarity onsets

ANNEX 8 - Stanford paper

ANNEX 1

Trajectory surveys of boreholes

4616, 4550, 4601 and EPS1

BRGM

GYRO MULTISHOT SURVEY

CHAMP : KUTZENHAUSEN

CLUSTER :

PUITS : 4616

JOB ref: 140591bis

REFERENCES PHASE : 4 1/2"

COORDONNEES tete de puits :

X: 1004635.95
Y: 152447.55

REFERENCE profondeur: TETE DE PUITS

ELEVATION TABLE DE ROTATION : 0 m

REFERENCE DIRECTION : NORD LAMBERT

Repere utilise pour l'orientation : GPK1

COORDONNEES de GPK1

X : 1004689.05
Y : 152057.34

BRGM
KUTZENHAUSEN
4616
Job :140591bis GYRO MULTISHOT SURVEY

D.DEPTH Meters	Vert.DEPTH Meters	Angle Deg	Azimut Deg	X(E/W) Departure	Y(N/S) (m)	PROJ Total	Dog.Leg Deg/10m
30.00	30.00	0.3	250.3	0.02W	0.01S	0.00	0.3
60.00	60.00	0.5	220.4	0.18W	0.13S	0.09	0.1
90.00	90.00	0.6	224.4	0.38W	0.35S	0.26	0.0
120.00	120.00	0.5	224.4	0.58W	0.55S	0.41	0.0
150.00	150.00	0.6	234.5	0.80W	0.74S	0.55	0.0
180.00	179.99	0.8	209.5	1.03W	1.01S	0.76	0.1
210.00	209.99	0.9	208.7	1.24W	1.40S	1.09	0.0
240.00	239.99	1.0	205.7	1.47W	1.84S	1.47	0.0
270.00	269.98	1.6	189.7	1.65W	2.49S	2.07	0.2
300.00	299.96	1.8	191.8	1.82W	3.36S	2.88	0.1
330.00	329.95	1.9	191.8	2.02W	4.30S	3.76	0.0
360.00	359.93	2.0	189.7	2.21W	5.30S	4.69	0.0
390.00	389.91	2.0	185.6	2.35W	6.34S	5.68	0.0
420.00	419.90	2.0	193.4	2.52W	7.37S	6.64	0.1
450.00	449.88	2.0	189.3	2.72W	8.40S	7.60	0.0
480.00	479.86	1.9	188.2	2.88W	9.40S	8.55	0.0
510.00	509.84	2.0	184.6	2.99W	10.41S	9.51	0.1
540.00	539.83	1.6	173.5	2.99W	11.35S	10.43	0.2
570.00	569.82	1.7	170.4	2.87W	12.21S	11.29	0.0
600.00	599.80	1.7	181.3	2.80W	13.09S	12.17	0.1
630.00	629.79	1.9	186.2	2.86W	14.03S	13.07	0.1
660.00	659.77	2.0	198.2	3.08W	15.02S	13.98	0.1
690.00	689.75	2.1	204.3	3.47W	16.01S	14.87	0.1
720.00	719.73	2.4	197.4	3.88W	17.10S	15.85	0.1
750.00	749.70	2.4	183.5	4.11W	18.33S	17.00	0.2
780.00	779.68	2.5	185.6	4.21W	19.61S	18.22	0.0
810.00	809.65	1.9	178.0	4.26W	20.75S	19.33	0.2
840.00	839.64	1.7	155.1	4.05W	21.65S	20.25	0.2
870.00	869.62	1.8	148.1	3.61W	22.46S	21.13	0.1
900.00	899.61	2.0	149.2	3.10W	23.31S	22.07	0.1
930.00	929.59	2.4	147.3	2.49W	24.28S	23.16	0.1
960.00	959.55	3.1	156.4	1.83W	25.55S	24.54	0.3
990.00	989.51	2.8	159.4	1.25W	26.98S	26.06	0.1
1020.00	1019.48	2.2	154.5	0.74W	28.19S	27.35	0.2
1050.00	1049.46	2.3	141.5	0.12W	29.18S	28.45	0.2
1080.00	1079.44	2.1	137.6	0.62E	30.05S	29.46	0.1
1110.00	1109.41	2.5	134.9	1.45E	30.91S	30.48	0.1
1140.00	1139.39	2.4	125.0	2.43E	31.73S	31.50	0.1
1170.00	1169.36	2.5	124.0	3.49E	32.46S	32.44	0.0
1200.00	1199.34	2.1	121.1	4.50E	33.11S	33.29	0.1
1230.00	1229.32	1.8	126.2	5.34E	33.66S	34.02	0.1
1260.00	1259.31	1.2	124.2	5.98E	34.12S	34.60	0.2
1290.00	1289.30	1.3	119.3	6.54E	34.46S	35.06	0.0
1320.00	1319.29	1.3	122.3	7.12E	34.81S	35.52	0.0
1350.00	1349.29	1.0	124.3	7.62E	35.13S	35.95	0.1

4616 GYRO MULTISHOT SURVEY

D.DEPTH Meters	Vert.DEPTH Meters	Angle Deg	Azimut Deg	X(E/W) Departure (m)	Y(N/S)	PROJ Total	Dog.Leg Deg/10m
1374.00	1373.28	1.0	148.4	7.90E	35.43S	36.30	0.2

LA PROJECTION TOTALE EST CALCULEE LE LONG DE 167.42
LE DEPLACEMENT HORIZONTAL EST 36.30 m DANS L'AZIMUT 167.42

BRGM

GYRO MULTISHOT SURVEY

CHAMP : KUTZENHAUSEN

CLUSTER :

PUITS : 4550

JOB ref: 140591

REFERENCES PHASE : 4 1/2"

COORDONNEES tete de puits :

X: 1004983.9
Y: 152308.84

REFERENCE profondeur: TETE DE PUITS

ELEVATION TABLE DE ROTATION : 0 m

REFERENCE DIRECTION : NORD LAMBERT

Repere utilise pour l'orientation : GPK1

COORDONNEES de GPK1

X : 1004689.05
Y : 152057.34

BRGM
KUTZENHAUSEN
4550
Job :140591

GYRO MULTISHOT SURVEY

D.DEPTH Meters	Vert.DEPTH Meters	Angle Deg	Azimut Deg	X(E/W) Departure	Y(N/S) (m)	PROJ Total	Dog.Leg Deg/10m
30.00	30.00	0.1	11.5	0.00E	0.01N	-0.01	0.1
60.00	60.00	0.1	336.6	0.00W	0.06N	-0.06	0.0
90.00	90.00	0.1	126.6	0.01E	0.07N	-0.07	0.1
120.00	120.00	0.2	120.7	0.07E	0.02N	-0.04	0.0
150.00	150.00	0.1	146.7	0.13E	0.02S	-0.00	0.0
180.00	180.00	0.7	231.8	0.01E	0.16S	0.15	0.2
210.00	210.00	0.9	226.8	0.31W	0.43S	0.49	0.1
240.00	239.99	1.3	204.8	0.62W	0.90S	1.01	0.2
270.00	269.98	1.8	198.0	0.91W	1.66S	1.81	0.2
300.00	299.96	2.0	191.1	1.16W	2.61S	2.80	0.1
330.00	329.94	2.1	198.1	1.43W	3.65S	3.87	0.1
360.00	359.93	2.0	192.2	1.71W	4.68S	4.93	0.1
390.00	389.91	1.8	191.2	1.91W	5.65S	5.93	0.1
420.00	419.90	1.5	192.3	2.08W	6.49S	6.79	0.1
450.00	449.89	1.0	182.5	2.18W	7.14S	7.44	0.2
480.00	479.88	1.0	182.6	2.20W	7.66S	7.95	0.0
510.00	509.88	0.9	183.8	2.23W	8.15S	8.44	0.0
540.00	539.88	0.8	189.9	2.28W	8.59S	8.87	0.0
570.00	569.87	1.2	196.6	2.41W	9.09S	9.40	0.1
600.00	599.86	1.7	197.8	2.63W	9.82S	10.15	0.2
630.00	629.85	1.8	216.9	3.05W	10.62S	11.02	0.2
660.00	659.83	2.4	204.0	3.59W	11.56S	12.06	0.3
690.00	689.80	3.0	200.2	4.11W	12.88S	13.46	0.2
720.00	719.77	2.2	211.4	4.68W	14.10S	14.78	0.3
750.00	749.75	1.8	215.7	5.26W	14.98S	15.76	0.1
780.00	779.73	1.6	213.9	5.77W	15.71S	16.58	0.1
810.00	809.72	1.8	202.1	6.18W	16.49S	17.43	0.1
840.00	839.70	2.5	190.4	6.47W	17.57S	18.54	0.3
870.00	869.68	2.1	167.6	6.47W	18.74S	19.69	0.3
900.00	899.66	1.3	168.8	6.29W	19.61S	20.50	0.3
930.00	929.66	1.3	200.1	6.34W	20.26S	21.15	0.2
960.00	959.65	1.5	205.3	6.63W	20.94S	21.87	0.1
990.00	989.63	1.8	204.6	6.99W	21.72S	22.71	0.1
1020.00	1019.62	2.0	200.4	7.36W	22.63S	23.69	0.1
1050.00	1049.59	2.7	188.9	7.66W	23.82S	24.91	0.3
1080.00	1079.56	2.5	185.9	7.83W	25.17S	26.26	0.1
1110.00	1109.53	2.5	187.2	7.98W	26.47S	27.57	0.0
1140.00	1139.50	2.6	183.4	8.10W	27.80S	28.89	0.1
1170.00	1169.47	2.9	182.2	8.17W	29.24S	30.31	0.1
1200.00	1199.43	3.0	182.4	8.24W	30.78S	31.83	0.0
1230.00	1229.38	3.5	183.6	8.32W	32.48S	33.51	0.2
1260.00	1259.33	3.3	184.7	8.45W	34.25S	35.27	0.1
1290.00	1289.28	3.0	188.9	8.64W	35.89S	36.91	0.1
1320.00	1319.24	3.0	183.0	8.81W	37.45S	38.47	0.1
1350.00	1349.20	3.2	183.0	8.89W	39.07S	40.07	0.1

4550 GYRO MULTISHOT SURVEY

D.DEPTH Meters	Vert.DEPTH Meters	Angle Deg	Azimut Deg	X(E/W) Departure	Y(N/S) (m)	PROJ Total	Dog.Leg Deg/10m
1380.00	1379.15	3.0	187.1	9.03W	40.69S	41.68	0.1
1406.00	1405.12	2.7	185.1	9.18W	41.97S	42.96	0.1

LA PROJECTION TOTALE EST CALCULEE LE LONG DE 192.34
LE DEPLACEMENT HORIZONTAL EST 42.96 m DANS L'AZIMUT 192.34

BRGM

GYRO MULTISHOT SURVEY

CHAMP : SOULTZ sous foret

CLUSTER :

PUITS : 4601

JOB ref: 150591

REFERENCES PHASE : 4 1/2"

COORDONNEES tete de puits :

X: 1003533.55
Y: 151165.3

REFERENCE profondeur: TETE DE PUITS

ELEVATION TABLE DE ROTATION : 0 m

REFERENCE DIRECTION : Nord Lambert

Repere utilise pour l'orientation : Pts 4589

COORDONNEES de Pts 4589

X : 1004890.75
Y : 151618.3

D.DEPTH Meters	Vert.DEPTH Meters	Angle Deg	Azimut Deg	X(E/W) Departure	Y(N/S) (m)	PROJ Total	Dog.Leg Deg/10m
30.00	30.00	0.1	242.1	0.01W	0.00S	-0.01	0.1
60.00	60.00	0.2	302.2	0.08W	0.01N	-0.06	0.1
90.00	90.00	0.4	277.1	0.22W	0.05N	-0.15	0.1
120.00	120.00	0.6	274.0	0.48W	0.08N	-0.36	0.1
150.00	150.00	0.6	278.0	0.80W	0.11N	-0.60	0.0
180.00	179.99	0.7	285.9	1.13W	0.18N	-0.83	0.0
210.00	209.99	0.8	289.9	1.50W	0.30N	-1.07	0.0
240.00	239.99	0.8	289.6	1.90W	0.45N	-1.31	0.0
270.00	269.99	0.9	303.6	2.29W	0.64N	-1.52	0.1
300.00	299.98	0.8	332.5	2.58W	0.96N	-1.59	0.1
330.00	329.98	0.7	339.5	2.74W	1.31N	-1.52	0.0
360.00	359.98	0.8	354.7	2.82W	1.69N	-1.37	0.1
390.00	389.97	1.1	12.0	2.78W	2.18N	-1.06	0.1
420.00	419.97	1.2	21.2	2.61W	2.76N	-0.59	0.1
450.00	449.96	1.3	17.5	2.39W	3.37N	-0.07	0.0
480.00	479.95	1.5	24.7	2.13W	4.06N	0.54	0.1
510.00	509.94	1.8	45.9	1.62W	4.74N	1.34	0.2
540.00	539.91	2.9	54.2	0.67W	5.51N	2.56	0.4
570.00	569.87	3.0	63.4	0.65E	6.30N	4.09	0.2
600.00	599.83	3.2	70.7	2.14E	6.93N	5.68	0.1
630.00	629.78	3.2	70.9	3.72E	7.48N	7.30	0.0
660.00	659.74	3.1	66.2	5.25E	8.08N	8.90	0.1
690.00	689.69	3.7	62.5	6.85E	8.85N	10.65	0.2
720.00	719.62	3.7	61.9	8.56E	9.76N	12.58	0.0
750.00	749.55	4.3	64.2	10.43E	10.70N	14.65	0.2
780.00	779.48	3.6	67.5	12.31E	11.55N	16.68	0.2
810.00	809.41	4.4	70.8	14.27E	12.29N	18.72	0.3
840.00	839.31	5.0	80.4	16.65E	12.89N	21.01	0.3
870.00	869.17	5.9	81.8	19.46E	13.32N	23.58	0.3
900.00	899.01	5.8	80.1	22.48E	13.81N	26.35	0.1
930.00	928.89	4.5	83.4	25.14E	14.20N	28.77	0.4
960.00	958.83	3.0	77.7	27.08E	14.50N	30.54	0.5
990.00	988.79	2.6	75.9	28.51E	14.84N	31.90	0.1
1020.00	1018.77	1.9	64.0	29.61E	15.22N	33.03	0.3
1050.00	1048.75	1.4	63.1	30.38E	15.60N	33.88	0.2
1080.00	1078.75	1.0	34.2	30.86E	15.98N	34.49	0.2
1110.00	1108.74	0.8	22.3	31.08E	16.39N	34.91	0.1
1140.00	1138.74	0.8	25.4	31.25E	16.77N	35.26	0.0
1170.00	1168.74	0.8	31.9	31.45E	17.14N	35.64	0.0
1200.00	1198.74	0.9	23.1	31.66E	17.54N	36.03	0.1
1230.00	1228.73	0.8	31.2	31.86E	17.93N	36.42	0.1
1260.00	1258.73	0.7	23.3	32.04E	18.28N	36.76	0.0
1290.00	1288.73	1.0	28.3	32.24E	18.68N	37.15	0.1
1320.00	1318.72	1.1	35.2	32.53E	19.14N	37.65	0.1
1350.00	1348.72	0.9	24.2	32.79E	19.59N	38.12	0.1

4601 GYRO MULTISHOT SURVEY

D.DEPTH Meters	Vert.DEPTH Meters	Angle Deg	Azimut Deg	X(E/W) Departure (m)	Y(N/S) (m)	PROJ Total	Dog.Leg Deg/10m
1380.00	1378.71	1.5	21.1	33.03E	20.18N	38.65	0.2
1410.00	1408.70	1.6	25.1	33.34E	20.92N	39.33	0.0
1440.00	1438.68	2.0	30.8	33.79E	21.75N	40.17	0.1
1470.00	1468.67	2.1	31.7	34.35E	22.67N	41.14	0.0
1500.00	1498.64	2.3	34.7	34.98E	23.63N	42.21	0.1
1515.00	1513.63	2.6	29.6	35.32E	24.17N	42.79	0.2

LA PROJECTION TOTALE EST CALCULEE LE LONG DE 55.61
LE DEPLACEMENT HORIZONTAL EST 42.79 m DANS L'AZIMUT 55.61

BRGM

GYRO MULTISHOT SURVEY

CHAMP : Soultz sous Forets

CLUSTER :

PUITS : 4589

JOB ref: 150591bis

REFERENCES PHASE : 4 1/2"

COORDONNEES tete de puits :

X: 1004890.75
Y: 151618.3

REFERENCE profondeur: TETE DE PUITS

ELEVATION TABLE DE ROTATION : 0 m

REFERENCE DIRECTION : NORD LAMBERT

Repere utilise pour l'orientation : Pts 4616

COORDONNEES de Pts 4616

X : 1004635.95
Y : 152447.55

D.DEPTH Meters	Vert.DEPTH Meters	Angle Deg	Azimut Deg	X(E/W) Departure	Y(N/S) (m)	PROJ Total	Dog.Leg Deg/10m
30.00	30.00	0.1	300.9	0.01W	0.00N	0.00	0.1
60.00	60.00	0.2	0.8	0.03W	0.07N	0.07	0.1
90.00	90.00	0.1	48.9	0.01W	0.14N	0.14	0.1
120.00	120.00	0.1	321.9	0.01W	0.18N	0.18	0.0
150.00	150.00	0.2	272.0	0.07W	0.20N	0.20	0.1
180.00	180.00	0.1	350.0	0.13W	0.23N	0.22	0.1
210.00	210.00	0.1	29.1	0.12W	0.27N	0.27	0.0
240.00	240.00	0.2	141.1	0.08W	0.25N	0.25	0.1
270.00	270.00	0.1	339.2	0.06W	0.24N	0.23	0.1
300.00	300.00	0.1	335.5	0.08W	0.29N	0.28	0.0
330.00	330.00	0.2	27.5	0.06W	0.36N	0.35	0.1
360.00	360.00	0.2	14.6	0.03W	0.45N	0.45	0.0
390.00	390.00	0.3	348.6	0.03W	0.58N	0.58	0.0
420.00	420.00	0.2	321.7	0.08W	0.70N	0.69	0.1
450.00	450.00	0.3	267.7	0.19W	0.74N	0.73	0.1
480.00	480.00	0.4	279.7	0.37W	0.75N	0.73	0.0
510.00	510.00	0.7	275.8	0.65W	0.79N	0.75	0.1
540.00	539.99	1.4	271.9	1.19W	0.82N	0.75	0.2
570.00	569.97	2.4	269.9	2.19W	0.83N	0.70	0.3
600.00	599.93	3.5	276.9	3.72W	0.94N	0.73	0.4
630.00	629.86	4.8	279.0	5.87W	1.24N	0.91	0.4
660.00	659.74	5.1	288.0	8.38W	1.85N	1.37	0.3
690.00	689.62	5.2	290.0	10.93W	2.73N	2.11	0.1
720.00	719.50	5.0	293.1	13.41W	3.71N	2.94	0.1
750.00	749.39	4.8	292.1	15.77W	4.69N	3.79	0.1
780.00	779.30	4.2	296.2	17.92W	5.65N	4.63	0.2
810.00	809.23	3.5	294.3	19.74W	6.51N	5.38	0.2
840.00	839.19	2.7	302.3	21.17W	7.26N	6.05	0.3
870.00	869.16	2.1	299.4	22.24W	7.91N	6.64	0.2
900.00	899.15	1.6	302.4	23.07W	8.40N	7.08	0.2
930.00	929.14	1.5	305.4	23.74W	8.85N	7.50	0.0
960.00	959.13	1.5	307.4	24.37W	9.32N	7.93	0.0
990.00	989.12	1.4	305.4	24.98W	9.77N	8.34	0.0
1020.00	1019.11	1.5	326.9	25.49W	10.31N	8.85	0.2
1050.00	1049.10	1.4	326.4	25.91W	10.94N	9.46	0.0
1080.00	1079.09	1.5	326.3	26.33W	11.57N	10.06	0.0
1110.00	1109.08	1.5	332.8	26.73W	12.25N	10.72	0.1
1140.00	1139.07	1.7	330.2	27.12W	12.98N	11.42	0.1
1170.00	1169.05	1.8	330.2	27.58W	13.77N	12.19	0.0
1200.00	1199.04	1.9	333.1	28.04W	14.62N	13.01	0.0
1230.00	1229.02	2.0	333.1	28.50W	15.53N	13.89	0.0
1260.00	1259.00	2.0	333.6	28.97W	16.47N	14.80	0.0
1290.00	1288.98	2.1	335.2	29.43W	17.43N	15.74	0.0
1320.00	1318.96	2.4	337.8	29.89W	18.50N	16.78	0.1
1350.00	1348.93	2.5	342.4	30.33W	19.71N	17.96	0.1

4589 GYRO MULTISHOT SURVEY

D.DEPTH Meters	Vert.DEPTH Meters	Angle Deg	Azimut Deg	X(E/W) Departure	Y(N/S) (m)	PROJ Total	Dog.Leg Deg/10m
1380.00	1378.90	2.8	344.0	30.73W	21.04N	19.27	0.1
1410.00	1408.87	2.5	347.1	31.08W	22.38N	20.59	0.1
1440.00	1438.84	2.9	349.1	31.37W	23.76N	21.95	0.1
1470.00	1468.79	3.2	354.2	31.60W	25.34N	23.51	0.1
1500.00	1498.74	3.5	359.3	31.69W	27.09N	25.25	0.1
1530.00	1528.68	3.7	357.4	31.75W	28.97N	27.13	0.1
1560.00	1558.61	4.1	5.5	31.69W	31.00N	29.16	0.2
1590.00	1588.53	4.6	10.3	31.37W	33.25N	31.42	0.2
1620.00	1618.42	5.0	13.3	30.86W	35.70N	33.90	0.2
1650.00	1648.30	5.5	17.7	30.12W	38.34N	36.58	0.2
1680.00	1678.15	5.8	21.1	29.14W	41.13N	39.41	0.1
1710.00	1707.98	6.4	23.7	27.92W	44.07N	42.42	0.2
1740.00	1737.77	7.1	27.7	26.39W	47.24N	45.67	0.3
1770.00	1767.50	8.5	30.1	24.42W	50.80N	49.34	0.5
1800.00	1797.15	9.0	34.0	22.00W	54.66N	53.33	0.3
1830.00	1826.74	9.9	37.4	19.12W	58.65N	57.48	0.4
1860.00	1856.25	10.8	42.4	15.66W	62.78N	61.79	0.4
1890.00	1885.69	11.5	45.3	11.65W	66.96N	66.20	0.3
1920.00	1915.03	12.6	47.2	7.12W	71.29N	70.77	0.4
1950.00	1944.21	14.2	48.0	1.99W	75.97N	75.74	0.5
1985.00	1978.08	15.0	49.4	4.64E	81.79N	81.92	0.3

LA PROJECTION TOTALE EST CALCULEE LE LONG DE 3.24
LE DEPLACEMENT HORIZONTAL EST 81.92 m DANS L'AZIMUT 3.24

ANNEX 2

List of events and locations

(X : Latitude - Y : Longitude - Z : Depths - In meters referred to GPK1 well head)

LIST OF THE EVENTS RECORDED AND LOCALIZED DURING THE PHASE 2A EXPERIMENTS

7 l/s EXPERIMENT

Exp.	Evt.	Date	Time	X	Y	Z	Amp.
1	10	11 Jul 1991	15:36:27				
1	11	11 Jul 1991	15:38:02				
1	12	11 Jul 1991	15:41:53				
1	14	11 Jul 1991	16:21:41	-10.1	-35.7	-2026.6	74
1	15	11 Jul 1991	16:38:28	-6.7	-45.3	-1980.5	57
1	16	11 Jul 1991	16:39:07				
1	17	11 Jul 1991	16:46:25	+14.9	-64.3	-2060.5	48
1	18	11 Jul 1991	16:47:37	+43.9	-60.4	-2064.0	40
1	19	11 Jul 1991	16:48:04	+18.3	-65.8	-2059.3	52
1	20	11 Jul 1991	16:49:47	+20.7	-63.3	-2061.3	245
1	21	11 Jul 1991	16:50:33	-23.1	-68.4	-1958.6	20
1	22	11 Jul 1991	16:58:42	-19.8	-53.2	-1964.8	45
1	23	11 Jul 1991	17:00:25	-.5	-55.8	-2065.9	109
1	24	11 Jul 1991	17:03:34	-4.1	-58.0	-1960.3	27
1	26	11 Jul 1991	17:27:54	-14.4	-33.1	-1991.9	408
1	27	11 Jul 1991	17:29:59				
1	31	11 Jul 1991	18:35:58				
1	32	11 Jul 1991	18:38:02	+8.5	-55.2	-2063.7	232
1	33	11 Jul 1991	18:40:48				
1	34	11 Jul 1991	19:33:52	+41.3	-25.3	-2097.8	405
1	36	11 Jul 1991	20:27:15	+11.5	-36.8	-2100.5	2742
1	37	11 Jul 1991	20:41:54	+71.5	-63.1	-2113.0	834
1	38	11 Jul 1991	21:40:20	-.6	-46.4	-2002.4	1266
1	39	11 Jul 1991	21:42:16	-12.6	-57.1	-2004.7	225
1	42	11 Jul 1991	22:33:37	+19.4	-103.7	-2071.0	1637
1	46	12 Jul 1991	00:21:51				
1	64	12 Jul 1991	15:45:27				
1	65	12 Jul 1991	15:58:33	+27.5	-50.7	-2061.5	800
1	66	12 Jul 1991	16:00:13	+22.8	-55.3	-2067.6	188
1	67	12 Jul 1991	16:08:45	+36.4	-35.1	-2062.2	984
1	68	12 Jul 1991	16:16:59	+6.0	-13.8	-2020.9	3474
1	101	12 Jul 1991	17:20:40	-10.5	-46.1	-1980.0	459
2	2	12 Jul 1991	18:34:04	+29.3	-110.4	-2114.8	605
2	4	12 Jul 1991	19:55:17	-36.9	-76.6	-2070.0	183
2	5	12 Jul 1991	20:08:22				
2	6	12 Jul 1991	20:13:47	+15.7	-19.5	-2128.9	341
2	7	12 Jul 1991	20:38:04	+34.0	-111.8	-1950.3	3499
2	8	12 Jul 1991	22:49:32	-136.3	+8.2	-2032.0	208
2	9	12 Jul 1991	22:51:53				
2	10	13 Jul 1991	00:19:58	+36.0	-53.7	-2102.1	3152
2	13	13 Jul 1991	01:22:33	-9.4	-18.3	-2015.0	122
2	15	13 Jul 1991	01:49:19				
2	16	13 Jul 1991	02:06:09	-7.1	-43.7	-1977.6	344
2	17	13 Jul 1991	02:19:16				
2	18	13 Jul 1991	04:10:00	-73.7	+50.7	-1963.1	1227
2	19	13 Jul 1991	05:28:57	+50.5	-36.7	-2147.6	1927
2	20	13 Jul 1991	05:51:39	+58.9	-105.2	-2133.9	1835
2	21	13 Jul 1991	05:56:08	-66.5	+46.3	-1956.2	3470
2	22	13 Jul 1991	06:25:04	-37.9	+34.8	-2000.8	317
2	23	13 Jul 1991	07:26:52	-71.0	+69.7	-2014.5	1036
2	24	13 Jul 1991	08:51:37	+104.5	-114.6	-2157.3	251
2	25	13 Jul 1991	09:34:11	+99.6	-102.3	-2158.5	389
2	26	13 Jul 1991	09:34:56				
2	27	13 Jul 1991	09:58:25	+32.6	-128.6	-2114.9	1021
2	28	13 Jul 1991	10:25:28	-13.8	+6.2	-2134.9	713

Exp.	Evt.	Date	Time	X	Y	Z	Amp.
2	29	13 Jul 1991	10:33:29				
2	30	13 Jul 1991	11:02:44				
2	31	13 Jul 1991	11:18:11				
2	32	13 Jul 1991	11:18:37				
2	33	13 Jul 1991	12:00:06				
2	34	13 Jul 1991	12:00:22				
2	35	13 Jul 1991	12:23:05				
2	36	13 Jul 1991	12:34:32	+4.8	-71.3	-2100.3	1410
2	37	13 Jul 1991	12:55:02	+27.9	+57.9	-1965.4	204
2	38	13 Jul 1991	13:16:07	-80.2	+55.8	-1997.6	115
2	39	13 Jul 1991	13:48:09				
2	40	13 Jul 1991	14:10:12	+14.3	-145.4	-2087.7	573
2	41	13 Jul 1991	14:15:07				
2	42	13 Jul 1991	14:15:19	-48.6	+23.0	-2137.5	309
2	43	13 Jul 1991	14:19:58				
2	44	13 Jul 1991	15:48:13				
2	46	13 Jul 1991	16:12:47	-61.4	+95.0	-2030.5	1490
2	47	13 Jul 1991	16:28:50				
2	48	13 Jul 1991	16:41:24				
2	49	13 Jul 1991	16:52:07	-38.8	+5.5	-2053.5	238
2	50	13 Jul 1991	16:59:48	-10.1	-93.9	-1932.8	3497
2	51	13 Jul 1991	17:11:40	-13.8	+6.5	-1955.8	123
2	52	13 Jul 1991	17:20:44	-40.3	+103.0	-2058.8	1071
2	53	13 Jul 1991	17:24:59	-65.0	+76.0	-2083.7	344
2	54	13 Jul 1991	17:35:32				
2	55	13 Jul 1991	17:41:32				
2	56	13 Jul 1991	17:53:48	+52.4	-41.5	-2141.5	1268
2	58	13 Jul 1991	18:07:14				
2	59	13 Jul 1991	18:08:15				
2	60	13 Jul 1991	18:26:58				
2	61	13 Jul 1991	20:05:11				
2	63	13 Jul 1991	21:11:18				
2	64	13 Jul 1991	21:31:22	-47.0	+4.7	-2069.5	352
2	66	13 Jul 1991	23:08:43	+30.0	+38.0	-2220.7	468
2	67	13 Jul 1991	23:52:13				
2	68	14 Jul 1991	00:03:53				
2	69	14 Jul 1991	00:43:48	+21.0	-1.5	-2116.3	492
2	70	14 Jul 1991	02:17:13				
2	73	14 Jul 1991	03:36:59				
2	74	14 Jul 1991	03:53:16				
2	75	14 Jul 1991	04:44:00				
2	76	14 Jul 1991	04:45:00	-63.4	+17.5	-2195.5	808
2	77	14 Jul 1991	04:51:42				
2	78	14 Jul 1991	05:52:09				
2	79	14 Jul 1991	06:29:36				
2	80	14 Jul 1991	06:42:20				
2	81	14 Jul 1991	06:59:17	+41.1	-121.4	-2109.1	327
2	82	14 Jul 1991	07:02:09				
2	83	14 Jul 1991	07:10:35	-79.5	+59.6	-2107.4	295
2	84	14 Jul 1991	07:58:48				
2	85	14 Jul 1991	08:10:17	-117.6	+35.6	-2170.6	845
2	86	14 Jul 1991	08:23:32	+15.3	-98.2	-1988.0	2389
2	87	14 Jul 1991	08:33:01	-88.8	+21.1	-2202.3	1659
2	88	14 Jul 1991	08:43:26				
2	89	14 Jul 1991	09:17:34	-73.9	-50.8	-2083.8	243

Exp.	Evt.	Date	Time	X	Y	Z	Amp.
2	90	14 Jul 1991	09:23:03				
2	91	14 Jul 1991	09:33:34				
2	92	14 Jul 1991	10:15:03				
2	94	14 Jul 1991	10:37:03				
2	95	14 Jul 1991	10:42:33	+28.5	-150.1	-2077.5	635
2	96	14 Jul 1991	10:48:24				
2	97	14 Jul 1991	11:01:31				
2	99	14 Jul 1991	12:06:52	+176.7	-108.0	-2141.8	247
2	100	14 Jul 1991	13:01:51				
2	101	14 Jul 1991	13:22:20				
2	102	14 Jul 1991	13:39:11				
2	103	14 Jul 1991	13:51:39				
2	104	14 Jul 1991	14:19:01	+63.2	-112.6	-2153.2	449
2	105	14 Jul 1991	15:00:38				
2	106	14 Jul 1991	15:01:40				
2	109	14 Jul 1991	16:02:17				
2	111	14 Jul 1991	16:34:12				
2	112	14 Jul 1991	16:59:43				
2	114	14 Jul 1991	18:06:14				
2	115	14 Jul 1991	18:12:33				
2	118	14 Jul 1991	22:49:44				
2	132	15 Jul 1991	03:30:06				

LIST OF THE EVENTS RECORDED AND LOCALIZED DURING THE PHASE 2A EXPERIMENTS

15 1/s EXPERIMENT

Exp.	Evt.	Date	Time	X	Y	Z	Amp.
3	11	18 Jul 1991	09:40:03	+26.5	-5.4	-2042.1	1021
3	12	18 Jul 1991	09:50:35	-17.0	-33.4	-2001.5	143
3	13	18 Jul 1991	09:58:17	-24.8	-20.0	-2022.6	216
3	14	18 Jul 1991	10:06:33	-41.5	-84.1	-1922.4	99
3	15	18 Jul 1991	10:09:56	+.6	-.8	-2040.1	166
3	16	18 Jul 1991	10:10:10	+28.9	-54.5	-2052.8	868
3	17	18 Jul 1991	10:10:22	+23.6	-55.4	-2053.6	1013
3	18	18 Jul 1991	10:10:35	+24.8	-51.8	-2060.9	1006
3	19	18 Jul 1991	10:11:08	-8.0	-41.3	-1983.3	404
3	20	18 Jul 1991	10:13:10	+9.4	-48.9	-2054.6	1609
3	21	18 Jul 1991	10:15:10	+21.4	-56.0	-2051.7	1637
3	22	18 Jul 1991	10:21:53				
3	24	18 Jul 1991	10:24:21				
3	26	18 Jul 1991	10:30:04	-21.7	-28.5	-2147.1	2263
3	27	18 Jul 1991	10:45:01	+12.7	-63.4	-2050.1	272
3	29	18 Jul 1991	11:08:15	-25.1	-43.2	-1961.1	79
3	30	18 Jul 1991	11:24:12	-14.4	+8.2	-2024.7	446
3	31	18 Jul 1991	11:39:58	-8.6	-146.8	-1929.5	3480
3	32	18 Jul 1991	11:56:23				
3	33	18 Jul 1991	12:09:01				
3	35	18 Jul 1991	12:35:19	+1.7	-48.2	-2076.5	780
3	36	18 Jul 1991	12:44:37	-7.1	-147.6	-1936.5	663
3	37	18 Jul 1991	12:56:51	+37.0	-1.4	-2020.1	122
3	38	18 Jul 1991	13:26:53	+11.2	-141.4	-1960.9	1050
3	40	18 Jul 1991	14:19:46	+56.2	-69.9	-2098.4	227
3	41	18 Jul 1991	14:21:35	+62.4	-103.2	-2015.6	1235
3	42	18 Jul 1991	14:21:55	+81.9	-96.9	-2035.3	3491
3	43	18 Jul 1991	14:22:22	-23.1	-39.1	-1966.5	237
3	44	18 Jul 1991	14:38:12	+43.6	-48.2	-2108.3	673
3	45	18 Jul 1991	14:46:15	+2.3	-17.4	-2111.2	1764
3	46	18 Jul 1991	14:53:40				
3	47	18 Jul 1991	15:03:37	-14.5	-66.9	-2087.5	586
3	48	18 Jul 1991	15:11:13	-17.2	+15.1	-1966.7	175
3	49	18 Jul 1991	15:16:11	-25.9	-77.6	-1903.7	198
3	50	18 Jul 1991	15:40:48	+38.6	-63.1	-2085.1	1042
3	51	18 Jul 1991	16:12:15	-13.8	-27.2	-1994.8	92
3	52	18 Jul 1991	16:17:40				
3	53	18 Jul 1991	16:17:52	+8.7	-47.8	-2104.6	1007
3	54	18 Jul 1991	16:33:46	+41.3	-110.2	-2113.6	413
3	56	18 Jul 1991	17:15:59	+39.8	-53.9	-2132.5	1816
3	57	18 Jul 1991	17:49:16	+83.9	-54.7	-2177.2	457
3	58	18 Jul 1991	17:50:50	-8.8	-19.2	-1997.9	229
3	59	18 Jul 1991	17:52:51	+31.8	-67.8	-2101.7	746
3	60	18 Jul 1991	18:06:59	+25.3	-128.7	-1966.2	229
3	61	18 Jul 1991	18:15:52	-21.5	-15.9	-1934.7	3486
3	62	18 Jul 1991	18:25:48				
3	63	18 Jul 1991	18:48:08				
3	64	18 Jul 1991	19:49:59				
3	67	18 Jul 1991	20:22:58	-25.4	-21.3	-1985.2	432
3	68	18 Jul 1991	20:27:41				
3	69	18 Jul 1991	20:39:05				
3	71	18 Jul 1991	20:53:36	+16.0	-104.9	-2046.4	250
3	72	18 Jul 1991	20:54:14	-87.2	+1.5	-2128.9	311
3	82	18 Jul 1991	21:12:24	-24.2	-17.1	-1928.2	1163
3	84	18 Jul 1991	21:47:08				

Exp.	Evt.	Date	Time	X	Y	Z	Amp.
3	86	18 Jul 1991	22:52:37				
3	89	19 Jul 1991	00:32:52	+49.9	-73.8	-2097.1	144
3	90	19 Jul 1991	01:22:52	+91.0	+102.5	-2200.6	302
3	92	19 Jul 1991	01:34:37				
3	93	19 Jul 1991	02:01:38	-7.3	+63.0	-2230.8	588
3	94	19 Jul 1991	02:15:28	-45.5	-20.2	-1958.9	585
3	95	19 Jul 1991	02:36:58	-57.9	+24.4	-2145.1	386
3	96	19 Jul 1991	02:41:51	+44.1	-140.9	-1948.1	2406
3	97	19 Jul 1991	02:59:15				
3	98	19 Jul 1991	03:05:50				
3	99	19 Jul 1991	03:08:47				
3	100	19 Jul 1991	03:10:16	-29.3	+51.6	-2175.1	265
3	101	19 Jul 1991	04:09:29	-62.4	+16.2	-2206.8	874
3	102	19 Jul 1991	04:19:20	-34.5	+32.8	-2194.6	459
3	103	19 Jul 1991	04:42:03	-39.3	+75.2	-2155.9	410
3	104	19 Jul 1991	04:53:38	-18.8	+70.5	-2034.1	593
3	105	19 Jul 1991	04:59:46	-78.7	+89.3	-2164.7	200
3	106	19 Jul 1991	05:10:35	-45.1	+36.6	-2108.9	74
3	107	19 Jul 1991	05:22:43	-11.8	+79.6	-2160.4	778
3	108	19 Jul 1991	05:37:03				
3	109	19 Jul 1991	05:51:32	-41.6	+98.2	-2107.0	95
3	110	19 Jul 1991	05:53:41				
3	111	19 Jul 1991	06:06:45	-78.1	+45.0	-2239.8	1490
3	112	19 Jul 1991	06:31:07				
3	113	19 Jul 1991	06:33:52				
3	114	19 Jul 1991	06:42:54				
3	115	19 Jul 1991	06:56:13				
3	116	19 Jul 1991	06:56:48	-59.8	+48.8	-2222.6	303
3	118	19 Jul 1991	07:03:38	-111.7	+72.5	-2168.7	770
3	119	19 Jul 1991	07:09:02	-102.2	+74.6	-2163.9	768
3	120	19 Jul 1991	07:43:32	-64.6	-4.2	-2189.4	497
3	121	19 Jul 1991	07:45:51				
3	122	19 Jul 1991	08:03:41	-77.3	-20.5	-2207.1	756
3	123	19 Jul 1991	08:09:11	-68.3	+77.0	-2163.6	413
3	124	19 Jul 1991	08:26:35	-75.8	-30.1	-2123.7	968
3	125	19 Jul 1991	08:28:13				
3	126	19 Jul 1991	08:38:14	-67.8	+76.9	-2161.0	366
3	127	19 Jul 1991	08:45:20	-58.2	+80.3	-2228.5	139
3	128	19 Jul 1991	08:52:28	-76.3	+50.4	-1932.1	95
3	129	19 Jul 1991	09:00:06				
3	130	19 Jul 1991	09:04:48	-87.4	+62.2	-2197.1	3475
3	134	19 Jul 1991	10:12:59	-54.7	+94.5	-2057.0	175
3	135	19 Jul 1991	10:22:40	-52.8	+75.0	-2168.9	150
3	136	19 Jul 1991	10:23:25				
3	137	19 Jul 1991	10:26:27	-65.9	+77.6	-2166.7	149
3	138	19 Jul 1991	10:37:56	-103.4	+32.6	-2230.4	895
3	139	19 Jul 1991	10:39:49	-59.4	+94.7	-2184.2	676
3	140	19 Jul 1991	10:58:55				
3	141	19 Jul 1991	11:03:19	-43.8	-51.0	-1939.6	317
3	142	19 Jul 1991	11:09:16				
3	143	19 Jul 1991	11:10:14				
3	144	19 Jul 1991	11:13:13	-57.5	+55.7	-2223.4	243
3	145	19 Jul 1991	11:17:12	-88.6	+56.7	-2208.6	183
3	146	19 Jul 1991	11:19:34	+8.7	-148.6	-1904.2	1567
3	147	19 Jul 1991	11:26:22	-81.9	+60.7	-2200.5	267

Exp.	Evt.	Date	Time	X	Y	Z	Amp.
3	148	19 Jul 1991	11:29:35	-97.0	+23.8	-2228.4	1130
3	149	19 Jul 1991	11:30:46				
3	151	19 Jul 1991	11:41:47	+51.9	-36.4	-2089.0	3474
3	153	19 Jul 1991	11:57:16				
3	154	19 Jul 1991	12:11:23	-34.0	+27.0	-2190.6	468
3	155	19 Jul 1991	12:30:37				
3	156	19 Jul 1991	12:55:45	-127.2	+16.0	-2212.9	1615
3	157	19 Jul 1991	13:04:49	-36.5	+39.3	-2214.1	455
3	158	19 Jul 1991	13:21:10	+36.9	-24.5	-2092.8	3376
3	159	19 Jul 1991	13:21:24	+44.5	-25.1	-2101.2	1616
3	160	19 Jul 1991	13:22:28				
3	161	19 Jul 1991	13:23:26				
3	162	19 Jul 1991	13:45:17	-85.8	+48.3	-2244.2	399
3	163	19 Jul 1991	14:02:10	-51.2	+29.7	-2216.2	1788
3	164	19 Jul 1991	14:03:23				
3	165	19 Jul 1991	14:03:37				
3	166	19 Jul 1991	14:09:46	-50.5	+29.5	-2208.0	792
3	167	19 Jul 1991	14:11:36	-59.6	+8.8	-2191.3	310
3	169	19 Jul 1991	14:50:08	-35.7	+73.1	-2195.8	295
3	171	19 Jul 1991	15:38:26				
3	172	19 Jul 1991	16:08:52				
3	173	19 Jul 1991	16:16:07				
3	176	19 Jul 1991	16:56:37	-55.1	+35.5	-2238.3	398
3	177	19 Jul 1991	17:34:11	-97.6	+61.1	-2011.0	103
3	178	19 Jul 1991	17:49:48	-108.4	+56.4	-2214.6	245
3	179	19 Jul 1991	17:57:03				
3	181	19 Jul 1991	18:20:05				
3	182	19 Jul 1991	18:29:28				
3	183	19 Jul 1991	18:35:26	-15.8	+85.7	-2188.5	3167
3	184	19 Jul 1991	19:16:06				
3	186	19 Jul 1991	19:24:50				
3	188	19 Jul 1991	19:31:54	-57.1	+80.2	-2171.6	804
3	189	19 Jul 1991	19:37:13	-92.0	+43.0	-2233.3	488
3	190	19 Jul 1991	19:41:16				
3	191	19 Jul 1991	20:54:17	-81.1	+73.0	-2177.7	1267
3	192	19 Jul 1991	21:09:33				
3	193	19 Jul 1991	21:32:38	-57.7	+86.4	-2196.7	583
3	194	19 Jul 1991	22:06:55				
3	195	19 Jul 1991	22:12:45	-105.7	+46.4	-2225.2	2402
3	197	19 Jul 1991	22:27:52	-92.2	+96.9	-1994.8	79
3	198	19 Jul 1991	22:29:39	-109.4	+40.3	-2228.5	834
3	199	19 Jul 1991	22:40:34				
3	200	19 Jul 1991	22:41:40	-38.6	+67.5	-2179.8	1973
3	201	19 Jul 1991	22:43:56				
3	202	19 Jul 1991	22:52:03	+21.6	-45.7	-2081.9	223
3	203	19 Jul 1991	22:52:53	-89.3	-10.0	-2198.1	521
3	204	19 Jul 1991	23:45:04	-35.1	+59.5	-2173.2	349
3	205	19 Jul 1991	23:45:58	-94.3	+59.4	-2187.9	795
3	206	19 Jul 1991	23:46:10	-37.6	+55.2	-2170.9	254
3	207	19 Jul 1991	23:57:36	-49.0	+83.8	-2097.5	100
3	208	20 Jul 1991	00:23:45				
3	209	20 Jul 1991	00:25:49	-59.7	+45.7	-2152.3	140
3	210	20 Jul 1991	00:57:43	-35.0	+63.9	-2172.8	774
3	211	20 Jul 1991	00:59:34	-147.7	-15.9	-2202.2	983
3	212	20 Jul 1991	01:07:40	-58.8	+44.8	-2161.1	363

Exp.	Evt.	Date	Time	X	Y	Z	Amp.
3	213	20 Jul 1991	01:19:54				
3	214	20 Jul 1991	02:11:26	-46.7	+98.3	-2185.5	1140
3	215	20 Jul 1991	02:40:08				
3	216	20 Jul 1991	02:41:38	-65.5	+10.2	-2192.2	375
3	217	20 Jul 1991	03:01:12				
3	218	20 Jul 1991	03:06:09	-89.9	-70.9	-2034.5	236
3	219	20 Jul 1991	03:16:43				
3	220	20 Jul 1991	03:38:11				
3	221	20 Jul 1991	03:42:14	-15.1	+58.5	-2165.0	353
3	222	20 Jul 1991	04:00:21	-19.2	+76.4	-2167.2	3496
3	223	20 Jul 1991	04:13:58	-56.2	+48.3	-2215.9	1667
3	224	20 Jul 1991	04:23:25	+122.4	-225.8	-1940.8	1917
3	225	20 Jul 1991	04:24:37				
3	226	20 Jul 1991	04:25:48	-23.7	+67.4	-2175.2	780
3	227	20 Jul 1991	04:34:10	-11.8	+74.4	-2173.1	2192
3	228	20 Jul 1991	04:34:33	-91.0	+61.5	-2210.7	1470
3	230	20 Jul 1991	05:05:27	-87.9	+46.3	-2254.4	348
3	231	20 Jul 1991	05:39:03	+45.4	-147.0	-1948.6	696
3	232	20 Jul 1991	05:46:28	-7.6	-47.8	-1993.5	1709
3	233	20 Jul 1991	05:48:21	-39.1	-29.4	-1868.5	2985
3	234	20 Jul 1991	06:05:52	-102.7	+4.0	-2212.0	1335
3	235	20 Jul 1991	06:43:38	-36.2	-15.1	-2100.0	366
3	236	20 Jul 1991	07:22:31				
3	237	20 Jul 1991	08:25:45	+29.5	-151.2	-1932.4	3479
3	238	20 Jul 1991	08:45:38	-10.5	+32.5	-1946.7	227
3	239	20 Jul 1991	08:48:45	-34.8	+71.2	-2172.8	328
3	240	20 Jul 1991	09:04:25	-96.7	-6.1	-2118.0	204
3	241	20 Jul 1991	09:23:29	-79.8	+28.4	-2196.9	525
3	242	20 Jul 1991	09:31:43	-104.0	-10.7	-2240.8	2650
3	243	20 Jul 1991	10:15:29	-113.0	+4.3	-2229.8	869
3	244	20 Jul 1991	10:35:44				
3	245	20 Jul 1991	10:36:48				
3	246	20 Jul 1991	10:38:17	-83.4	+78.3	-2045.2	131
3	247	20 Jul 1991	11:06:13	-6.6	+25.5	-1967.1	221
3	248	20 Jul 1991	11:08:11	-86.5	+27.0	-2225.5	542
3	249	20 Jul 1991	11:11:38	+1.1	-66.2	-1974.0	735
3	250	20 Jul 1991	11:41:03	-1.8	-181.9	-1932.2	856
3	251	20 Jul 1991	11:51:45	-15.1	+36.1	-1976.8	815
3	252	20 Jul 1991	12:00:50	-111.9	+12.4	-2211.3	2716
3	253	20 Jul 1991	12:03:24	-106.9	+10.4	-2214.2	2284
3	254	20 Jul 1991	12:09:41	-107.0	+34.2	-2236.1	182
3	255	20 Jul 1991	12:15:32				
3	256	20 Jul 1991	12:28:16	-31.3	-63.3	-1966.0	295
3	258	20 Jul 1991	13:07:14	-98.5	+17.1	-2223.1	2698
3	259	20 Jul 1991	13:07:38	-72.0	+23.2	-2235.4	326
3	260	20 Jul 1991	13:11:33	-65.7	+17.5	-2182.5	425
3	266	20 Jul 1991	13:53:29	-129.8	+28.0	-2247.2	576
3	267	20 Jul 1991	14:27:06	-123.1	+41.4	-2193.1	571
3	268	20 Jul 1991	14:41:16	-79.7	-2.8	-2247.8	3286
3	269	20 Jul 1991	15:04:04				
3	270	20 Jul 1991	15:54:20				

LIST OF THE EVENTS RECORDED AND LOCALIZED DURING THE PHASE 2A EXPERIMENTS

POST_STIMULATION EXPERIMENT

Exp.	Evt.	Date	Time	X	Y	Z	Amp.
4	2	20 Jul 1991	16:13:04				
4	3	20 Jul 1991	17:06:32				
4	5	20 Jul 1991	17:39:26				
4	6	20 Jul 1991	18:01:25				
4	7	20 Jul 1991	19:01:22				
4	8	20 Jul 1991	19:38:40				
4	9	20 Jul 1991	20:03:57	+40.3	+144.7	-1815.9	178
4	10	20 Jul 1991	20:16:44	-102.0	-28.0	-2215.9	1589
4	11	20 Jul 1991	21:06:20				
4	13	20 Jul 1991	21:50:57	-95.9	+20.1	-2251.8	3491
4	16	20 Jul 1991	23:36:11				
4	17	20 Jul 1991	23:48:30	-48.7	-52.2	-1829.4	117
4	18	20 Jul 1991	23:59:19	+42.5	+84.6	-1991.2	194
4	19	21 Jul 1991	00:09:40				
4	20	21 Jul 1991	00:27:33				
4	21	21 Jul 1991	00:41:41	-76.8	-21.2	-2207.9	966
4	26	21 Jul 1991	07:37:10	-98.6	+61.7	-2258.7	316
4	33	21 Jul 1991	13:05:57				
4	34	21 Jul 1991	16:55:35				
4	43	22 Jul 1991	11:13:05	-174.2	-63.4	-2162.2	2307
4	44	22 Jul 1991	14:24:56				
4	54	22 Jul 1991	20:35:38				
4	59	23 Jul 1991	01:45:10				
4	82	24 Jul 1991	08:52:35	-69.6	-1.7	-1898.0	82
4	84	24 Jul 1991	11:12:11				
5	20	26 Jul 1991	07:41:34				
5	22	26 Jul 1991	09:49:32				
5	32	26 Jul 1991	23:54:44				
5	34	27 Jul 1991	03:51:03				
5	44	27 Jul 1991	23:39:50				
5	50	28 Jul 1991	11:25:37	-107.7	-45.9	-1907.2	175
5	51	28 Jul 1991	15:37:25	+10.5	+97.0	-2015.1	522
5	54	28 Jul 1991	19:36:59	-38.4	-32.1	-2201.8	743
5	55	28 Jul 1991	19:58:50	+22.7	+25.0	-1923.1	624
5	56	28 Jul 1991	21:05:32				
5	57	28 Jul 1991	22:34:01				
5	61	29 Jul 1991	11:05:47				
5	82	1 Aug 1991	04:11:01				
5	94	4 Aug 1991	14:21:26				

ANNEX 3

Seismic event examples

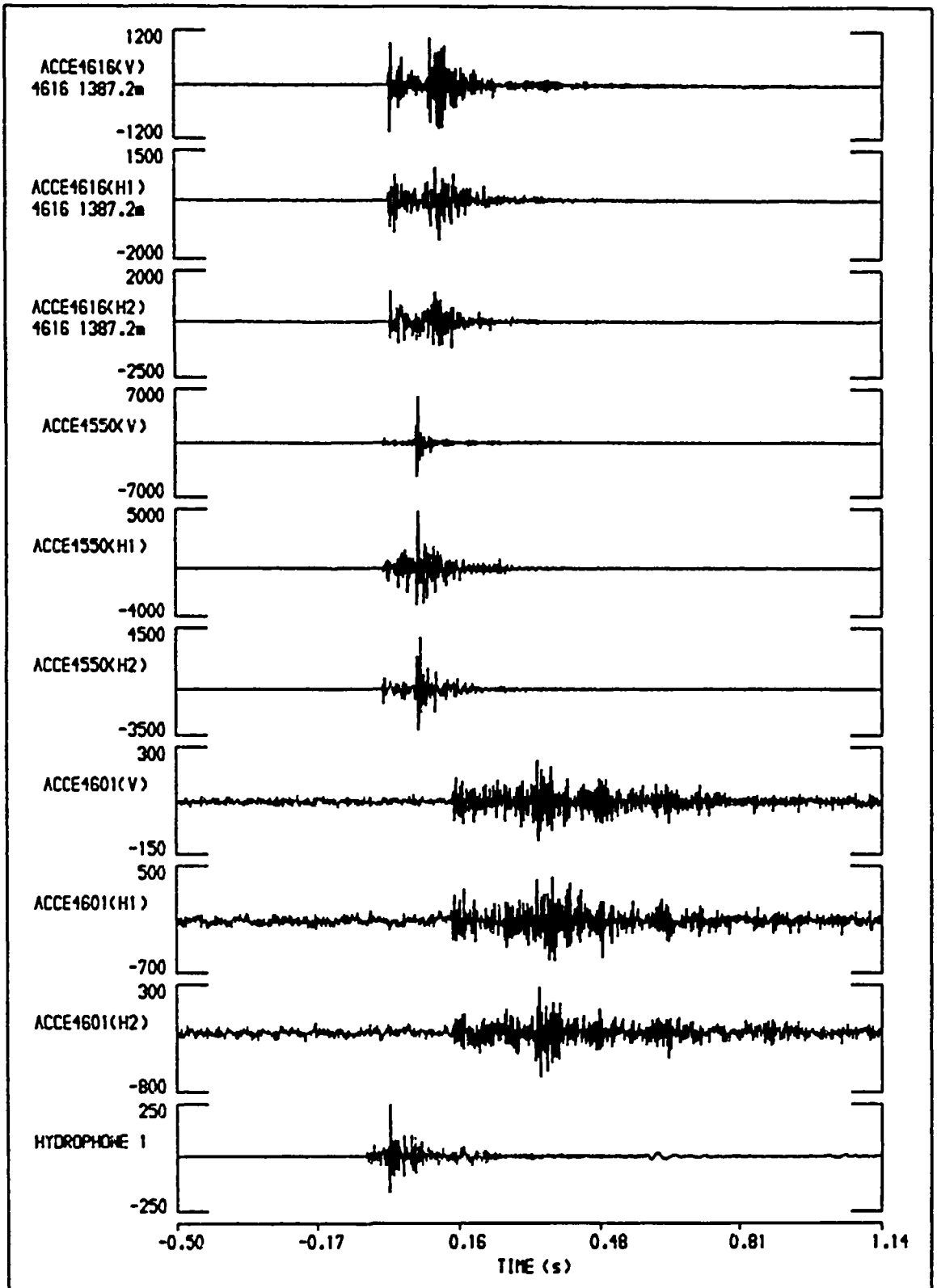

TEST STZSTI01 Event N° 26 Time : 11 Jul 1991 17:27:54.51

Event location : X = -14 m Y = -33 m Z = -1992 m

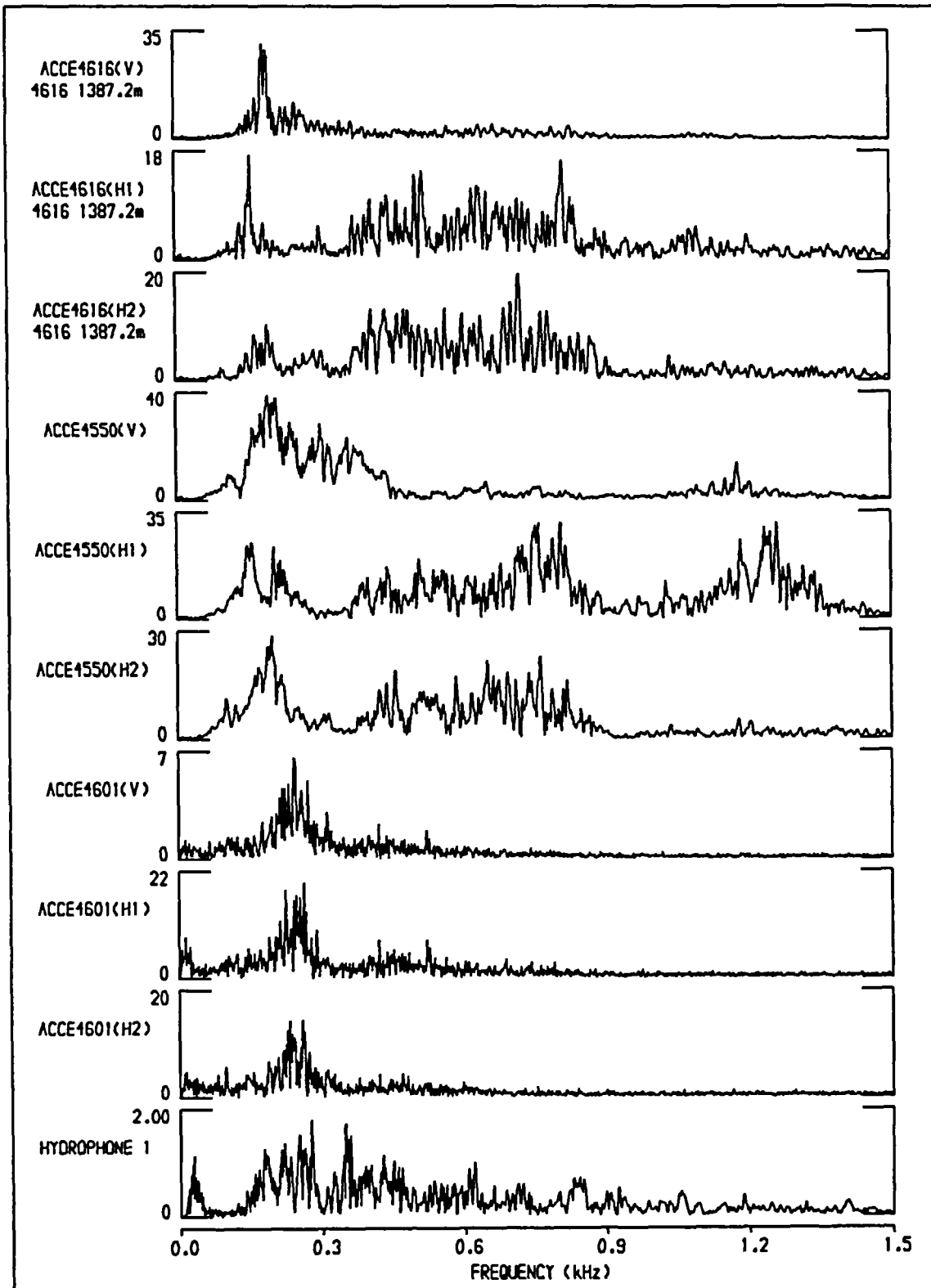

TEST STZSTI01 Event N° 26 Time : 11 Jul 1991 17:27:54.51

Event location : X = -14 m Y = -33 m Z = -1992 m

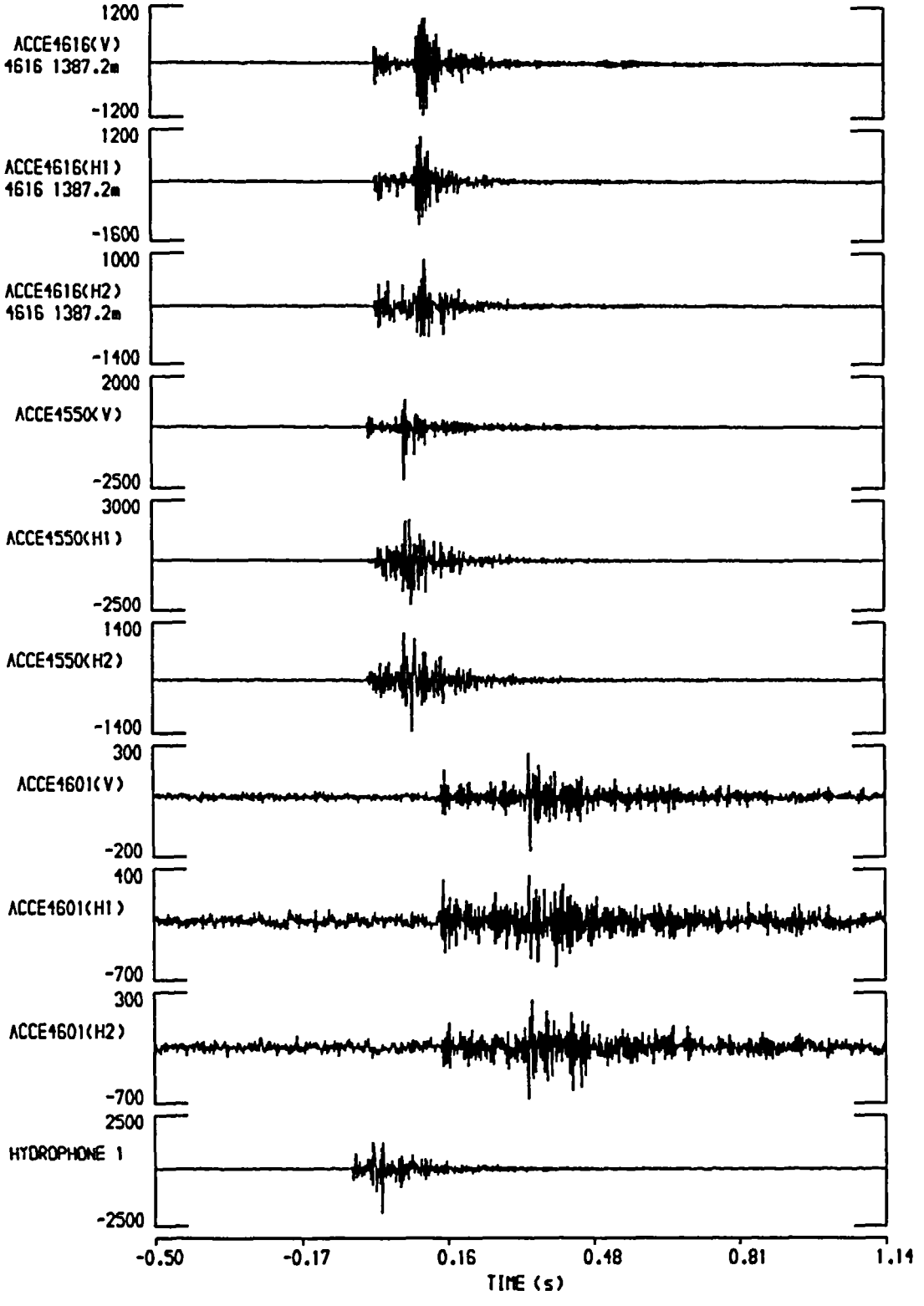

TEST STZSTI01 Event N° 68 Time : 12 Jul 1991 16:16:59.66

Event location : X = 6 m Y = -14 m Z = -2021 m

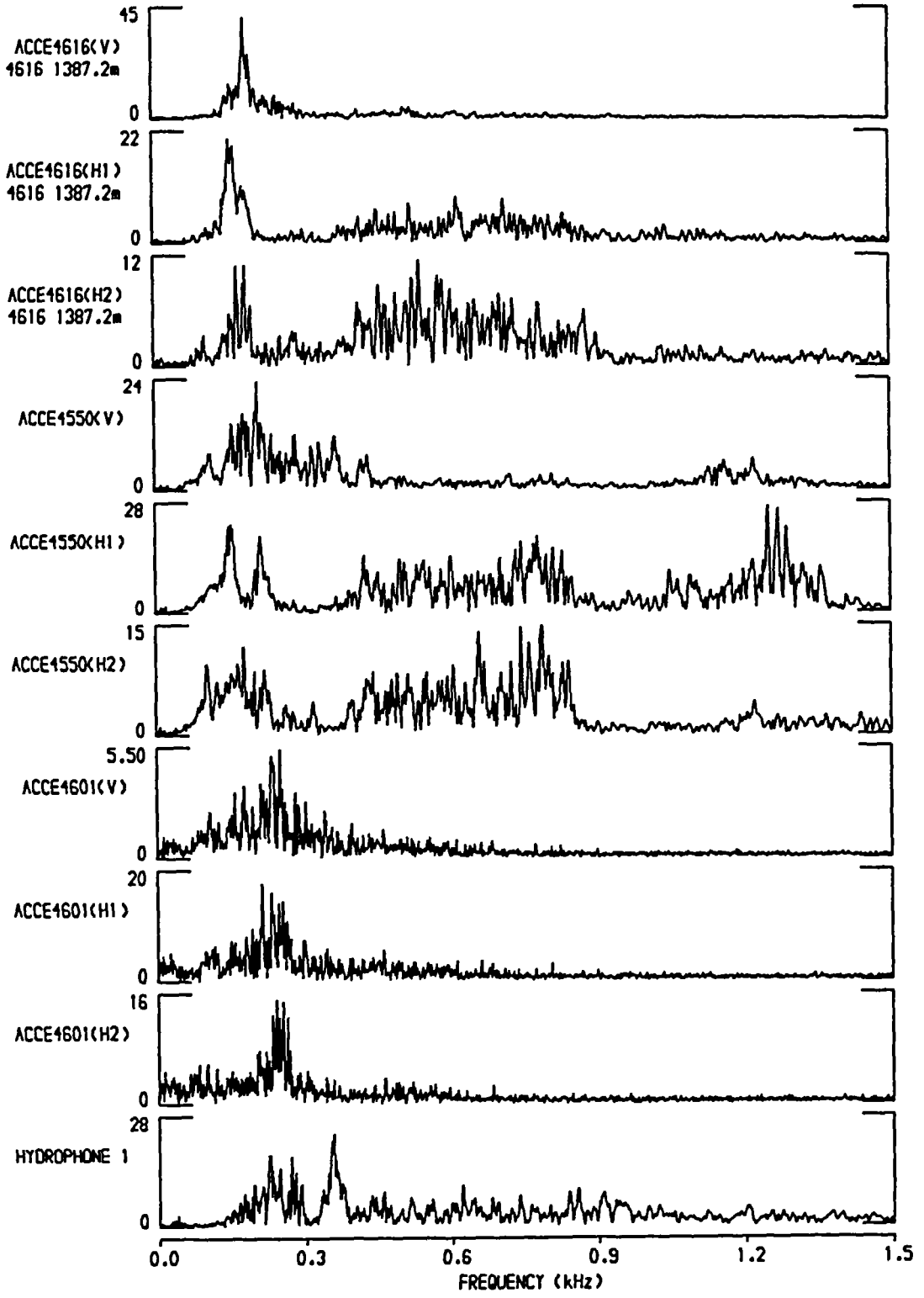

TEST STZSTI01 Event N° 68 Time : 12 Jul 1991 16:16:59.66

Event location : X = 6 m Y = -14 m Z = -2021 m

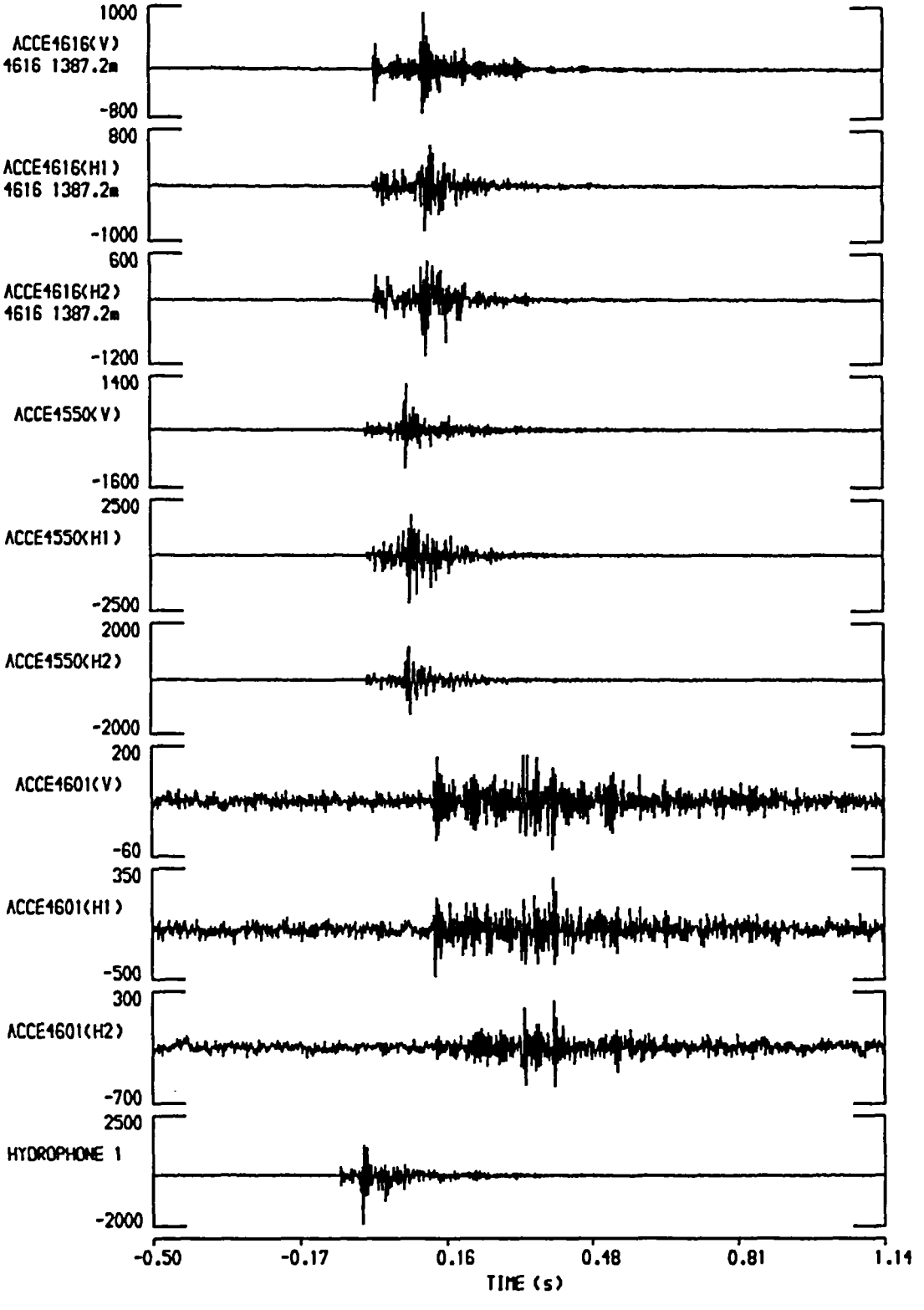

TEST STZSTI02 Event N° 10 Time : 13 Jul 1991 00:19:58.98

Event location : X = 36 m Y = -54 m Z = -2102 m

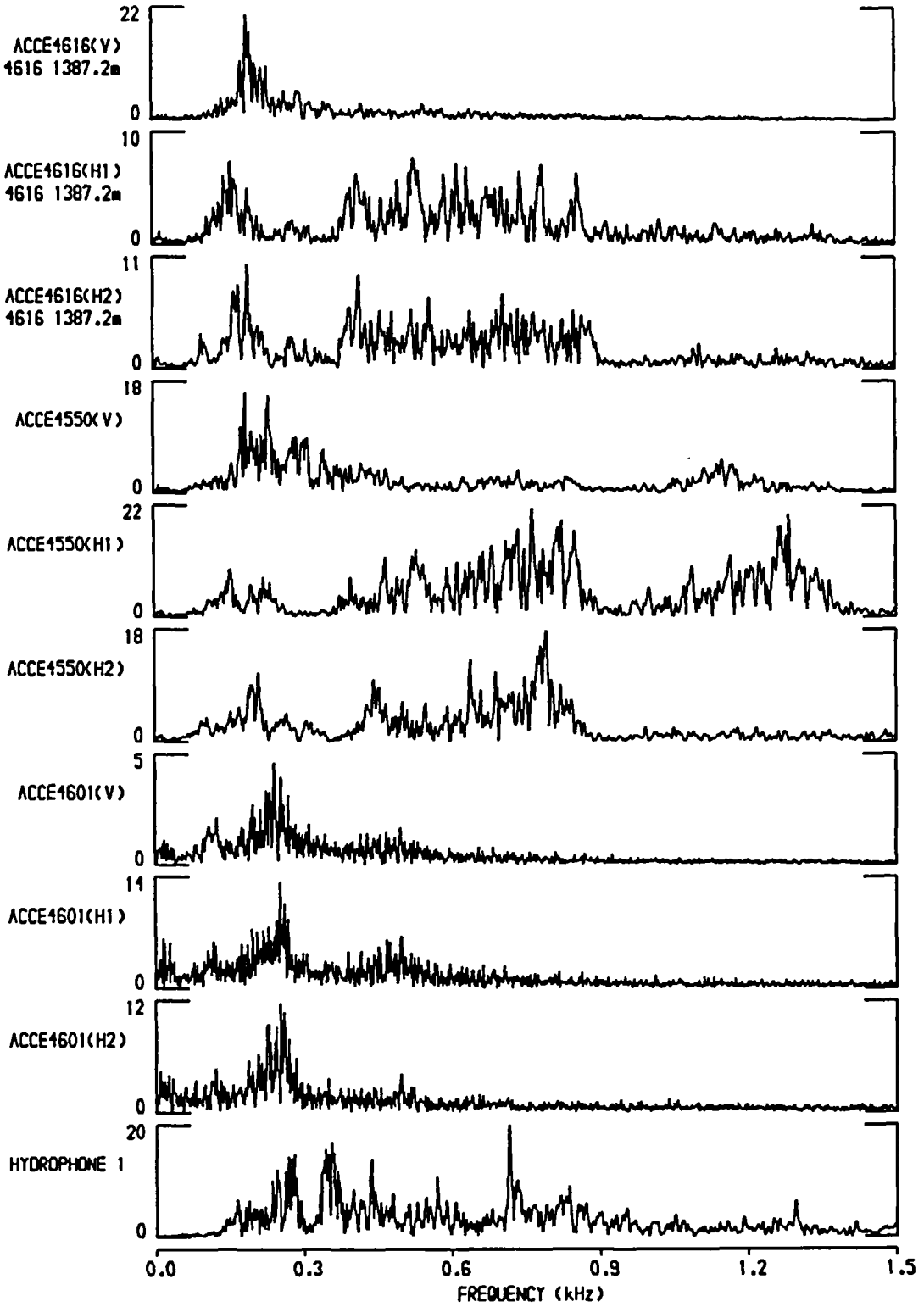

TEST STZSTI02 Event N° 10 Time : 13 Jul 1991 00:19:58.98

Event location : X = 36 m Y = -54 m Z = -2102 m

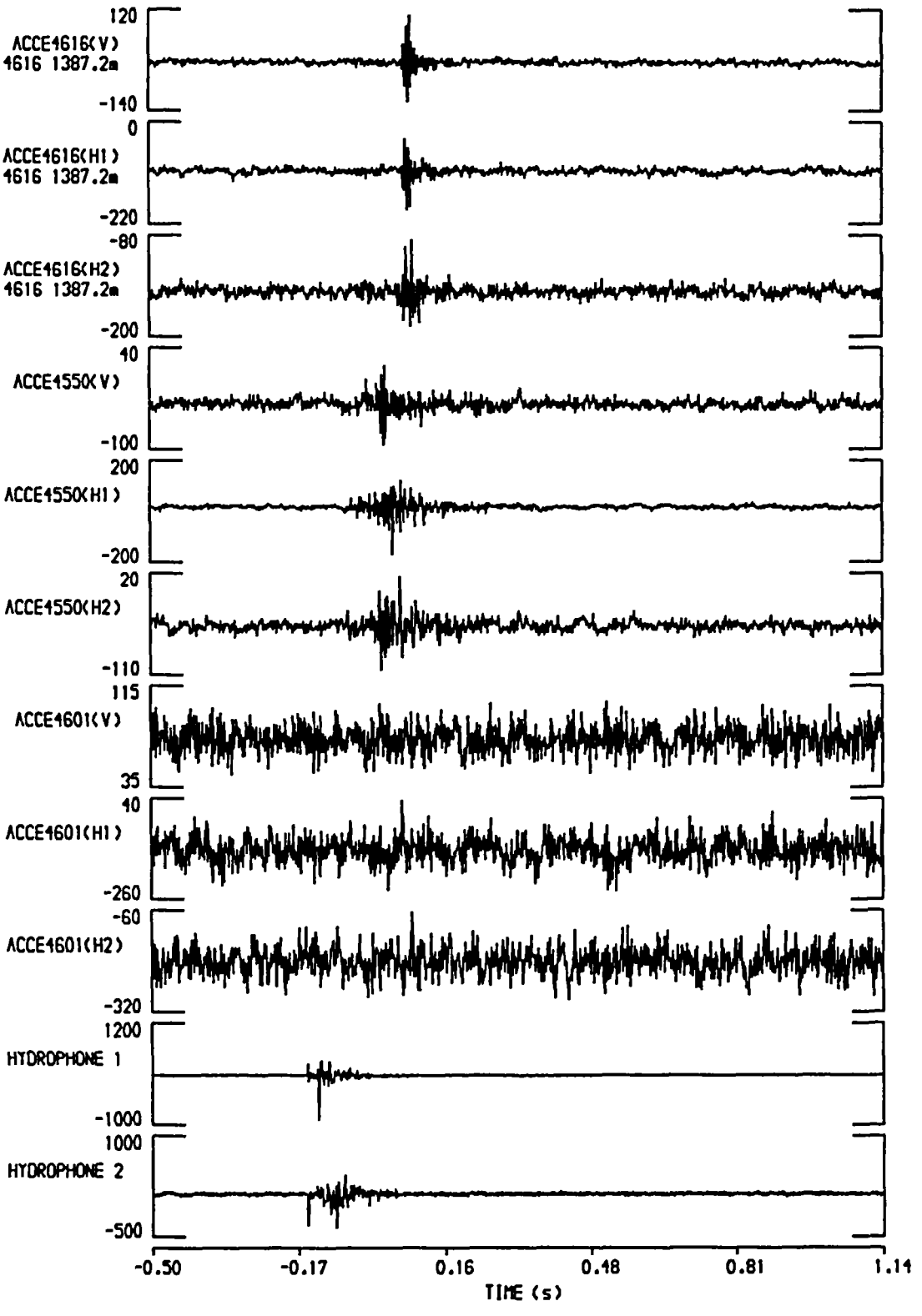

TEST STZSTI03 Event N° 224 Time : 20 Jul 1991 04:23:25.33

Event location : X = 122 m Y = -226 m Z = -1941 m

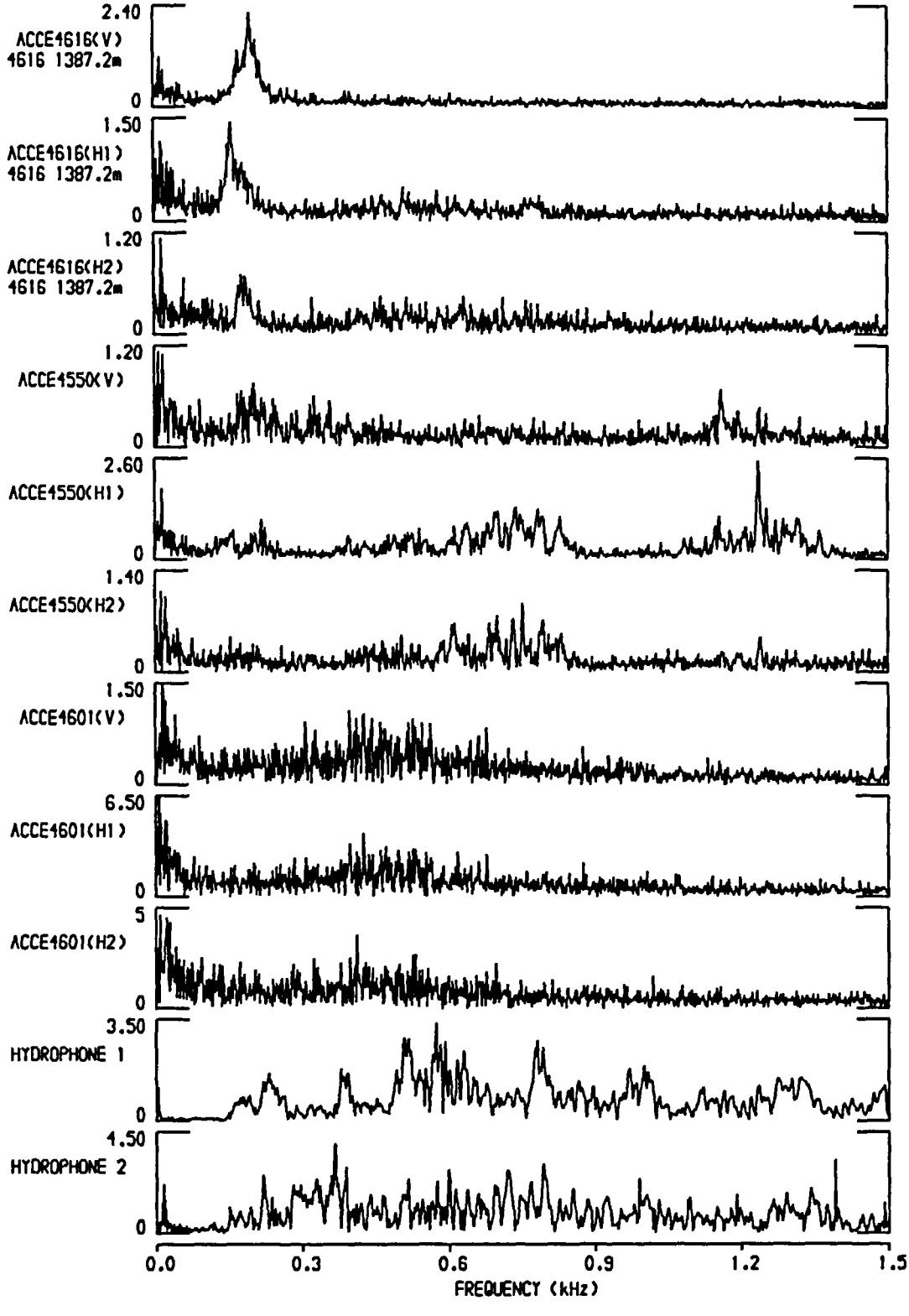

TEST STZSTI03 Event N° 224 Time : 20 Jul 1991 04:23:25.33

Event location : X = 122 m Y = -226 m Z = -1941 m

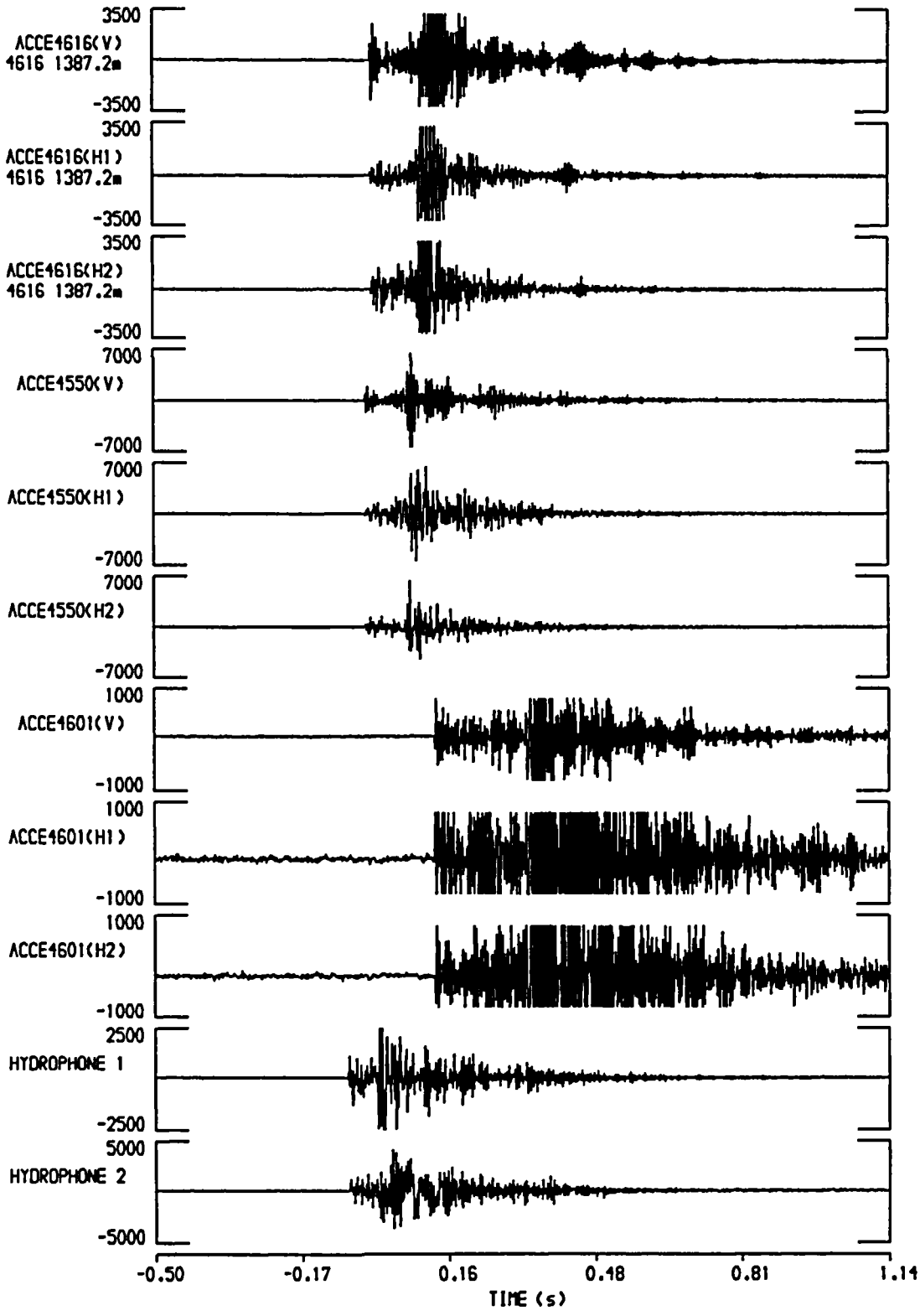

TEST STZSTI03 Event N° 222 Time : 20 Jul 1991 04:00:21.27

Event location : X = -21 m Y = 74 m Z = -2165 m

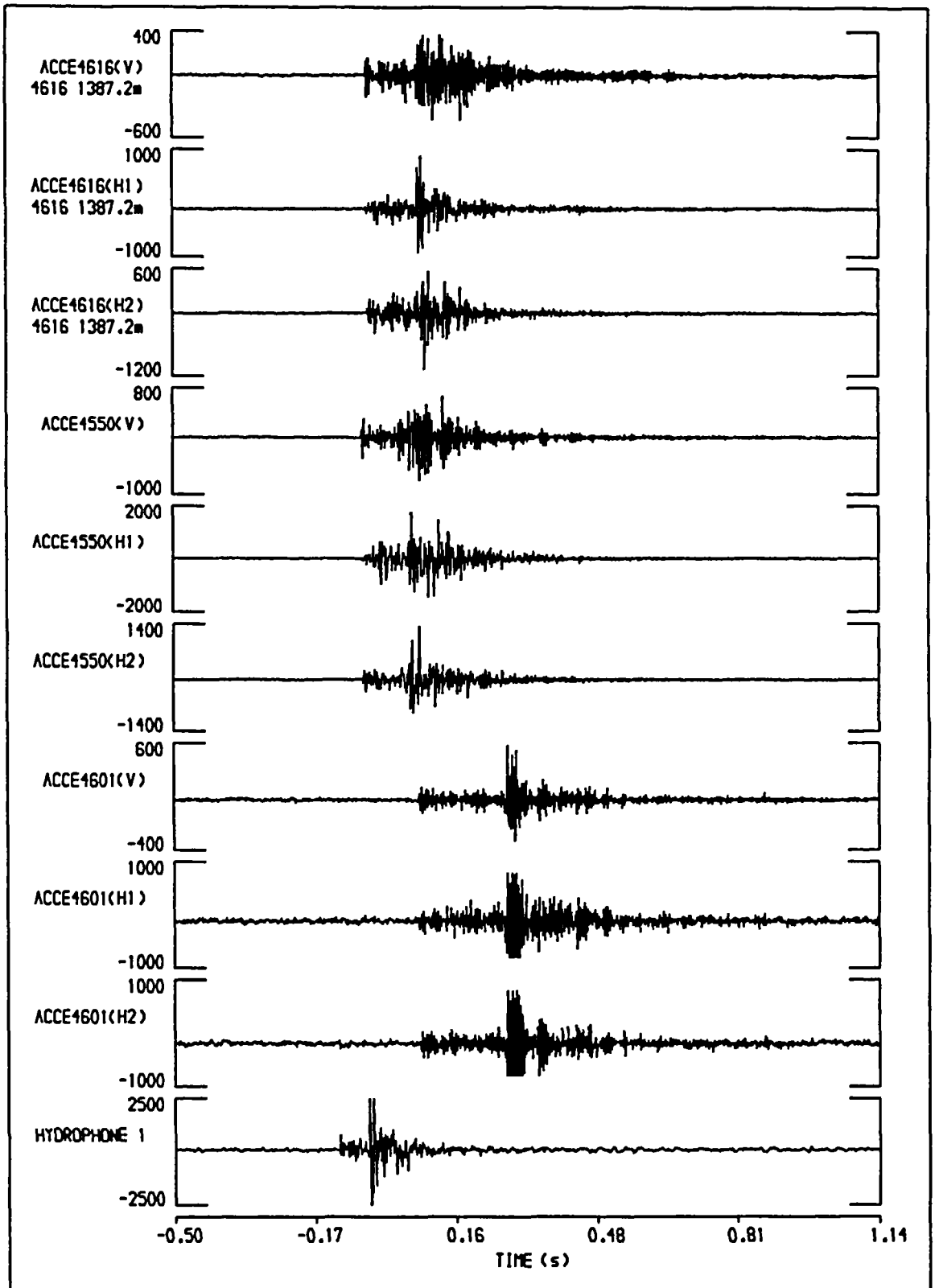

TEST STZSTI04 Event N° 13 Time : 20 Jul 1991 21:50:57.79

Event location : X = -93 m Y = 22 m Z = -2253 m

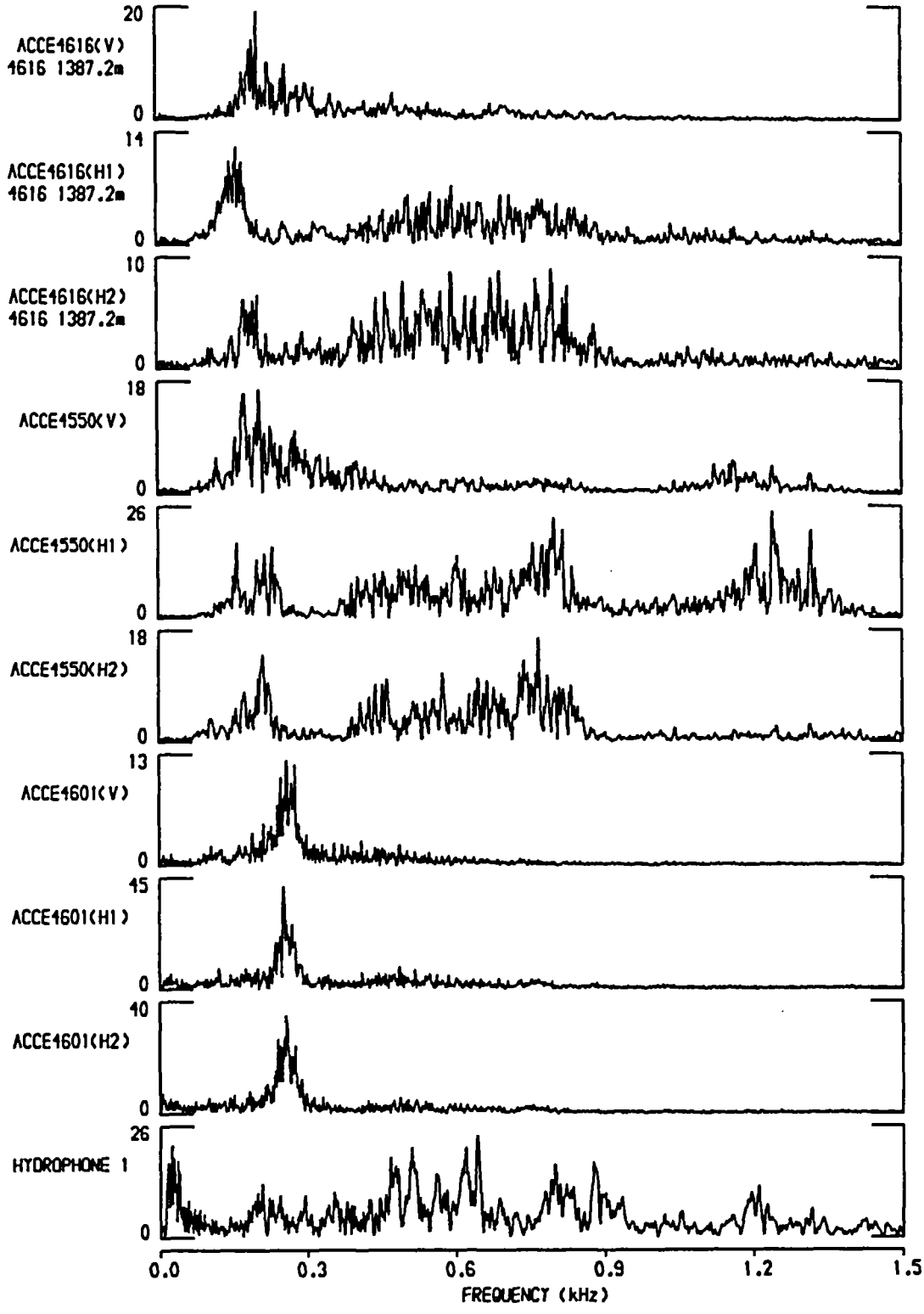

TEST STZSTI04 Event N° 13 Time : 20 Jul 1991 21:50:57.79

Event location : X = -93 m Y = 22 m Z = -2253 m

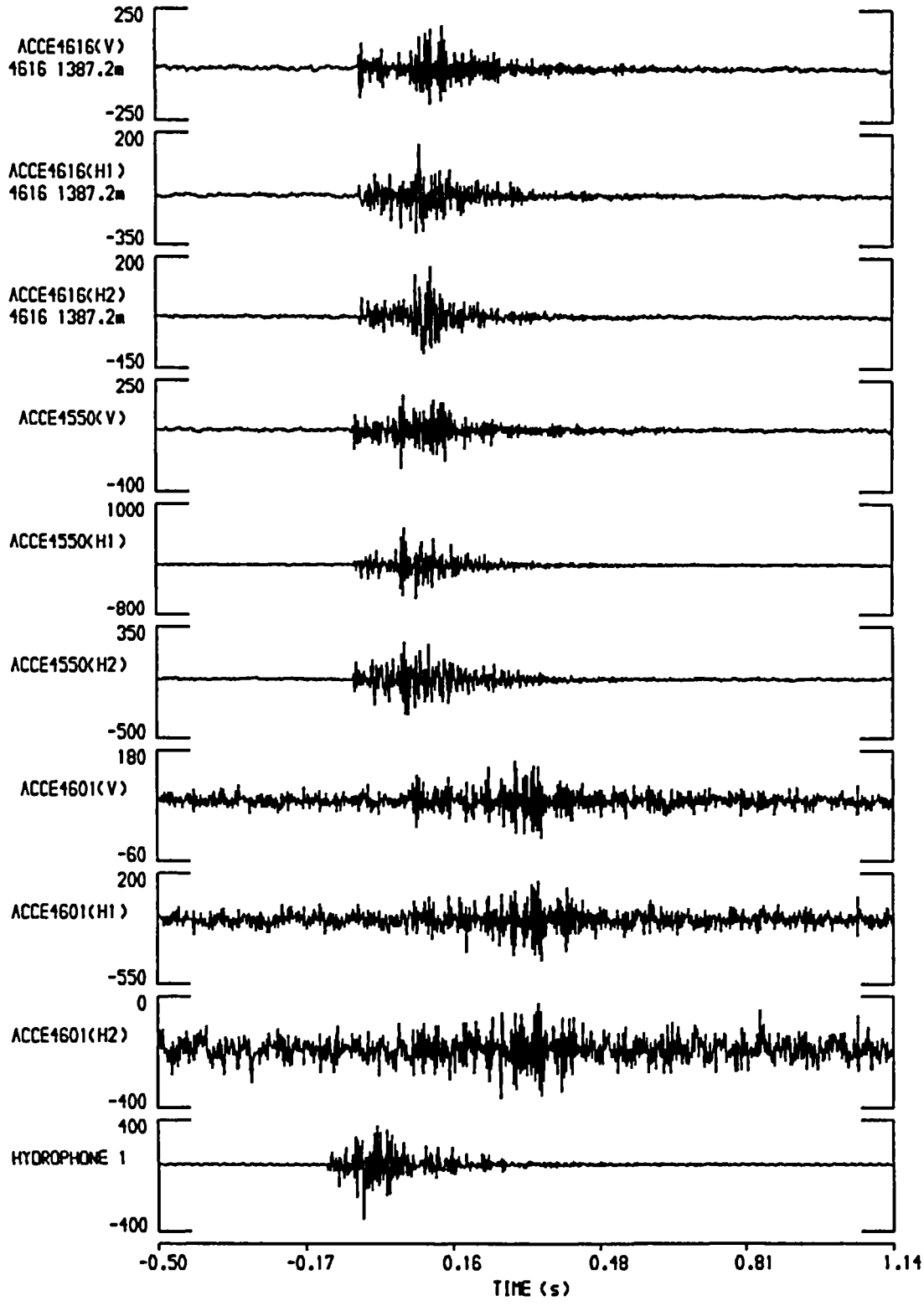

TEST STZSTI05 Event N° 54 Time : 28 Jul 1991 19:36:59.31

Event location : X = -38 m Y = -32 m Z = -2202 m

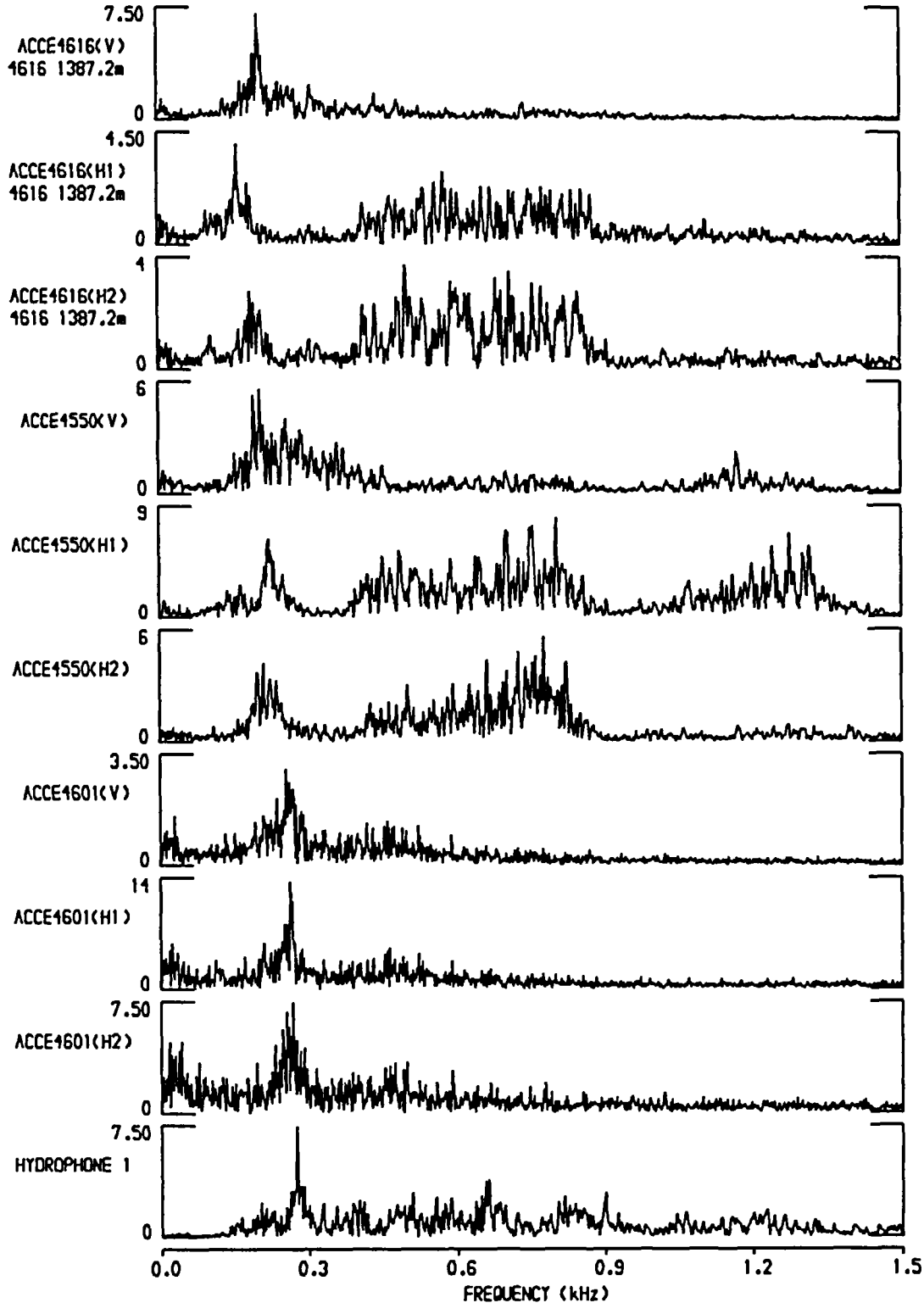

TEST STZSTI05 Event N° 54 Time : 28 Jul 1991 19:36:59.31

Event location : X = -38 m Y = -32 m Z = -2202 m

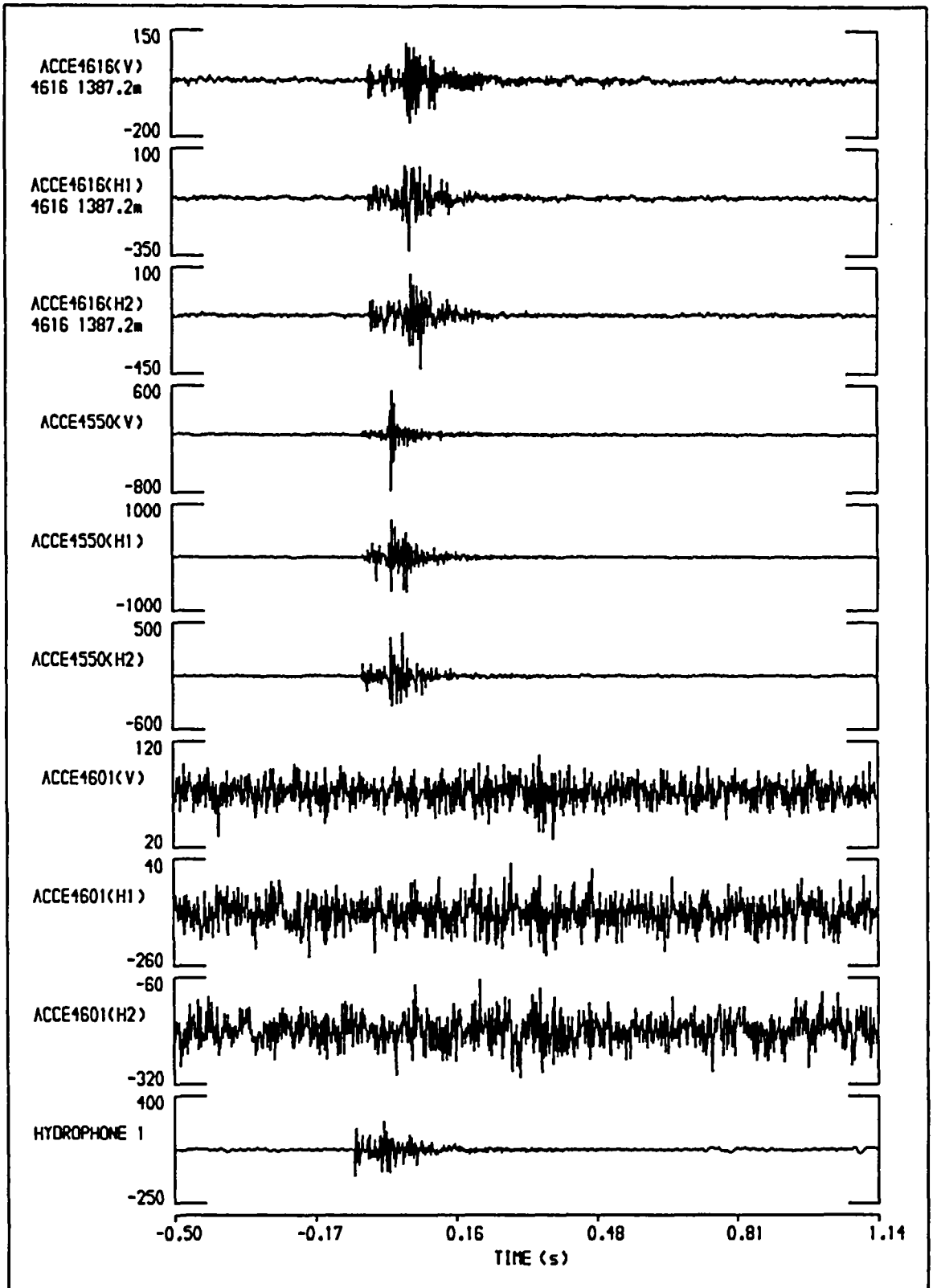

TEST STZSTI05 Event N° 55 Time : 28 Jul 1991 19:58:50.07

Event location : X = 23 m Y = 25 m Z = -1923 m

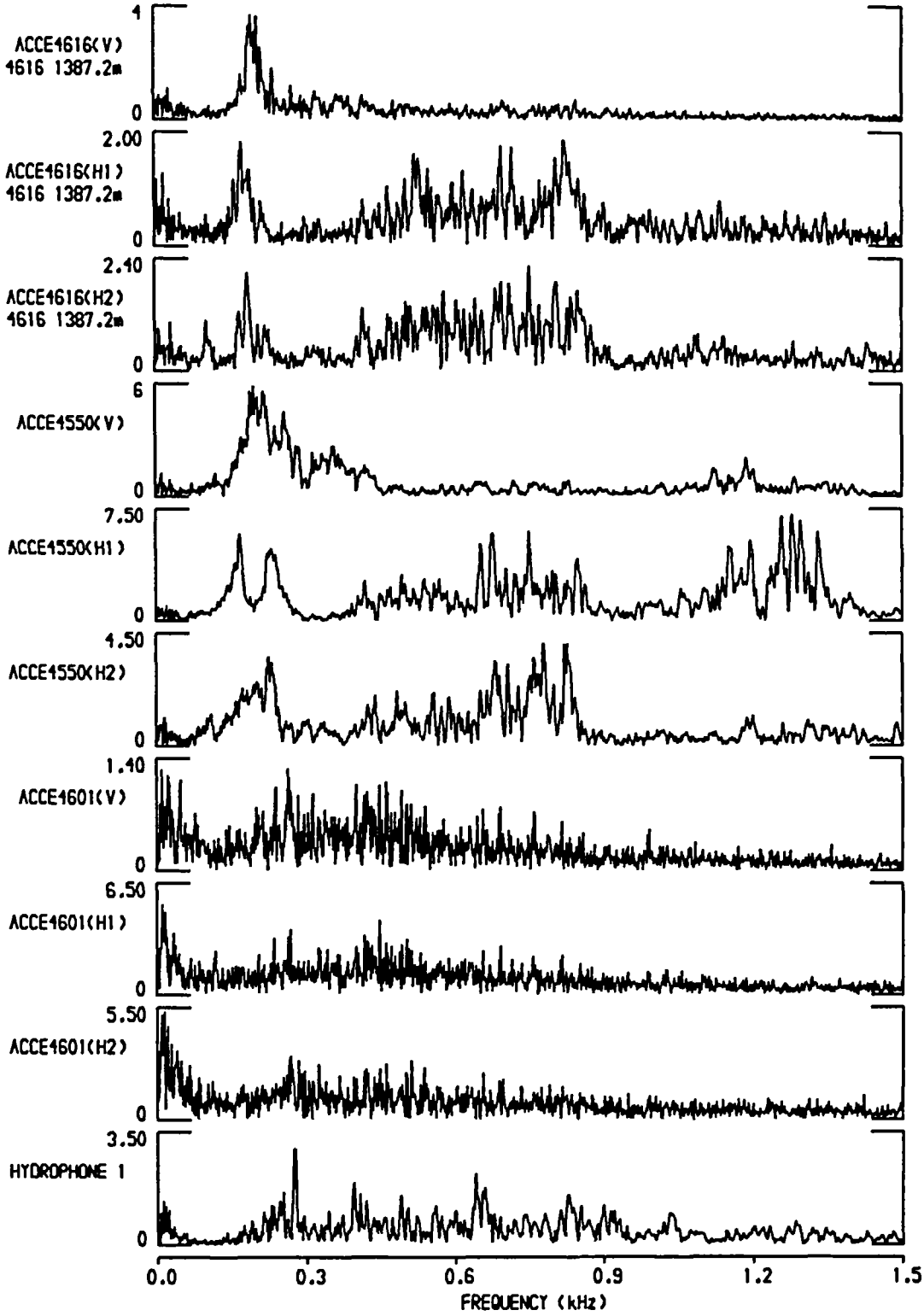

TEST STZST105 Event N° 55 Time : 28 Jul 1991 19:58:50.07

Event location : X = 23 m Y = 25 m Z = -1923 m

ANNEX 4

Evolution of the induced seismicity during the 7 l/s experiment

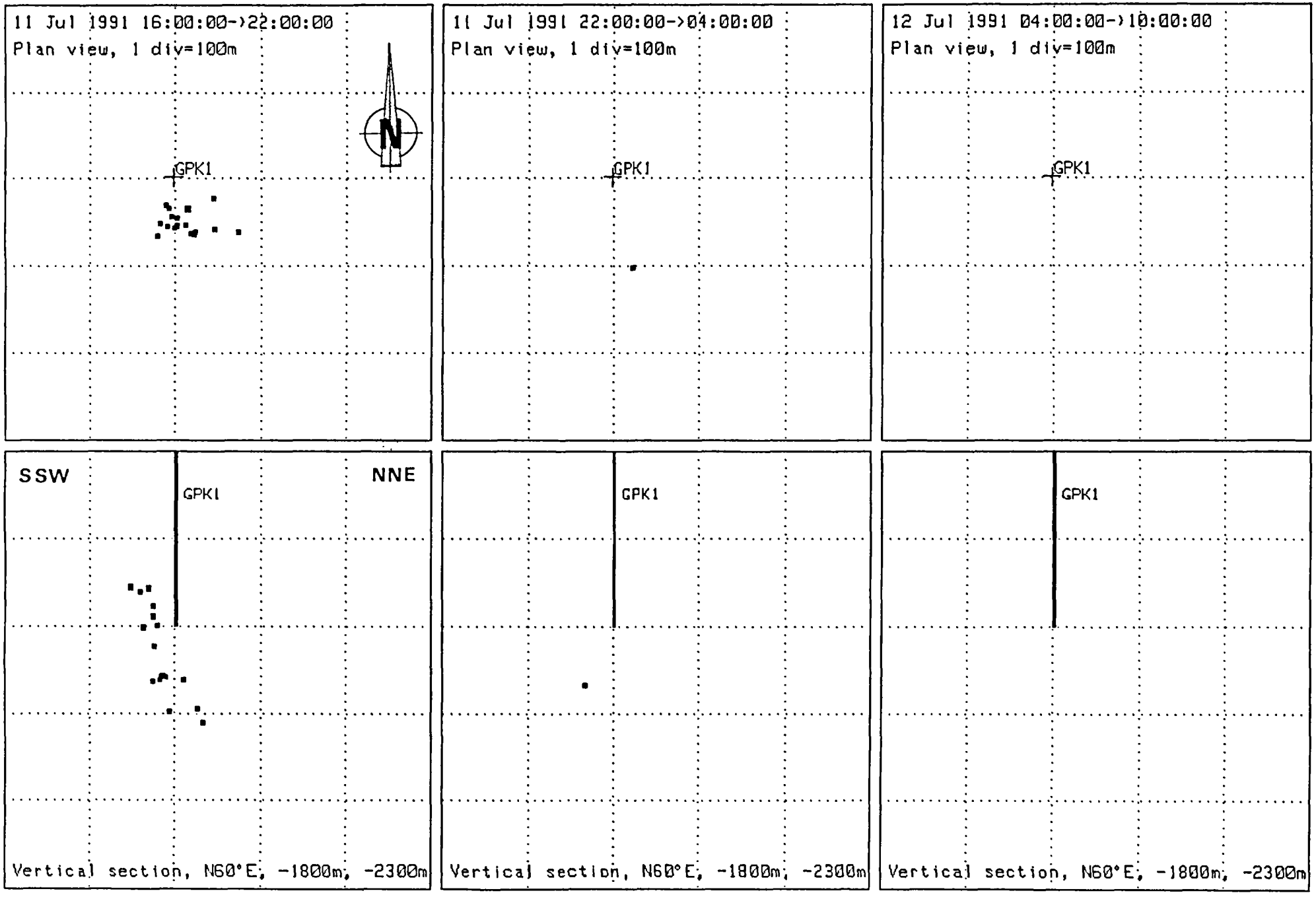
11 Jul 1991 16:00:00->22:00:00
Plan view, 1 div=100m
N
GPK1
11 Jul 1991 22:00:00->04:00:00
Plan view, 1 div=100m
GPK1
12 Jul 1991 04:00:00->10:00:00
Plan view, 1 div=100m
GPK1
SSW
NNE
GPK1
Vertical section, N60°E, -1800m, -2300m
GPK1
Vertical section, N60°E, -1800m, -2300m
GPK1
Vertical section, N60°E, -1800m, -2300m

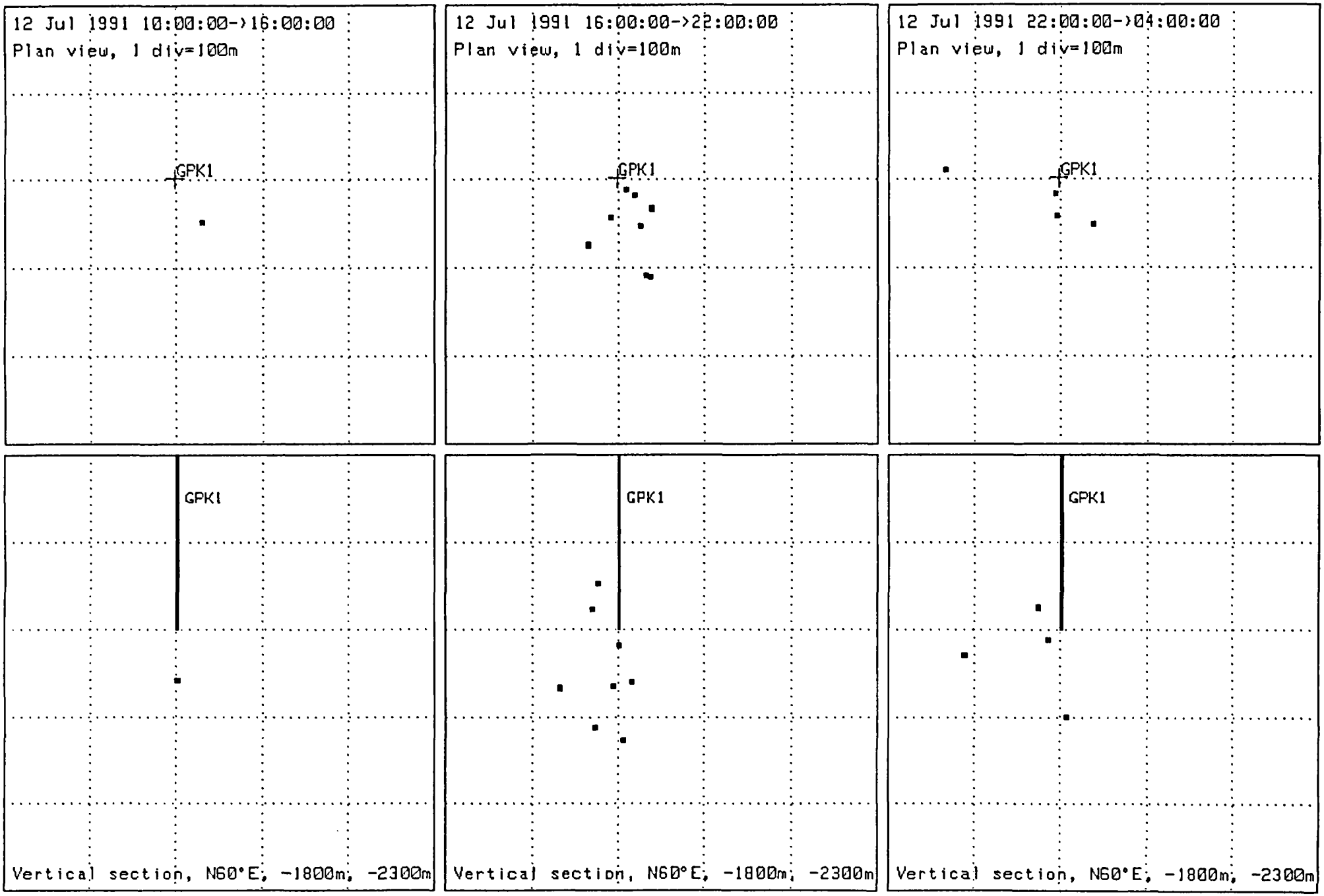
12 Jul 1991 10:00:00->16:00:00
Plan view, 1 div=100m
GPK1
12 Jul 1991 16:00:00->22:00:00
Plan view, 1 div=100m
GPK1
12 Jul 1991 22:00:00->04:00:00
Plan view, 1 div=100m
GPK1
GPK1
Vertical section, N60°E, -1800m, -2300m
GPK1
Vertical section, N60°E, -1800m, -2300m
GPK1
Vertical section, N60°E, -1800m, -2300m

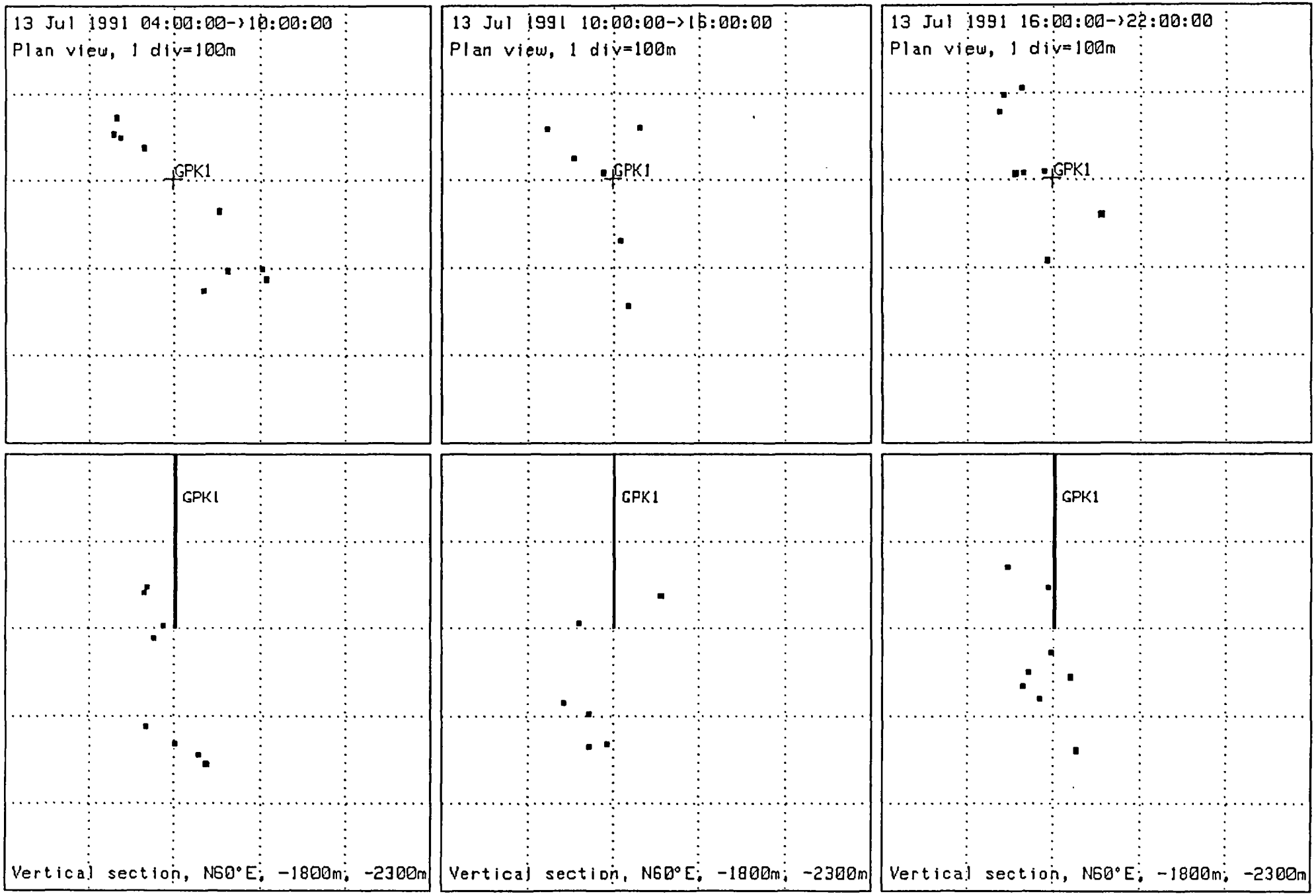
13 Jul 1991 04:00:00->10:00:00
Plan view, 1 div=100m
GPK1
13 Jul 1991 10:00:00->16:00:00
Plan view, 1 div=100m
GPK1
13 Jul 1991 16:00:00->22:00:00
Plan view, 1 div=100m
GPK1
GPK1
Vertical section, N60°E, -1800m, -2300m
GPK1
Vertical section, N60°E, -1800m, -2300m
GPK1
Vertical section, N60°E, -1800m, -2300m

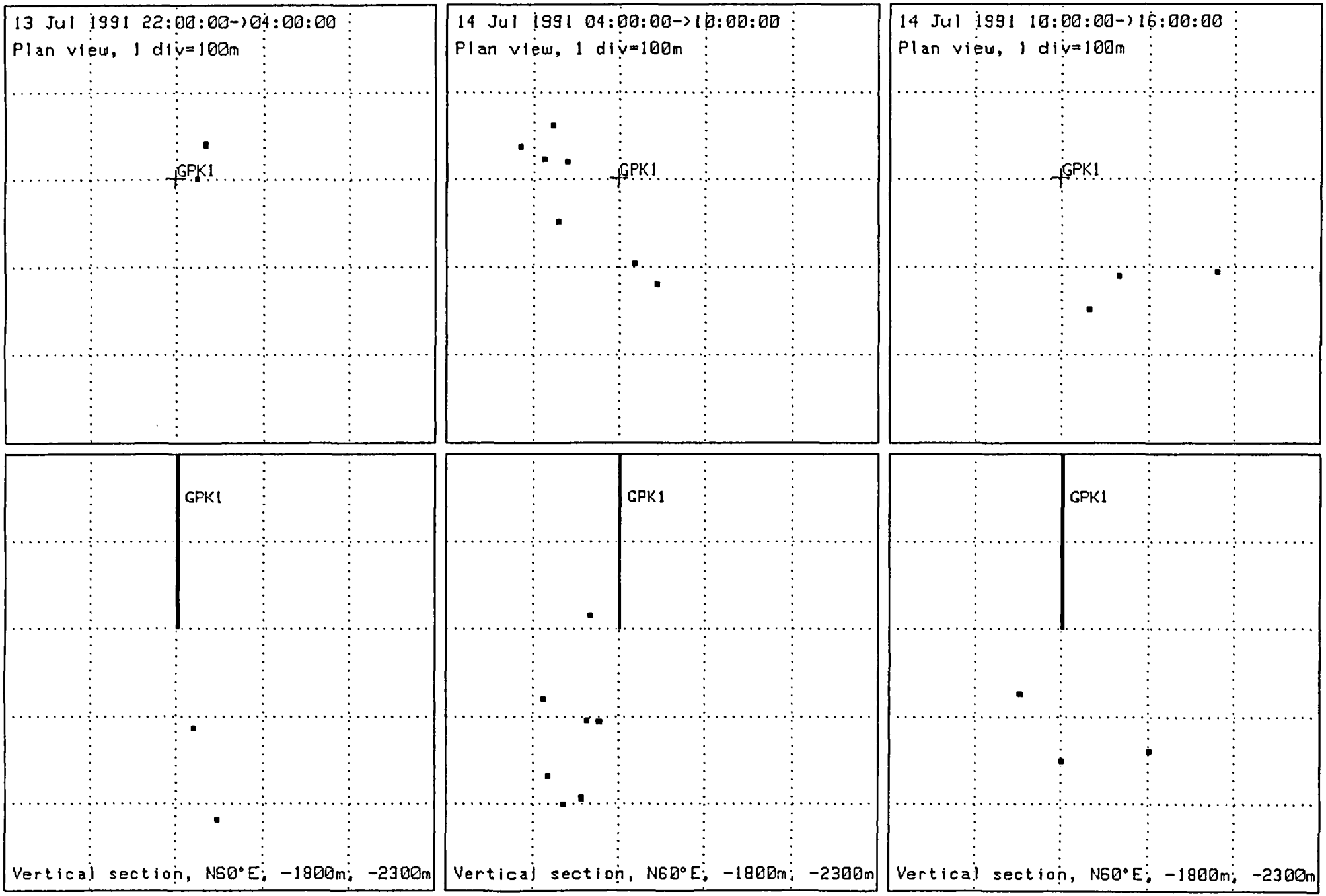
13 Jul 1991 22:00:00->04:00:00
Plan view, 1 div=100m
GPK1
14 Jul 1991 04:00:00->10:00:00
Plan view, 1 div=100m
GPK1
14 Jul 1991 10:00:00->16:00:00
Plan view, 1 div=100m
GPK1
GPK1
Vertical section, N60°E, -1800m, -2300m
GPK1
Vertical section, N60°E, -1800m, -2300m
GPK1
Vertical section, N60°E, -1800m, -2300m

ANNEX 5

Evolution of the induced seismicity during the 15 l/s experiment

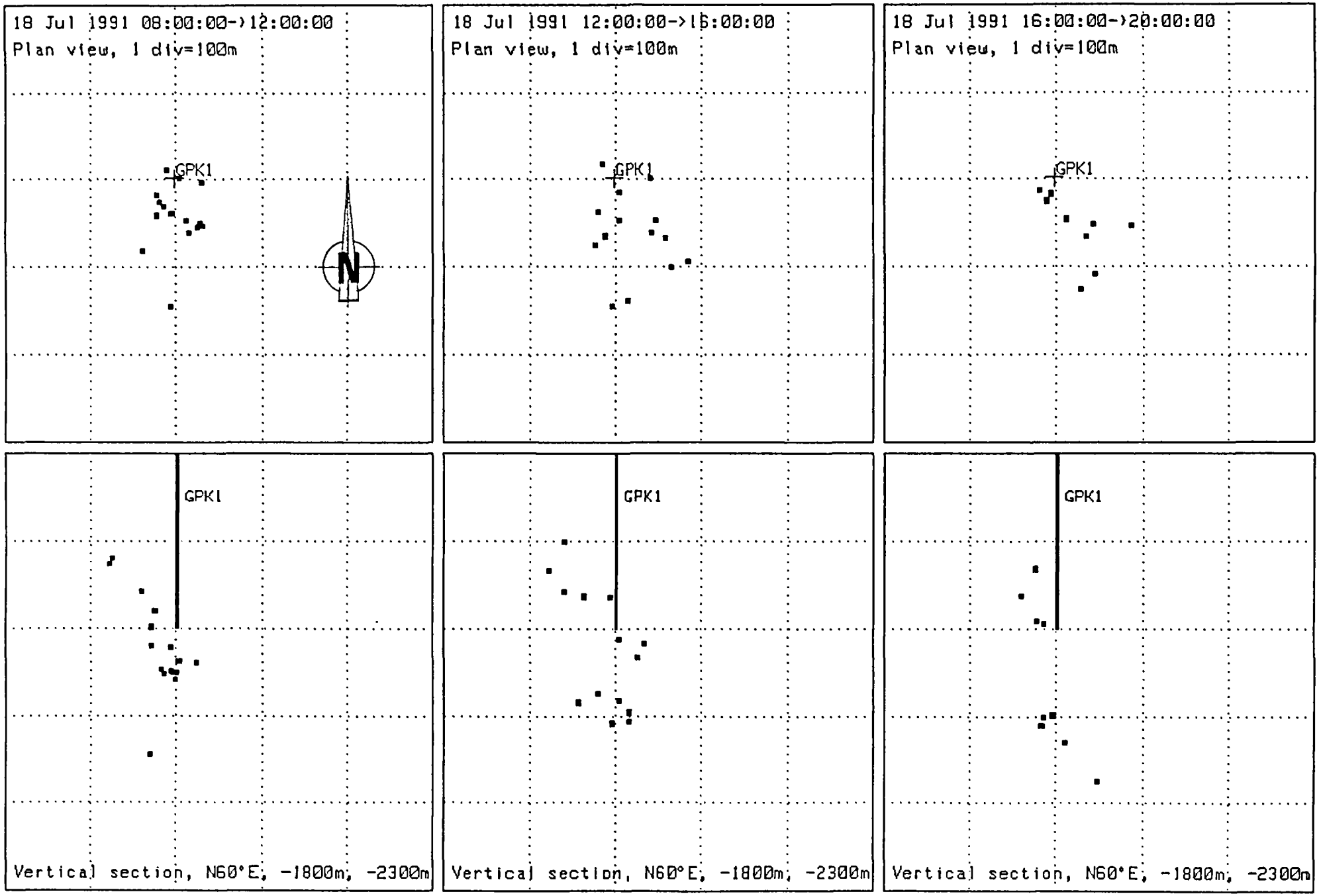
18 Jul 1991 08:00:00->12:00:00
Plan view, 1 div=100m
GPK1
N
18 Jul 1991 12:00:00->16:00:00
Plan view, 1 div=100m
GPK1
18 Jul 1991 16:00:00->20:00:00
Plan view, 1 div=100m
GPK1
GPK1
Vertical section, N60°E, -1800m, -2300m
GPK1
Vertical section, N60°E, -1800m, -2300m
GPK1
Vertical section, N60°E, -1800m, -2300m

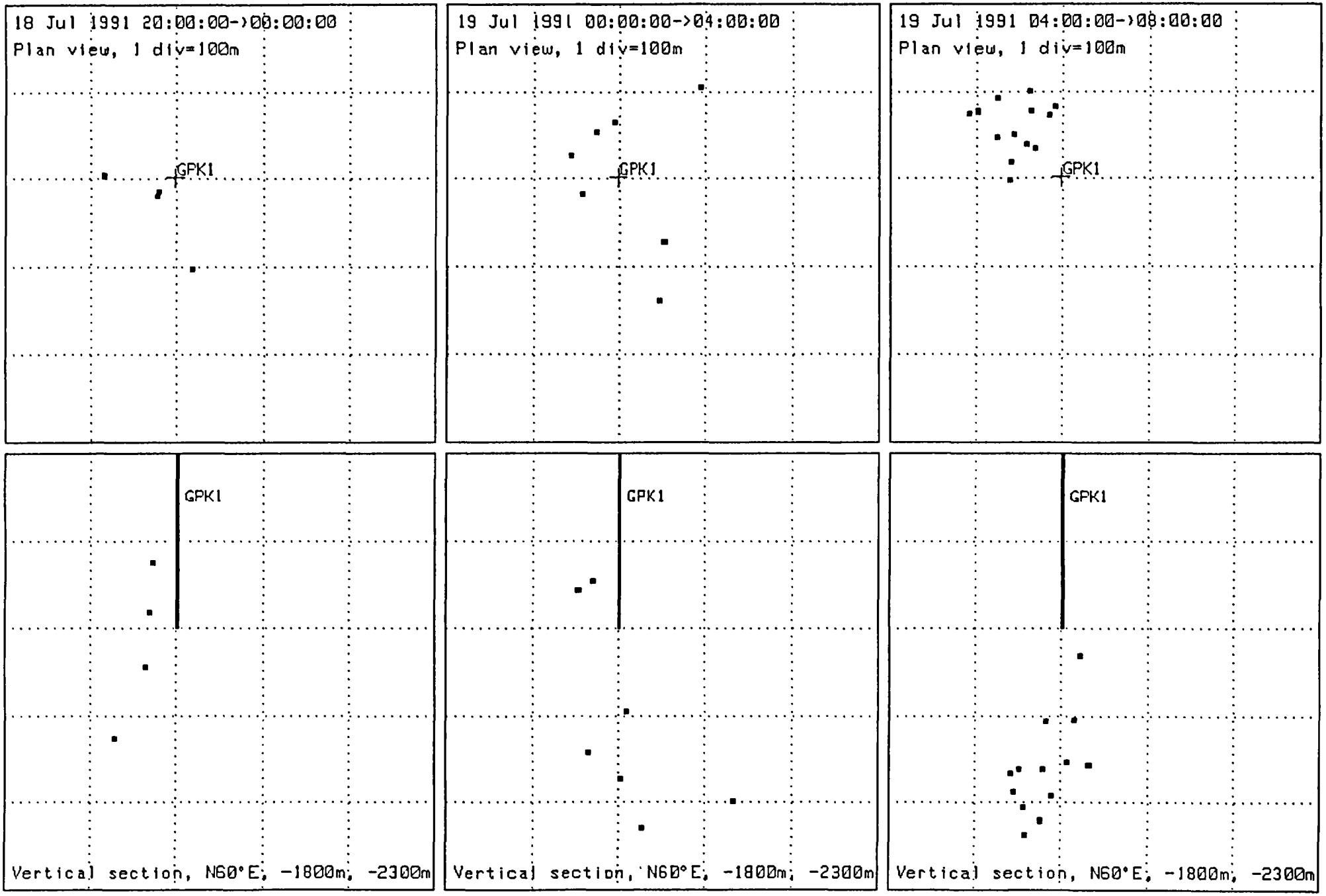
18 Jul 1991 20:00:00->00:00:00
Plan view, 1 div=100m
GPK1
19 Jul 1991 00:00:00->04:00:00
Plan view, 1 div=100m
GPK1
19 Jul 1991 04:00:00->08:00:00
Plan view, 1 div=100m
GPK1
GPK1
Vertical section, N60°E, -1800m, -2300m
GPK1
Vertical section, N60°E, -1800m, -2300m
GPK1
Vertical section, N60°E, -1800m, -2300m

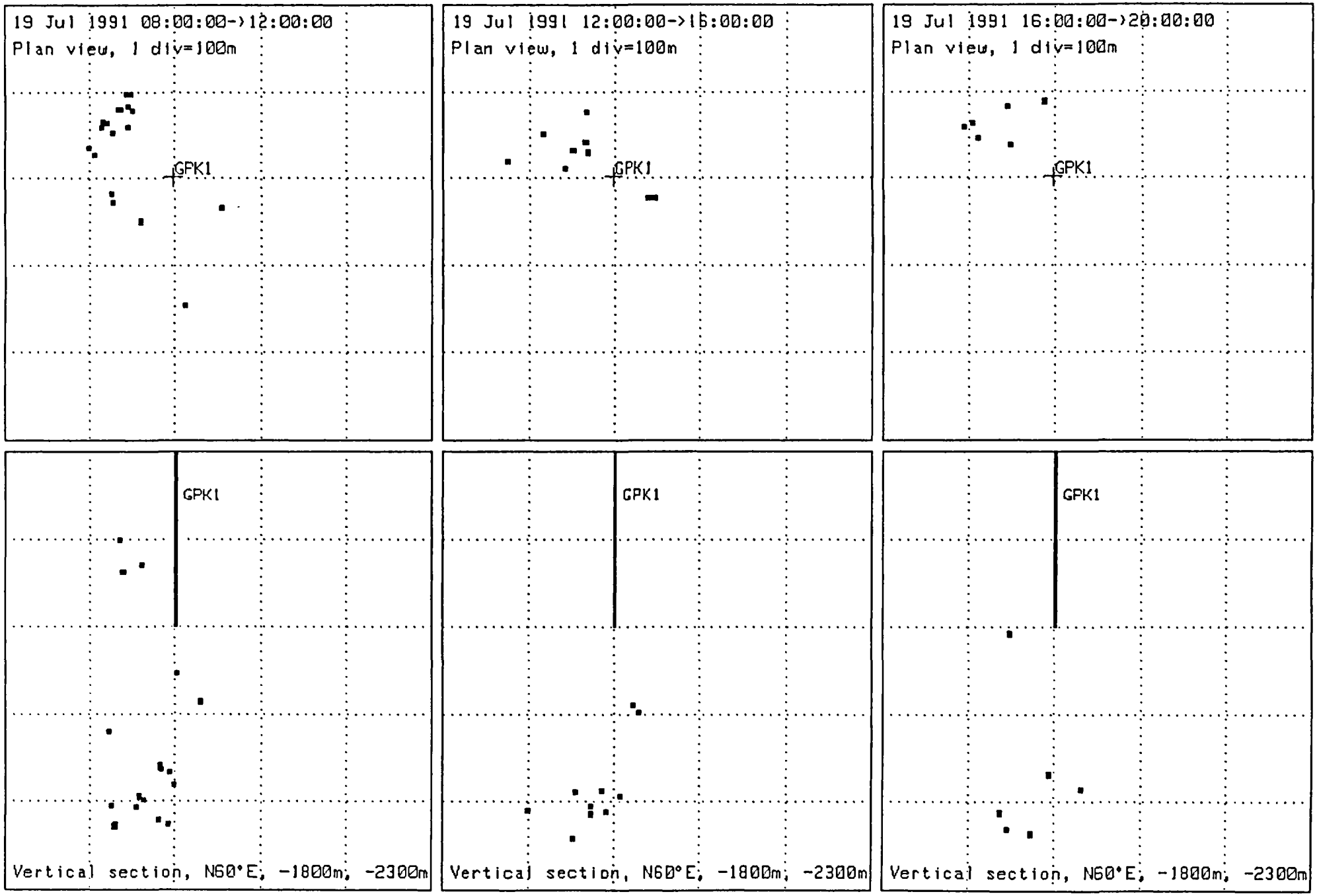
19 Jul 1991 08:00:00->12:00:00
Plan view, 1 div=100m
GPK1
19 Jul 1991 12:00:00->16:00:00
Plan view, 1 div=100m
GPK1
19 Jul 1991 16:00:00->20:00:00
Plan view, 1 div=100m
GPK1
GPK1
Vertical section, N60°E, -1800m, -2300m
GPK1
Vertical section, N60°E, -1800m, -2300m
GPK1
Vertical section, N60°E, -1800m, -2300m

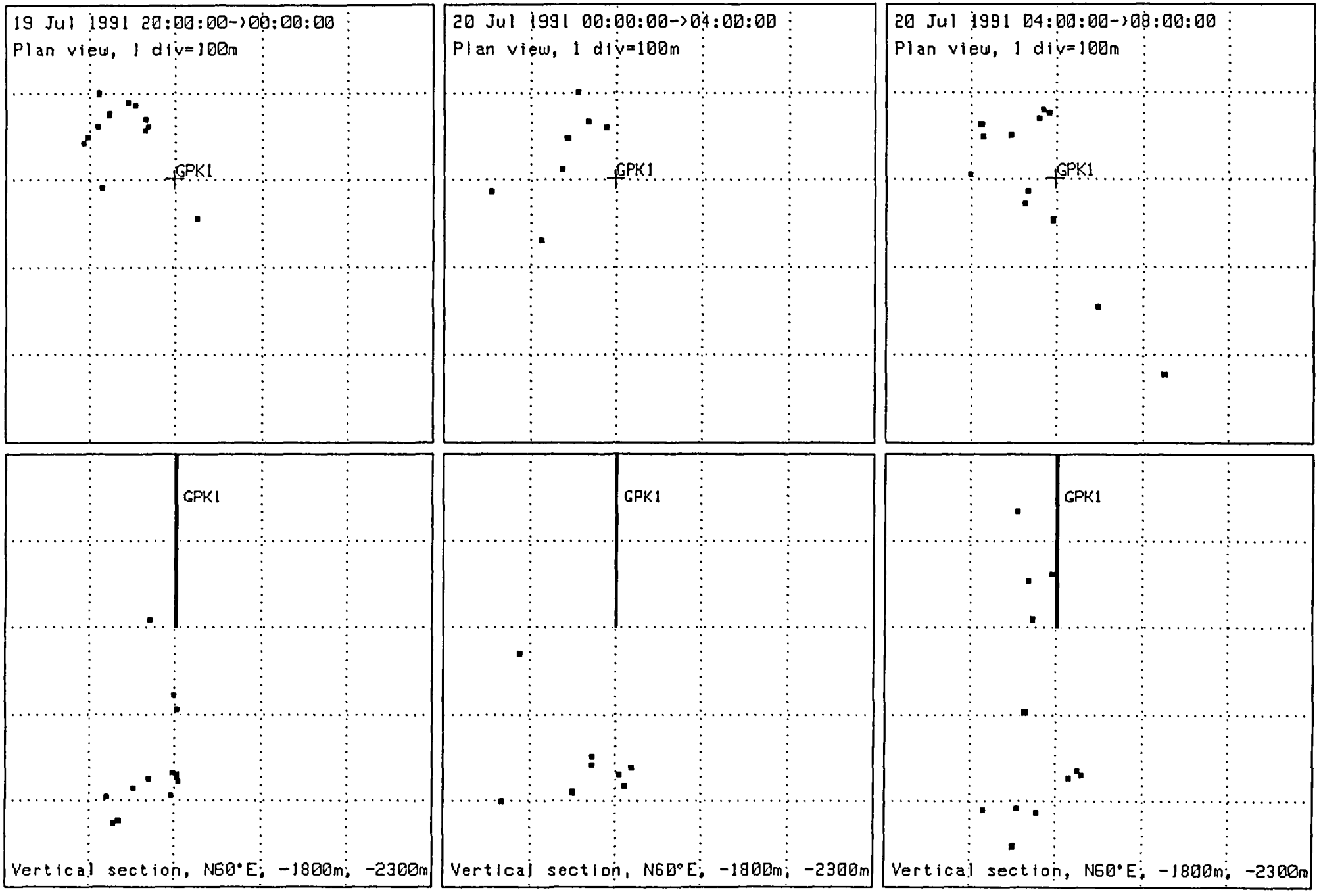
19 Jul 1991 20:00:00->00:00:00
Plan view, 1 div=100m
GPK1
20 Jul 1991 00:00:00->04:00:00
Plan view, 1 div=100m
GPK1
20 Jul 1991 04:00:00->08:00:00
Plan view, 1 div=100m
GPK1
GPK1
Vertical section, N60°E, -1800m, -2300m
GPK1
Vertical section, N60°E, -1800m, -2300m
GPK1
Vertical section, N60°E, -1800m, -2300m

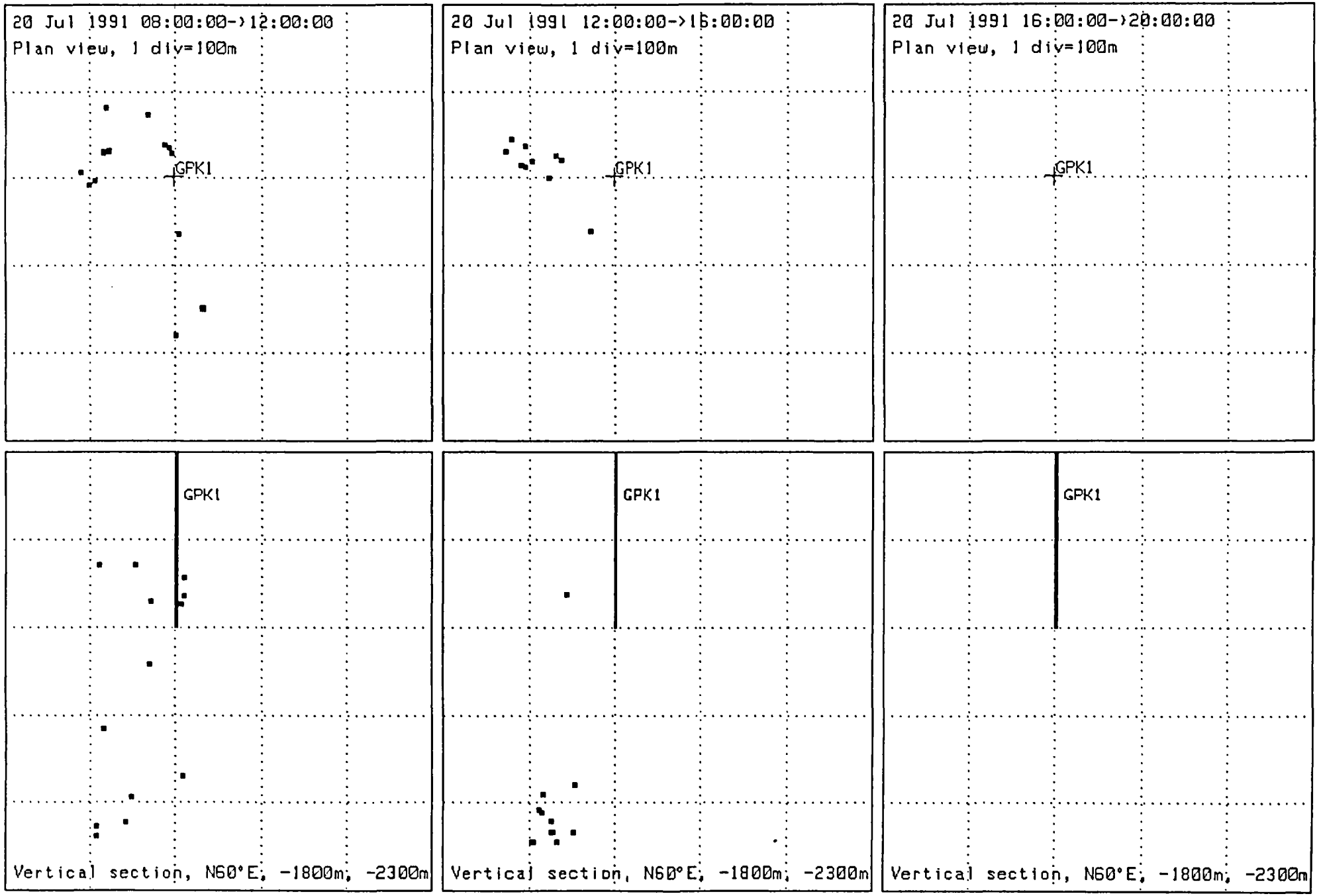
20 Jul 1991 08:00:00->12:00:00
Plan view, 1 div=100m
GPK1
20 Jul 1991 12:00:00->16:00:00
Plan view, 1 div=100m
GPK1
20 Jul 1991 16:00:00->20:00:00
Plan view, 1 div=100m
GPK1
GPK1
Vertical section, N60°E, -1800m, -2300m
GPK1
Vertical section, N60°E, -1800m, -2300m
GPK1
Vertical section, N60°E, -1800m, -2300m

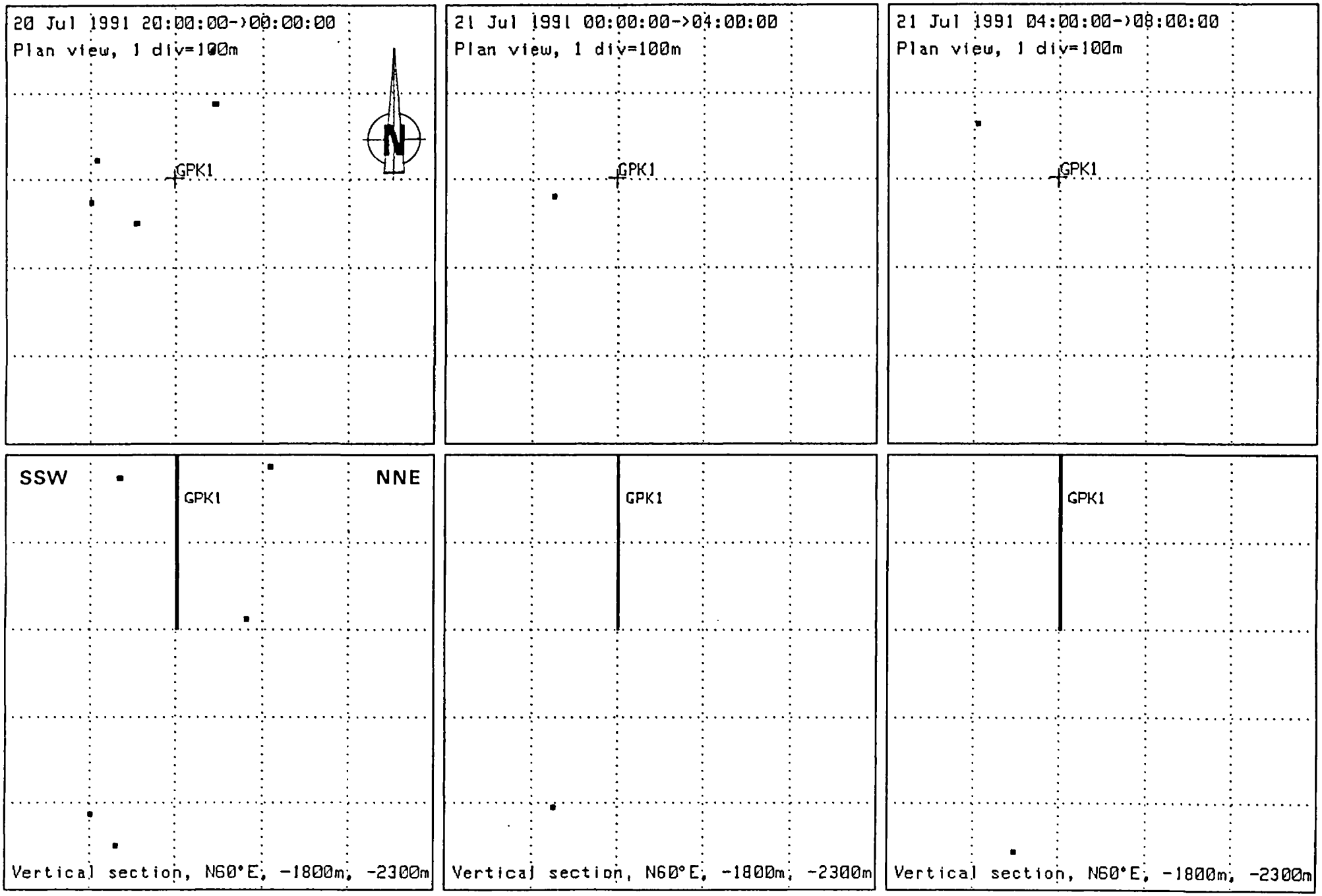
20 Jul 1991 20:00:00->00:00:00
Plan view, 1 div=100m
N
GPK1
21 Jul 1991 00:00:00->04:00:00
Plan view, 1 div=100m
GPK1
21 Jul 1991 04:00:00->08:00:00
Plan view, 1 div=100m
GPK1
SSW
NNE
GPK1
Vertical section, N60°E, -1800m, -2300m
GPK1
Vertical section, N60°E, -1800m, -2300m
GPK1
Vertical section, N60°E, -1800m, -2300m

ANNEX 6

Location errors on selected events

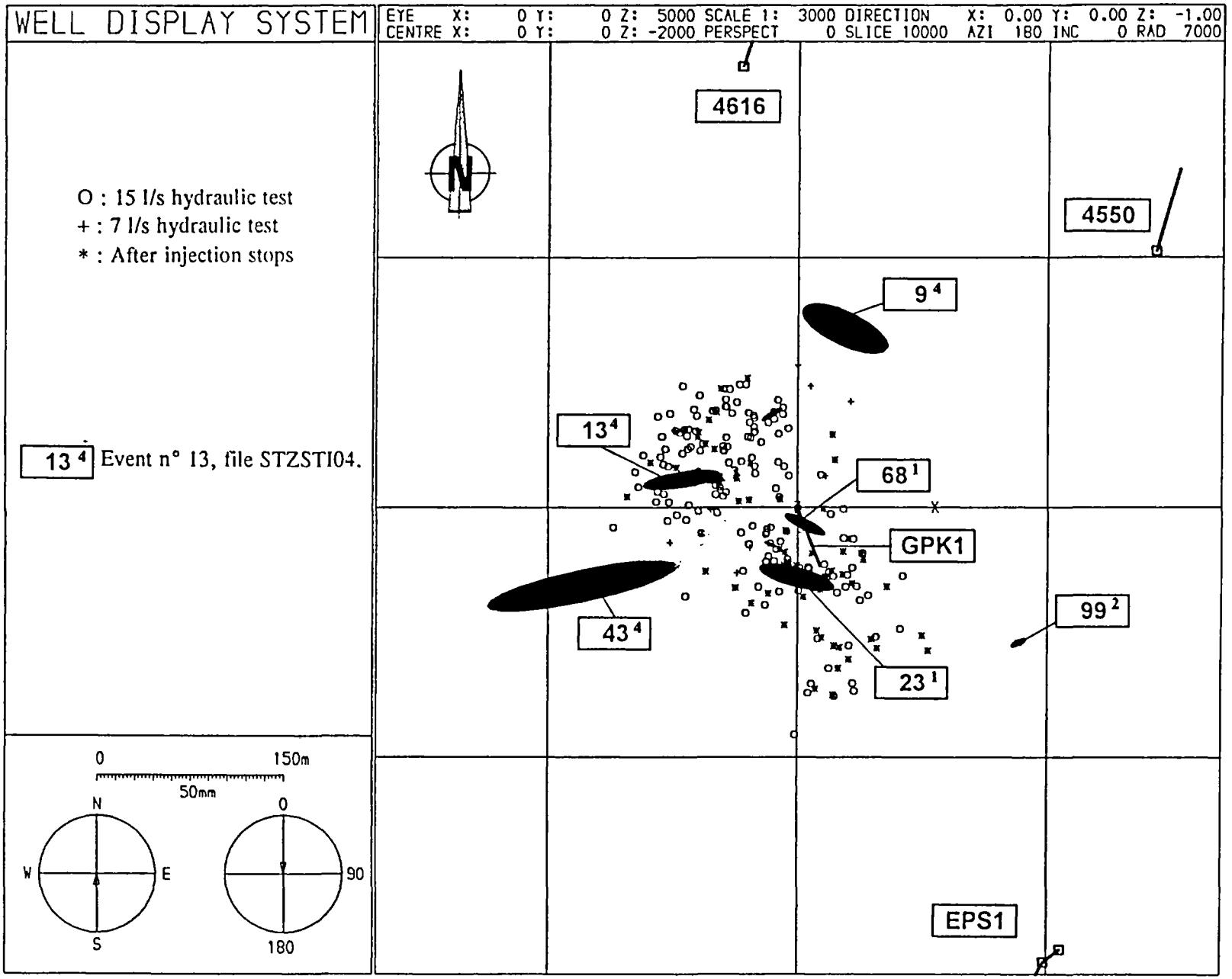

Ellipse errors on selected events recorded during the 7 l/s injection test and after the 15 l/s test.
Map view

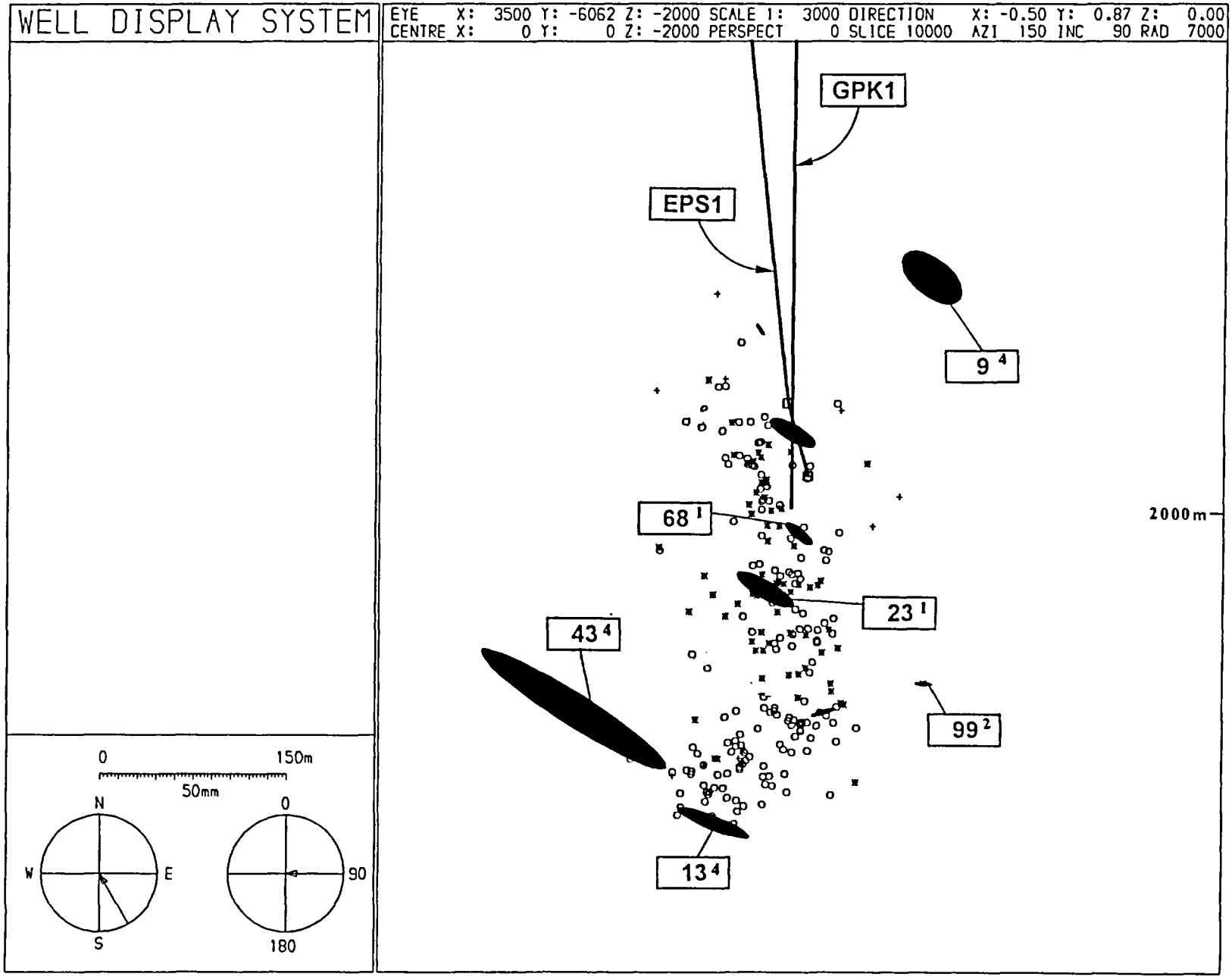

Ellipse errors on selected events recorded during the 7 l/s injection test and after the 15 l/s test.
Cross-section N 60°

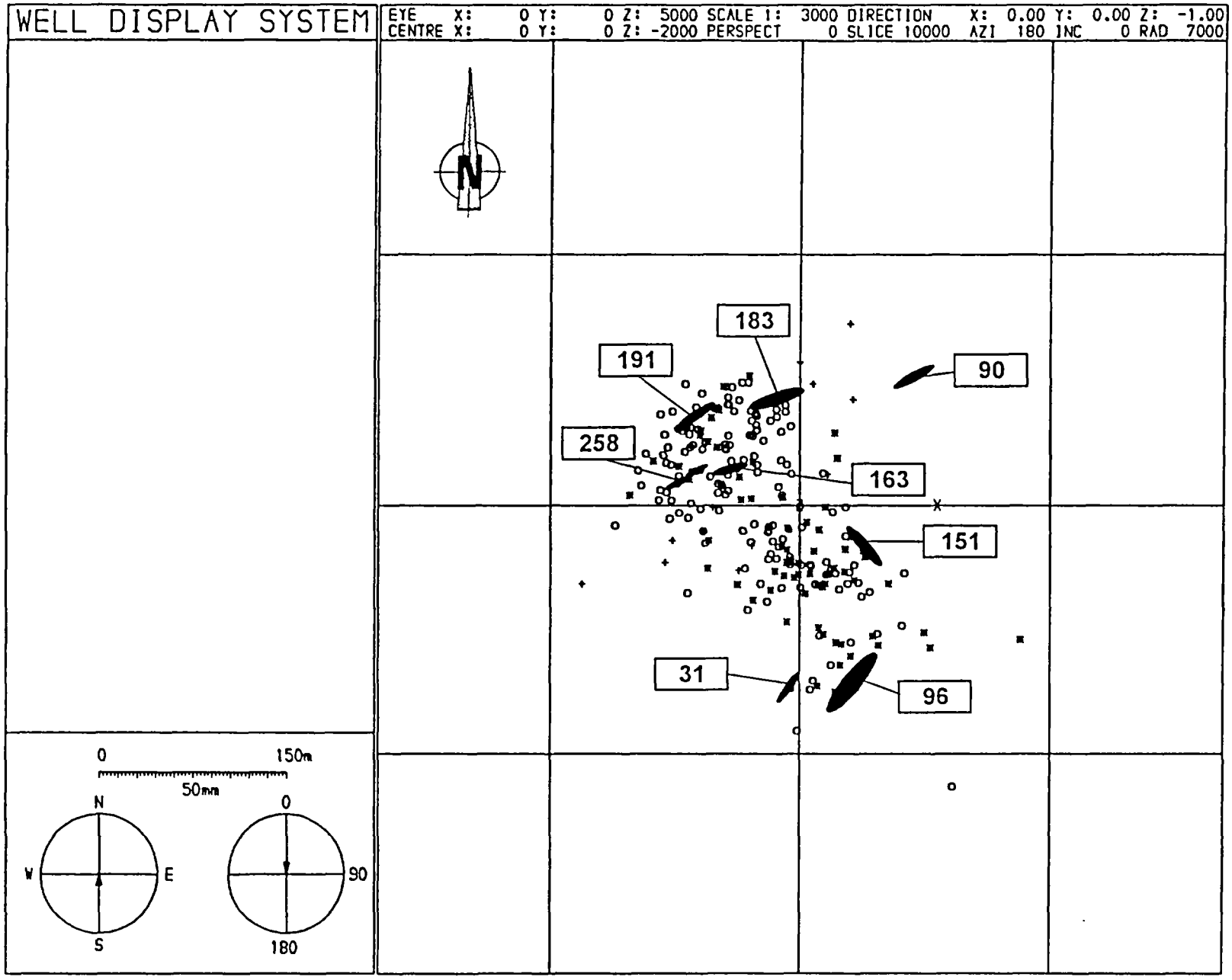

Ellipse errors on selected events recorded during the 15 l/s injection test. (Only on STZSTI03 file) Map view.

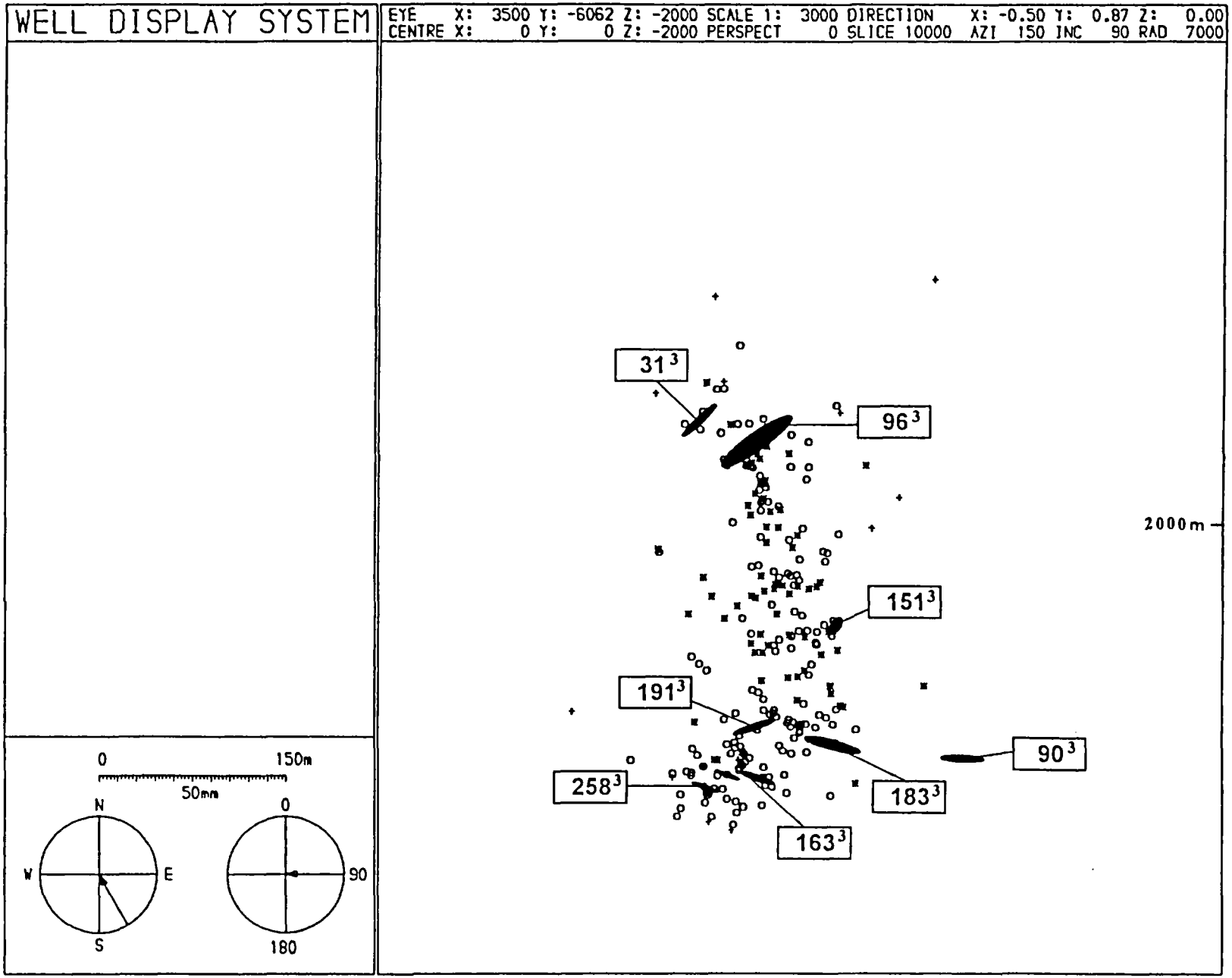

Ellipse errors on selected events recorded during the 15 l/s injection test. (Only on STZSTI03 file)
Cross-section N 60°

ANNEX 7

List of events characterized by their P-wave polarity onsets

Population	Symbol	4616	4550	Hydr. (top)	Hydr. (bot)	Number of events
1	□	U	U	U	U	12
2	×	U	U	U	D	2
3	+	U	U	D	D	12
4	O	U	D	D	D	2
5	*	U	D	D	U	4
6	Δ	D	D	D	D	2
7	∇	U	U		U	13
8	◊	U	U		D	3

(P-wave polarities distributions on vertical sensor for seismic probes; U: Up D: Down)

Definition of the populations of events recorded on the network as a function of the observed combination of P-wave polarity picks

N° TEST	STZSTI01	STZSTI02	STZSTI03	STZSTI04	STZSTI05
Population 1			11, 16, 17, 19, 20, 21, 26, 30, 35, 45, 53, 56 59, 61, 67, 232		
Population 2			94, 239		
Population 3			41, 42, 101, 130, 151, 158, 159, 195, 214, 245, 252, 258		
Population 4			31, 93		
Population 5		8, 50	50, 222		
Population 6	23		234		
Population 7	19, 20, 26, 65, 67, 68	19, 20, 21, 46, 69		26	54
Population 8		86		13, 43	

List of events belonging to the various populations according to the P-wave polarity distributions recorded on the network

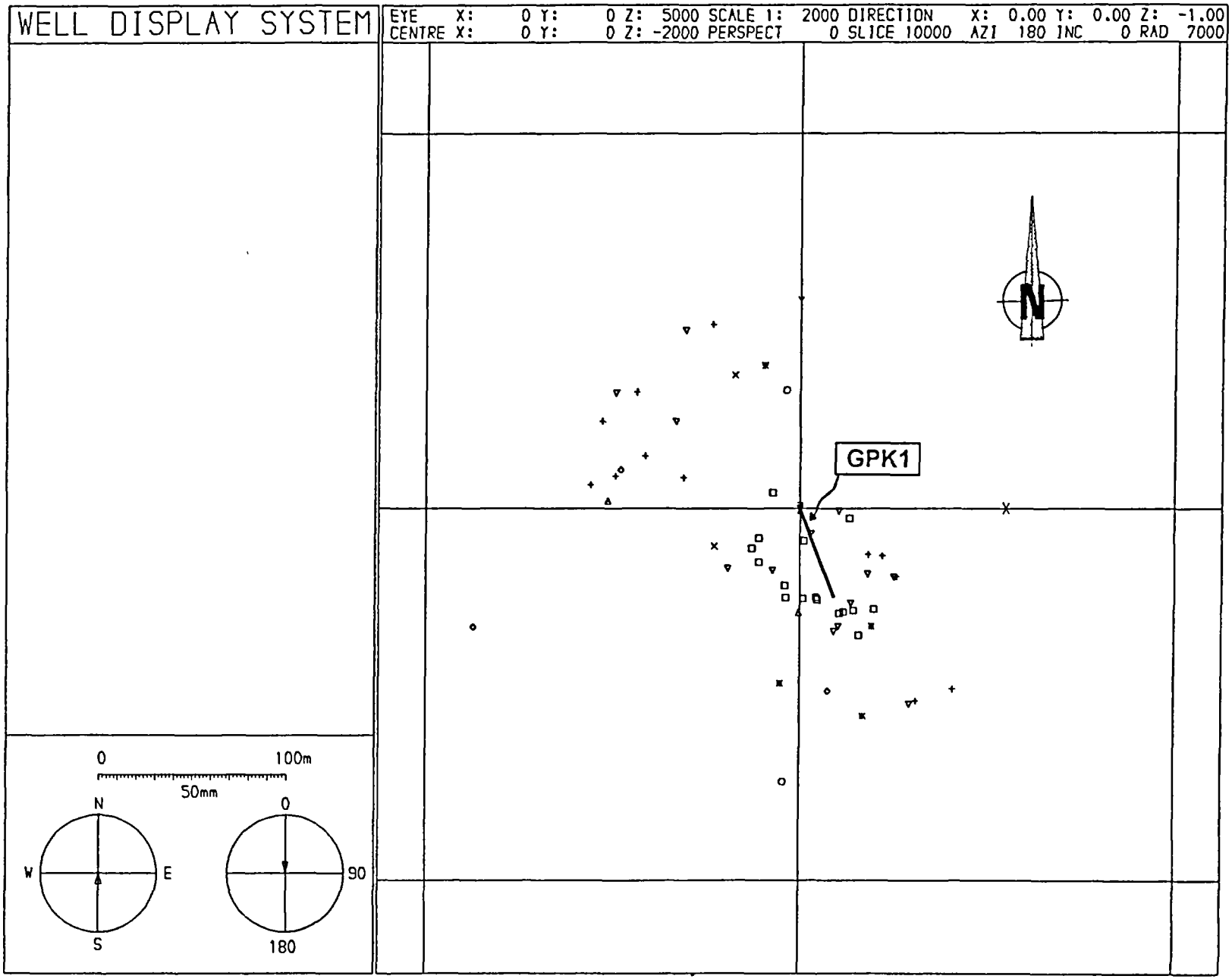

Locations of the various populations of events as a function of the observed combination of P-wave polarity picks. Map view.

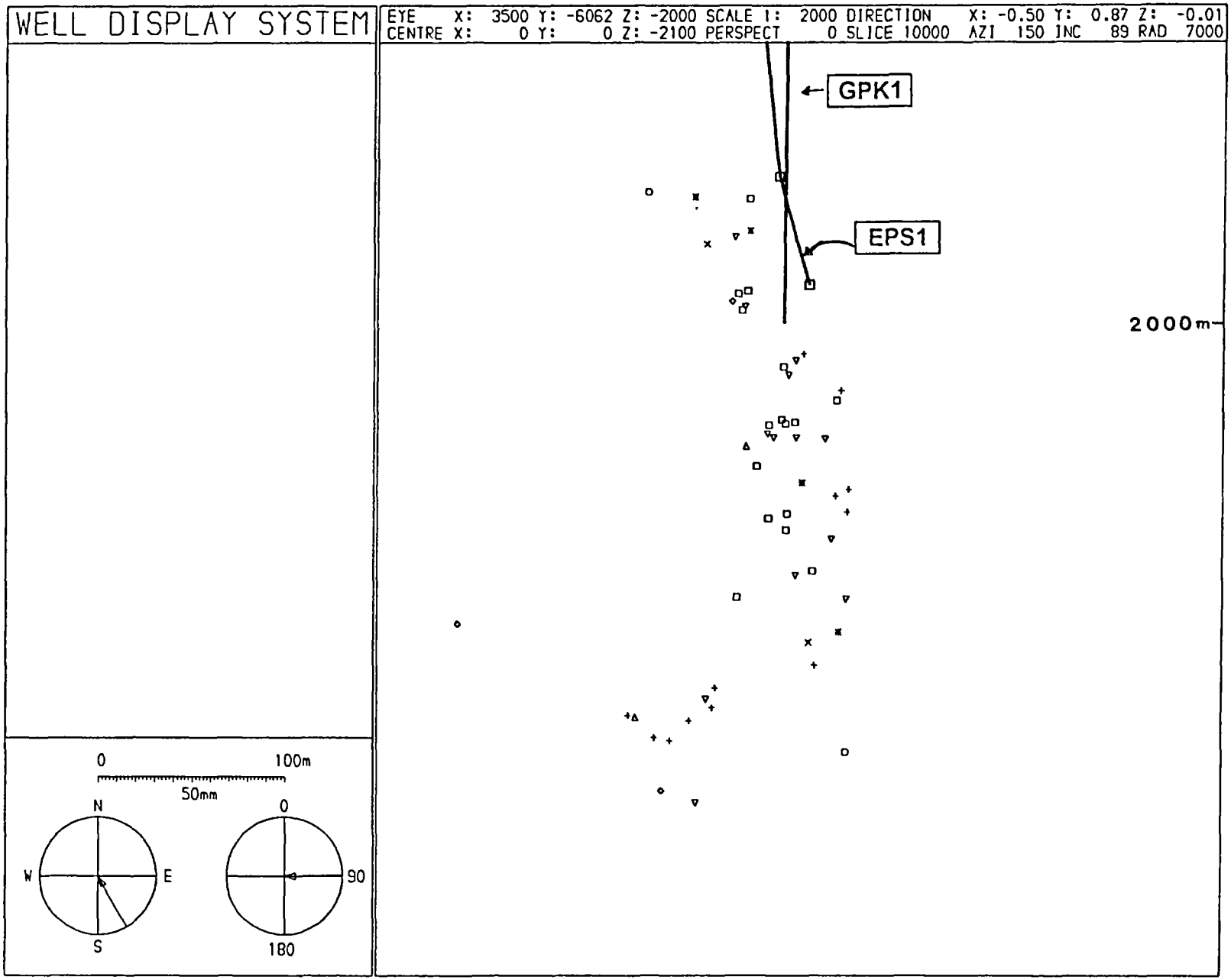

Locations of the various populations of events as a function of the observed combination of P-wave polarity picks. Vertical N150° cross-section.

ANNEX 8

Stanford paper

"Microseismic monitoring of hydraulic experiments undertaken during Phase IIa of the Soultz HDR project (Alsace, France)" - Presented on 17th Workshop on Geothermal Reservoir engineering, Stanford (USA), Jan. 29-31, 1992.

MICROSEISMIC MONITORING OF HYDRAULIC EXPERIMENTS UNDERTAKEN DURING PHASE IIA OF THE SOULTZ HDR PROJECT (ALSACE, FRANCE)

A. Beauce, R. Jones**, H. Fabriol*, C. Twose**, C. Hulot**

*BRGM/IMRG, BP. 6009, 45060 Orléans Cedex 2, France
**CSMA, Rosemanowes Quarry, Herniss, Penryn, Cornwall, UK

ABSTRACT

In the framework of the European HDR Project of SOULTZ, co-sponsored by European Community, two 50 hour-hydraulic injections were carried out in the main borehole GPK1. This borehole reached a depth of 2000 m (600 m of granite under a 1400-m-thick sedimentary cover) and a bottom hole temperature of 140°C. Both injections tests were made between a packer sited at 1968 m and bottom hole, with injection flow-rates of 7 l/s and 15 l/s.

3-axis accelerometer probes designed to withstand high temperatures up to at least 135°C were installed at the bottom of three boreholes which reached the granite. This network was supplemented by high temperature hydrophone sensors deployed in a fourth borehole (EPS1) at depth of about 2000 m. Data were transmitted to an on-line computer to perform preliminary interpretations.

During the tests, 135 and 239 induced microseismic events respectively were recorded. Present results show that seismicity starts off very close to the injection point and spreads out to form a cloud with a North-West to South-East elongation.

According to previous interpretations, the direction of the maximum horizontal stress component deduced by BHTV data analysis and hydrofracture in-situ stress measurements led to values of respectively 175°N and 155°N. During the second injection experiment a concentration of seismicity was revealed to the N-W of GPK1. This cloud also shows a trend to grow downwards and no seismicity extends more than 300 m away from the injection interval.

INTRODUCTION

Within the frame of the validation of a new power generation concept, research into the development of "Hot Dry Rock" geothermal energy began in the early 1970's in the US (Los Alamos) and later on, in Europe - Camborne (UK), Urach (Germany), Mayet de Montagne (France) - and in Japan. In all these projects, the monitoring of the microseismicity induced during hydraulic injection tests has proved to be fundamental in the understanding of the growth and size of the stimulated regions (Baria,R. & al.,1989; Matsunaga, I., 1990; Mock, J., 1989).

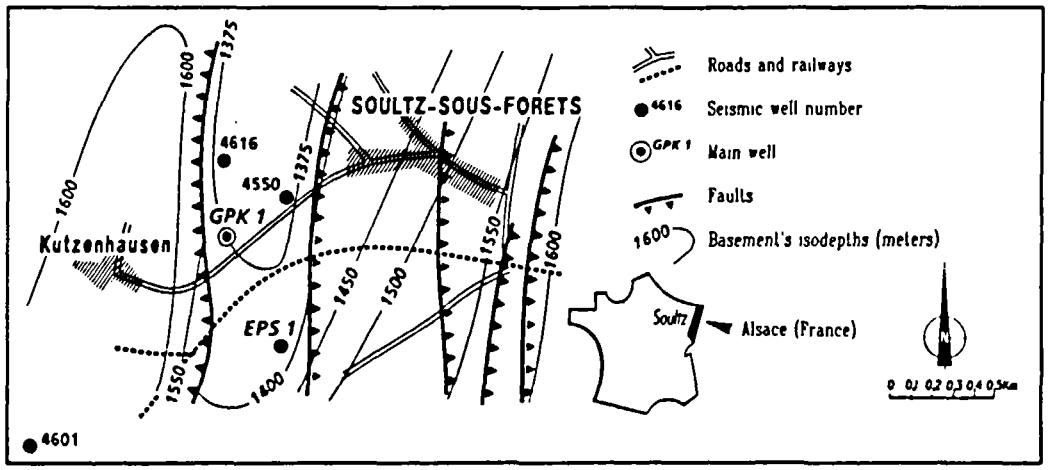

Fig. 1 - Location map of the project

The HDR site of Soultz, situated in the northeastern part of France in Alsace, was chosen in 1986 on top of a very large thermal anomaly which extend over about 4000 km^2 in the Rhine graben (Figure 1).

Prefeasability studies (Phase I) began in 1987 after the drilling of the main well GPK1 down to 2000 m (Kappelmeyer & al. , 1991). This borehole reached temperatures of 125°C at the top of the granite and 140°C at bottom-hole. A first small scale hydraulic stimulation (at a flowrate of 3 l/s for 3 days) took place in GPK1 at the end of 1988, and the associated seismicity was monitored (Beauce,A. & al., 1991).

In 1990, Phase IIa of the project started with the drilling of a second exploratory borehole (EPS1), sited at about 500 m S-E of GPK1 and planned to reach 3500 m; but, due to technical reasons and a very significant deviation of more than 15°, this well was stopped at about 2000 m. At total depth, final temperature of this borehole was 150°C.

During this phase, two 50-hour hydraulic stimulation experiments were undertaken in GPK1 between a packer set at 1968 m and bottom-hole: one of 7 l/s and one of 15 l/s.

MICROSEISMIC MONITORING NETWORK

To monitor the site during these experiments, three old oil wells (4616, 4550, 4601, see Figure 1) were successfully recovered in the surroundings of GPK1. As deduced from Phase I, and in order to avoid the attenuation effects observed on the seismic signals during their propagation in the sedimentary layers, these boreholes were deepened inside the granite. The coordinates of the sensors are given in Table 1, where the origin of the coordinate system is the wellhead of GPK1.

TABLE 1

SENSOR	X (m)	Y (m)	Z (m)	MD (m)	Depth in granite (m)
4516	-45.03	353.61	1382.81	1387.2	7
4550	285.23	205.12	1492.63	1492.0	87
4601	-1118.05	-864.35	1580.76	1599.0	26
Hydro 1	197.45	-363.95	1917.24	1945.0	-500
Hydro 2	210.45	-353.95	1974.82	2004.53	-500

Three 3-axis accelerometer probes were especially designed by CSM Associates Ltd to withstand the rough temperature and corrosion conditions, and deployed at the bottom of each of these wells. Various technical problems connected with borehole completion, prevented the correct cementation of these units before the hydraulic stimulations.

Data delivered by the accelerometer and hydrophone units were lowpass filtered downhole at 1500 Hz and analog transmitted using wires to the computer room in order to be continously monitored and pre-processed on a micro-VAX. Sampling rate was 5000 cps/channel and a window of 1.6 s (including pre-trigger) of data was stored on disk when an event was detected.

During the hydraulic stimulations either a single hydrophone (during the 7 l/s test), either a pair of hydrophones (during the 15 l/s test) were used. When only the single unit was deployed, then it was placed at the same position as the lower of the pair when that was used.

All the trajectories of these boreholes were measured using a gyroscopic tool.

An additionnal analog telemetry link seismic network composed of 8 mobile stations was also deployed on surface at about 1 km from the GPK1 wellhead by Institut de Physique du Globe de Strasbourg (IPGS); but no seismicity was recorded during the injection experiments.

VELOCITY MODEL

In order to obtain a velocity field around GPK1, and thus to allow reliable locations, a calibration shot of 300 g of explosives was fired at a depth of 1992 m in GPK1. Clear P-wave onsets were produced on all the sensors of the network; only one S-wave arrival was observed (on probe 4616).

The P-wave calculated velocities are given in Table 2:

TABLE 2

SENSOR	P-wave velocity (km/s)
4616	5.715
4550	5.745
4601	5.465
Hydrophone 1	5.940
Hydrophone 2	5.930

The deduced velocities between borehole pairs GPK1-4616 and GPK1-4550 are similar and in agreement with the results obtained in Phase I, i.e. an average velocity of 5.680 km/s.

However, an important discrepency is observed for the path GPK1-EPS1 that could be due to well survey errors, as borehole EPS1 was highly deviated.

More problematic is the low velocity measured between GPK1 and 4601 and the preceeding reason seems to be unlikely as both boreholes are almost vertical. At present, the problem of velocity anisotropy is not completely resolved but it could be

due to the conjonction of two factors: its relative long distance of this probe from the injection interval (around 1470 m) and the presence of an important NE-SW fault affecting the sedimentary layers and the granite which was revealed by a past reflection seismic survey. In order to not perturbate the location results of the microseismic events and to preserve a relative homogeneity in the results, it has been decided not to use the data from this probe at this stage of interpretation.

Bearing in mind these factors, it has been decided to adopt for locations an isotropic average P-wave velocity model of 5.85 km/s and to apply respective calculated time delays to the monitoring stations. As it was not really possible to deduced a good S-wave velocity model from the calibration shot data, no station delays were considered for these waves and a Vp/Vs ratio of 1.73 has been chosen.

INDUCED MICROSEISMICITY DURING THE 7 l/s HYDRAULIC INJECTION TEST

The 7 l/s hydraulic stimulation started on July 11th at 1 p.m., over a 30-m-long vertical section of GPK1 well, between a packer sited at 1968 m and bottom-hole. After eight and a half hours, and an injected volume of about 160 m^3, the experiment was stopped as the pressure in the annulus began to increase. The injection restarted at 1:15 p.m. on 12th and carried on from the next 50 hours.

Figure 2 shows a plot of the seismic event rate and down-hole pressure recorded during this period. A total of 135 microseismic events were induced during this test and seismic rate decreased immediatly when the injection stopped.

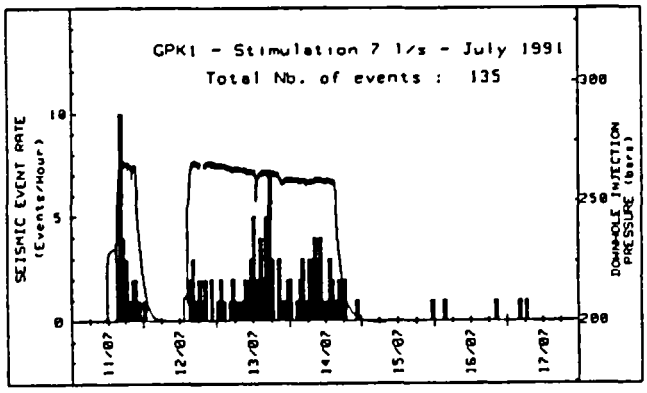

Fig. 2 - Hydraulic and seismic event rate data recorded during the 7 l/s stimulation in GPK1

These events have shown clear P and S wave onsets on the different probes of the network (see figure 3). It must be noted that the probe deployed in the borehole 4601 recorded only about 20% of the whole recorded seismic activity.

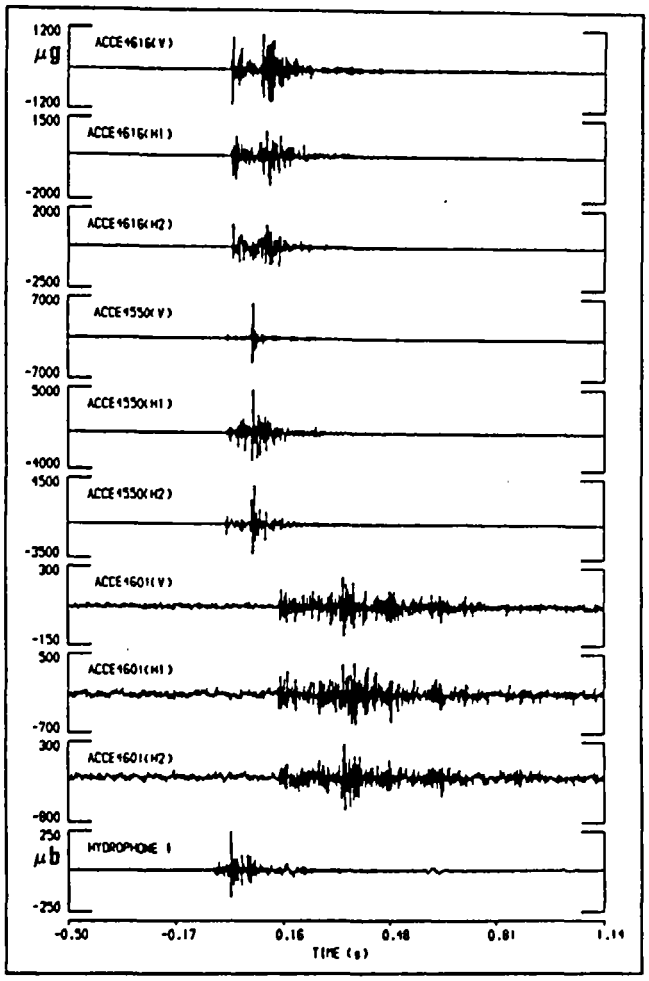

Fig. 3 - Signatures from down-hole accelerometers and hydrophone recorded during the 7 l/s hydraulic injection in GPK1
Event 26 - 11/07/1991 - 17:27:54

Microseismic location results

Of all the seismicity recorded during this test, 60% of the events have been interpreted and located (see figure 4) using the isotropic velocity model presented above. During this test only one hydrophone was deployed in the borehole EPS1. In consequence, as data from 4601 probe was not used for the locations, we only have a coplanar network. So, location results gave dual solutions images which form a mirror image in the plane defined by these sensors: the decision to choose the deepest solutions was based on the results obtained when we have more sensors and a non-coplanar network, i.e. during the 15 l/s injection test.

The plan view of figure 4 shows how the seismicity develops during this test to form an overall cloud with a N-W to S-E elongation, while the vertical plan view from 150°N shows a trend to grow downward.

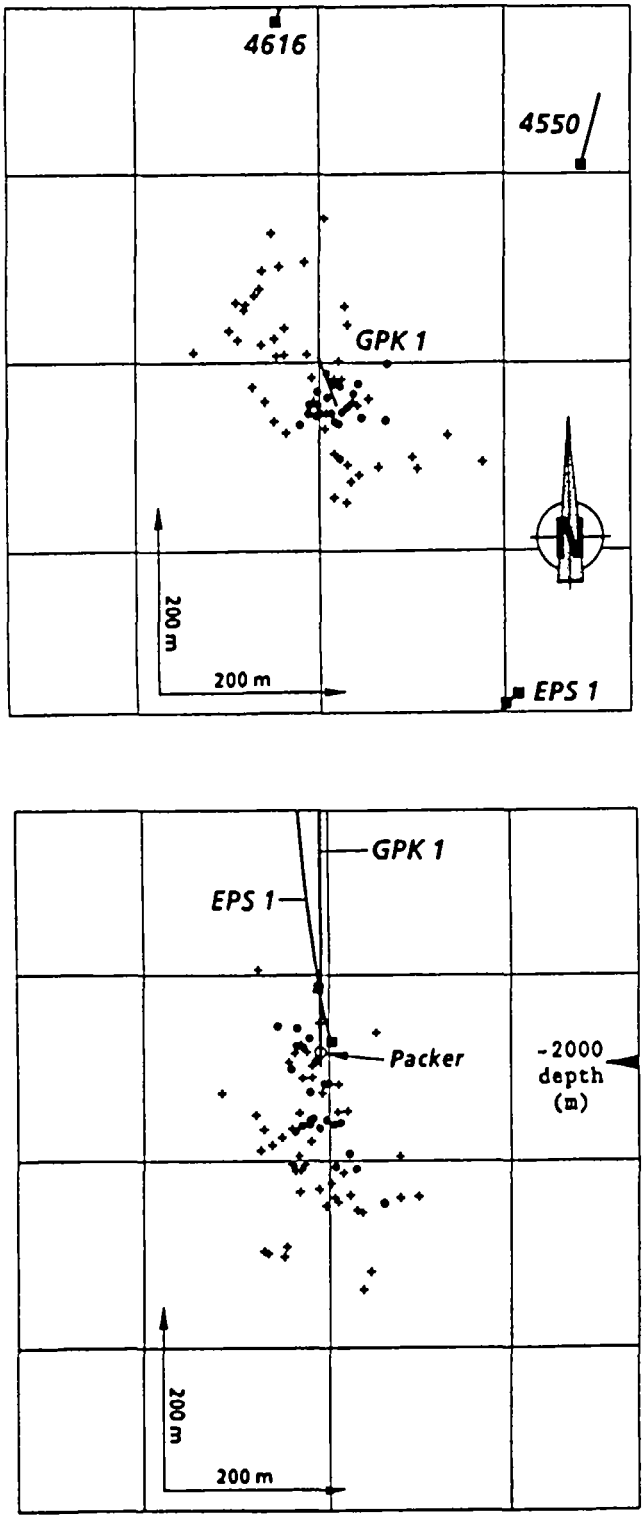

Fig. 4 - Microseismicity during the 7 l/s hydraulic injection in GPK1
Plan view and vertical section view (azimuth 150°N)
● first phase, + second phase
■ seismic probe

More precisely, on the first phase (full circles) the seismicity mainly concentrates near GPK1 and only on the south-southeastern side at depths between 1950 m and 2100 m. These results are in agreement with what was found during Phase I of the project with an hydraulic test with a flowrate of 3 l/s.

During the second phase, the seismicity extends away from GPK1 and at depths down to 2150 m, but in addition and corresponding to the second peak of seismicity observed on figure 2, a new seismic active zone appears on the north-northeastern side of GPK1 during the third day of the injection.

INDUCED MICROSEISMICITY DURING THE 15 L/S HYDRAULIC INJECTION TEST

The 15 l/s injection in GPK1 started on 18th of July at 9 a.m. and lasted about 50 hours in similar conditions to the previous experiment. A total volume of 2300 m^3 of fresh water was injected. Figure 5 shows the downhole injection pressure recorded during this test and the associated seismic event rate. The first event occured after an injected volume of 35 m^3 and a total of 239 induced events were recorded. In comparaison with the previous test, the average seismic rate (4 events/hour) was double. Moreover, the seismicity still persisted after the end of the stimulation, suggesting the existence of a remanent pressurized zone sited away from the borehole injection interval.

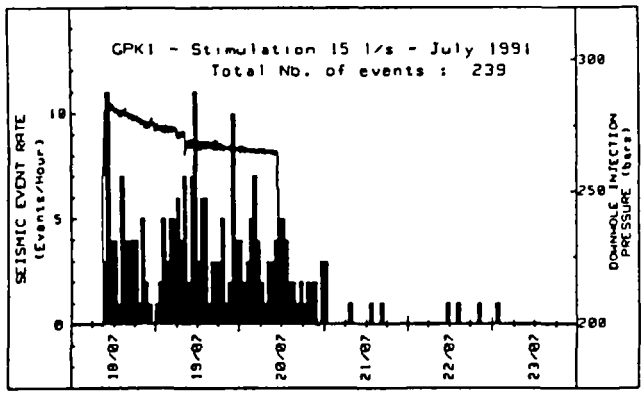

Fig. 5 - Hydraulic and seismic event rate data recorded during the 15 l/s stimulation in GPK1

Microseismic location results

During this injection the string of 2 hydrophones was deployed in EPS1, and again data recorded by the probe sited in borehole 4601 were not used for the locations of the events.

Figure 6 illustrates the chronological migration of the induced microseismicity as a function of days of injection in plan view and associated vertical plane viewed from the azimuth 150°N. During the first day, the seismicity grows downward to a maximum depth of 2150 m but only on the S-SE sector from GPK1 wellhead as it was observed during the beginning of preceeding test. On the second day, this seismic zone ceases to be active and a migration of the seismicity towards the N-W of GPK1 clearly appears; this new cloud concentrates at depths between 2150 m and 2250 m and still remains the principal active zone during the last day. When the injection stopped, this zone still also remained active for a few hours.

Once more, the general trend of seismicity is the same as observed during the 7 l/s injection test, that is along a NW-SE axis.

CONCLUSIONS

These preliminary results, both for the 7 l/s and 15 l/s hydraulic stimulations, have shown that the respective seismic clouds seem to organize along a NW-SE axis, and to grow downward from the injection interval. This trend must be associated with the present knowledge of the stress field which indicates an extension regime typical of a graben system with a maximum horizontal stress component of the tensor oriented 155°N to 175°N (Rummel F. & al., 1991).

However, the seismicity did not grow symmetrically along this axis in reference to GPK1 wellhead; in a first stage, the events appeared in the SE sector around the injection interval and deepened as the injection went on. Afterwards, this volume ceased to be seismically active - that was clear in a more obvious way during the second test after an injected volume of about 1000 m^3 - and a new zone sited on the NE sector and at depths between 2150 m and 2250 m began to activate.

At this stage of interpretation, it is therefore also necessary to point out that the network configuration will cause difficulties in the forthcoming detailed interpretations of fault plane solutions and source mechanisms.

ACKNOWLEDGEMENTS

This work was financially supported by the Commission of the European Communities, the Bureau de Recherches Géologiques et Minières and the Agence Française pour la Maîtrise de l'Energie.

The work described in this research note was also carried out under contract to the UK Department of Energy's Renewable Energy Research and Development programme, managed by the Energy Technology Support Unit (ETSU) at Harwell. The views and judgements expressed in this research note are those of the authors and do not necessarily reflect those of ETSU or the Department of Energy.

REFERENCES

Baria, R., Green, A.S.P, (1989), "Microseismics: a key to understanding reservoir growth", International HDR Geothermal Energy Conference, Camborne(UK), 27-30 June 1989, pp 363-377.

Beauce, A., Fabriol, H., Le Masne, D., Cavoit, C., Mechler, P., Chen, XK., (1991), "Seismic studies on the HDR site of Soultz-sous-Forêts (Alsace-France)", Geotherm. Sci. & Tech., Vol. 3 (1-4), pp. 239-266.

Kappelmeyer, O., Gérard, A., Schloemer, W., Ferrandes, R., Rummel, F., Benderitter, Y., (1991), "European HDR project at Soultz-sous-Forêts: general presentation", Geotherm. Sci. & Tech., Vol. 2 (4), pp. 263-289.

Matsunaga, I., (1990), "Development of hydrothermal power generation plants: development of technologies for a power generation system in HDR", 10th annual NEDO conference on Geothermal Energy Technologies, Oct. 1990, pp. 69-86.

Mock, J., 1989, "The U.S. Hot Dry Rock program", International HDR Geothermal Energy Conference, Camborne (U.K.), 27-30 June 1989, pp 149-158.

Rummel ,F., and Baumgartner, J., (1991) "Hydraulic fracturing stress measurements in the GPK1 borehole, Soultz-sous-Forêts", Geotherm. Sci. & Tech., Vol. 3 (1-4), pp. 119-148.

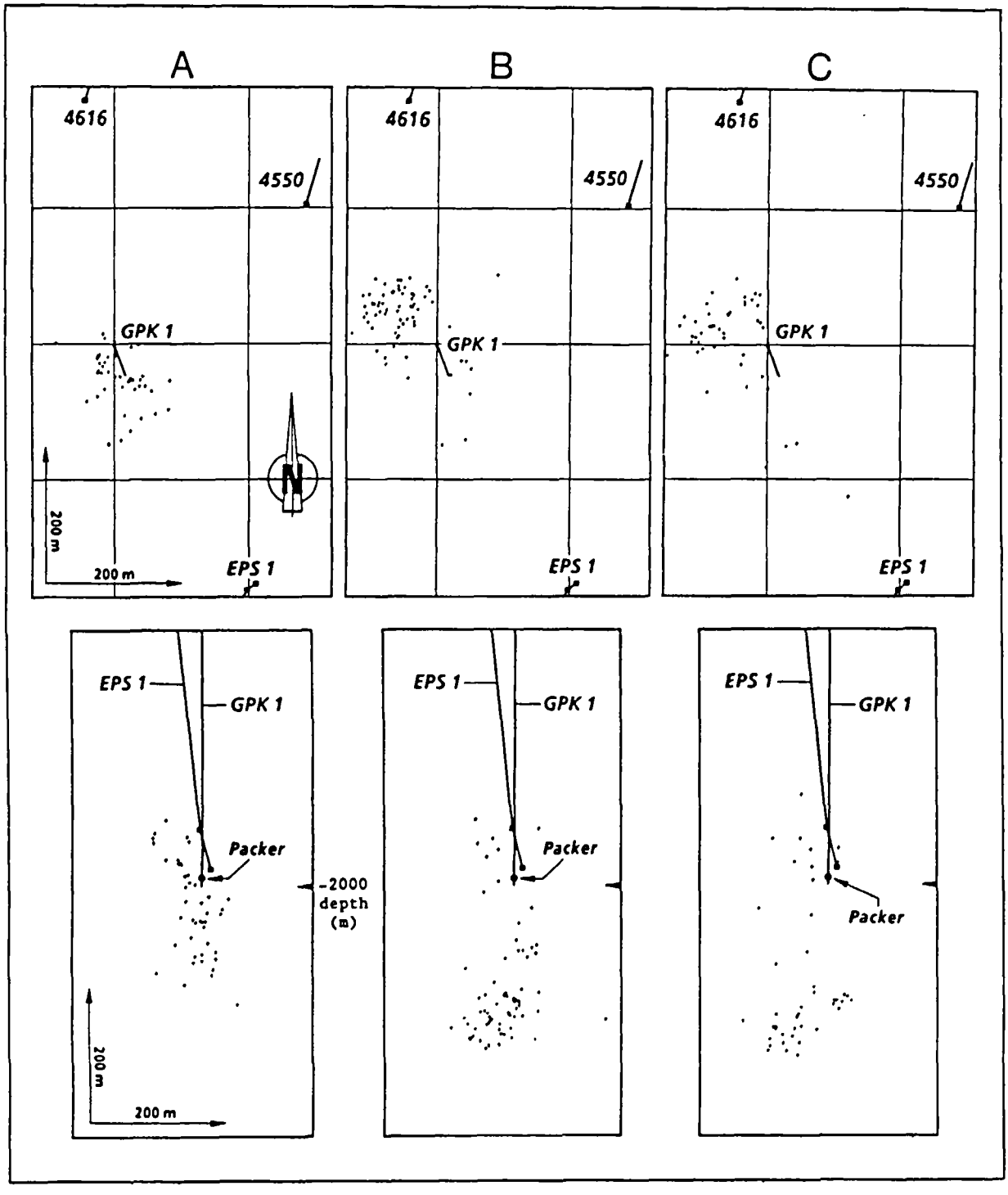

Fig. 6 - Microseismicity during the 15 l/s injection in GPK1
Plan view and vertical section view (azimuth 150°N)
A = first day, B = second day, C = third day
■ : seismic probe

RÉALISATION BRGM

impression et façonnage :
SERVICE REPROGRAPHIE